ASSESSING AND COMMUNICATING THE IMPACTS OF CLIMATE CHANGE ON THE SOUTHERN CALIFORNIA COAST

A Report for:

California's Fourth Climate Change Assessment

Prepared By:
Li H. Erikson[1], Patrick L. Barnard[1], Andrea O'Neill[1], Patrick Limber[1], Sean Vitousek[1], Juliette Finzi-Hart[1], Maya Hayden[2], Jeanne Jones[1], Nathan Wood[1], Michael Fitzgibbon[2], Amy Foxgrover[1], Jessica Lovering[1]

[1]U.S. Geological Survey
[2]Point Blue Conservation Science

Edmund G. Brown, Jr. *Governor*

August 2018
CCCA4-CNRA-2018-013

ACKNOWLDEGEMENTS

Support for this project was provided by the California Natural Resources Agency (BECI SUBAWARD NO.: EM4CX4-03A), California Coastal Conservancy, California Department of Fish and Wildlife, City of Imperial Beach, Tijuana River National Estuarine Research Reserve, and the USGS Coastal and Marine Geology Program.

Many individuals, organizations, and agencies helped make this work possible by providing data, information, input, and review of the final paper. We owe thanks, in particular, to Lesley Ewing and Carrey Batha at the Coastal Commission for engaging discussions on products and needs, as well as Phylis Grifman, Alyssa Newton, and Nick Sadrpour from USC Sea Grant for shouldering a tremendous outreach role and serving as such positive advocates for our science.

We thank Dr. Dan Cayan, Mary Tyree, and David Pierce of Scripps Institution of Oceanography for providing the CaRD10 data early in the stages of their work.

PREFACE

California's Climate Change Assessments provide a scientific foundation for understanding climate-related vulnerability at the local scale and informing resilience actions. These Assessments contribute to the advancement of science-based policies, plans, and programs to promote effective climate leadership in California. In 2006, California released its First Climate Change Assessment, which shed light on the impacts of climate change on specific sectors in California and was instrumental in supporting the passage of the landmark legislation Assembly Bill 32 (Núñez, Chapter 488, Statutes of 2006), California's Global Warming Solutions Act. The Second Assessment concluded that adaptation is a crucial complement to reducing greenhouse gas emissions (2009), given that some changes to the climate are ongoing and inevitable, motivating and informing California's first Climate Adaptation Strategy released the same year. In 2012, California's Third Climate Change Assessment made substantial progress in projecting local impacts of climate change, investigating consequences to human and natural systems, and exploring barriers to adaptation.

Under the leadership of Governor Edmund G. Brown, Jr., a trio of state agencies jointly managed and supported California's Fourth Climate Change Assessment: California's Natural Resources Agency (CNRA), the Governor's Office of Planning and Research (OPR), and the California Energy Commission (Energy Commission). The Climate Action Team Research Working Group, through which more than 20 state agencies coordinate climate-related research, served as the steering committee, providing input for a multisector call for proposals, participating in selection of research teams, and offering technical guidance throughout the process.

California's Fourth Climate Change Assessment (Fourth Assessment) advances actionable science that serves the growing needs of state and local-level decision-makers from a variety of sectors. It includes research to develop rigorous, comprehensive climate change scenarios at a scale suitable for illuminating regional vulnerabilities and localized adaptation strategies in California; datasets and tools that improve integration of observed and projected knowledge about climate change into decision-making; and recommendations and information to directly inform vulnerability assessments and adaptation strategies for California's energy sector, water resources and management, oceans and coasts, forests, wildfires, agriculture, biodiversity and habitat, and public health.

The Fourth Assessment includes 44 technical reports to advance the scientific foundation for understanding climate-related risks and resilience options, nine regional reports plus an oceans and coast report to outline climate risks and adaptation options, reports on tribal and indigenous issues as well as climate justice, and a comprehensive statewide summary report. All research contributing to the Fourth Assessment was peer-reviewed to ensure scientific rigor and relevance to practitioners and stakeholders.

For the full suite of Fourth Assessment research products, please visit www.climateassessment.ca.gov. This report assesses the coastal impacts of climate change for the California coast, including the combination of sea level rise, storms, and coastal change and translates that information into two simple, user-friendly online web tools.

ABSTRACT

Over the course of this and the next century, the combination of rising sea levels, severe storms, and coastal erosion will threaten the sustainability of coastal communities, development, and ecosystems as we currently know them. To clearly identify coastal vulnerabilities and develop appropriate adaptation strategies for projected increased levels of coastal flooding and erosion, coastal managers need user-friendly planning tools based on the best available climate and coastal science. In anticipation of these climate change impacts, many communities are in the early stages of climate change adaptation planning but lack the scientific information and tools to adequately address the potential impacts. In collaboration with leading scientists world-wide, the USGS designed the Coastal Storm Modeling System (CoSMoS) to assess the coastal impacts of climate change for the California coast, including the combination of sea level rise, storms, and coastal change. In this project, we directly address the needs of coastal resource managers in Southern California by integrating a vast range of global climate change projections and translate that information using sophisticated physical process models into planning-scale physical, ecological, and economic exposure, shoreline change, and impact assessments, all delivered in two simple, user-friendly, online tools. Our results show that by the end of the 21st century, over 250,000 residents and nearly $40 billion in building value across Southern California could be exposed to coastal flooding from storms, sea level rise, and coastal change. Results for the other major population center in California (the greater San Francisco Bay Area) are also available but not explicitly discussed in this report. Together, CoSMoS has now assessed the exposure of 95% of the 26 million coastal residents of the State (17 million in Southern California).

Keywords:

Sea level rise (SLR), future coastal storms, coastal flood hazards, long-term shoreline change, socio-economic exposure, Southern California

Please use the following citation for this paper:

Erikson, Li, H., Patrick L. Barnard Andrea O'Neill, Patrick Limber, Sean Vitousek, Juliette Finzi Hart, Maya Hayden, Jeanne Jones, Nathan Wood, Michael Fitzgibbon, Amy Foxgrover, Jessica Lovering. (U.S. Geological Survey and Point Blue Conservation Science). 2018. ***Assessing and Communicating the Impacts of Climate Change on the Southern California Coast.*** California's Fourth Climate Change Assessment, California Natural Resources Agency. Publication number: CCCA4-CNRA-2018-013.

HIGHLIGHTS

- CoSMoS provides coastal hazard vulnerability projections due to climate change for the 17 million coastal residents of Southern California. The results are being extensively used in local adaptation and resilience planning.
- Over 250,000 people, >2,300 km of road, and $38 billion worth of constructed buildings (present-day value, not accounting for inflation) are prone to coastal flooding across the region for the 200 cm SLR in combination with anticipated 100-year coastal storm events.
- Including storms increases population and property exposure from 10% (annual storm) to 350% (100-year) compared to the no-storm, SLR only scenarios.
- Of the five Southern California coastal counties, San Diego, Orange, and Los Angeles are most vulnerable to residential and infrastructure exposure. Ventura County is most prone to flooding of agricultural land whereas San Diego County hosts the majority of wetlands that are prone to permanent inundation (assuming no wetland accretion).
- Long-term average beach loss is projected to range from ~10 to 70 m for the 25 and 200 cm SLRs, potentially eliminating 2/3 of Southern California's beaches if sediment supply is limited.
- Average cliff retreat (including armored sections) is projected to range from 5 to 30 m for the 25 and 200 cm SLRs, representing an increase of ~20% to 150% compared to historical rates.

WEB LINKS

Coastal Storm Modeling System (CoSMoS):
http://walrus.wr.usgs.gov/coastal_processes/cosmos/

Our Coast, Our Future (OCOF) web tool: *www.ourcoastourfuture.org*

Hazard Exposure and Reporting Analytics (HERA): *www.usgs.gov/apps/hera*

TABLE OF CONTENTS

1: Introduction

Changes in atmospheric conditions such as temperatures, winds, and sea level pressures (SLPs) can impart deviations in both magnitude and frequency of storm events compared to the past which, combined with sea level rise (SLR), will affect coastal erosion patterns and coastal flood potentials. Coastal California continues to undergo extensive development which, combined with rising SLR and changing climatic conditions, could potentially exasperate the region's vulnerability to coastal flooding unless vulnerable areas are identified and appropriate development strategies and adaptations are implemented. In this study, we aim to identify potential vulnerabilities associated with coastal hazards brought about by projected climatic conditions and SLR during the 21st Century.

When considering the influence of climate change, global climate models (GCMs) are currently the best tools available to drive oceanographic and coastal models for assessing future flood hazards. Because of the coarse resolution and inability of GCMs to represent regional and local conditions that are essential for coastal impact studies (IPCC, 2007), outputs from GCMs cannot be used directly and require downscaling to regional and local scales (Wood et al., 2004). A number of studies have conducted regional downscaling of GCMs for evaluation of changes in future storm surges and wave conditions (e.g., Harper et al. 2009; Smith et al 2010; Mousavi et al., 2011; Graham et al. 2012; Hoeke et al 2013; Camus et al., 2014), but only a few have translated that work to the coastal zone and developed flood hazard maps from the combined impacts of projected SLR, wave run-up, storm surge, and other coastal water level contributors.

One such study is the Coastal Storm Modeling System (CoSMoS, Barnard et al., 2014) which employs a predominantly deterministic approach to make detailed predictions (10s of meters/feet) of storm-induced coastal flooding over large geographic scales (100s of kilometers/miles). The prototype system, developed for the California coast where swell waves generated in the large Pacific basin are a dominant factor in coastal storm-induced flooding, uses the global WaveWatchIII wave model, the TOPEX/Poseidon satellite altimetry-based global tide model, and atmospheric forcing data from GCMs to determine regional wave and water level boundary conditions. These physical processes are dynamically downscaled using a series of nested SWAN and Delft3D-FLOW models and are linked at the coast to tightly spaced XBeach (eXtreme Beach) cross-shore profile models.

The first version of CoSMoS was developed by USGS in collaboration with Deltares for the Southern California Bight (Barnard et al., 2014; http://cosmos.deltares.nl/SoCalCoastalHazards/index.html). That first iteration of CoSMoS focused on evaluating flood hazards associated with historical storms and two SLR scenarios as well as the hypothetical ARkStorm (Porter et al., 2011); the system continues to run operationally for near-term forecasts of regional wave climate and water levels. That initial work was expanded upon across the greater San Francisco Bay Area (https://walrus.wr.usgs.gov/coastal_processes/cosmos/norcal/index.html; https://walrus.wr.usgs.gov/coastal_processes/cosmos/sfbay/index.html) and up to Pt. Arena (https://walrus.wr.usgs.gov/coastal_processes/cosmos/ptarena/index.html) by including 40-50 SLR and storm scenarios and incorporating downscaled atmospheric forcing and river flows within San Francisco Bay. The work presented here builds upon the earlier CoSMoS work in Southern California to include 1) high resolution grids for better representation of harbors,

lagoons, bays, estuaries, and overland flow, 2) fluvial discharges that might locally impede and amplify flooding associated with coastal storms, 3) long-term morphodynamic change (i.e., beach change and cliff/bluff retreat) and its effect on coastal flooding projections, 4) uncertainty associated with terrain models, numerical model errors, and vertical land motion, and 5) alterations to coastal storm intensity and frequency associated with a changing climate.

Resulting model projections include flood extent, depth, duration, uncertainty, water elevation, wave run-up, maximum wave height, maximum current velocity, and long-term shoreline change and bluff retreat. To assess the socioeconomic impacts and communicate those risks and vulnerabilities associated with the coastal change and flood hazards, the data is made available on publicly accessible web-tools.

The Our Coast, Our Future (OCOF; www.ourcoastourfuture.org) web tool developed by Point Blue Conservation Science provides coastal managers and the general public with a user-friendly means to visualize how future scenarios of coastal flooding will impact local roads, property, businesses, and critical utilities. Users can export summary tables and reports detailing changes in flood extent by scenario on a scale relevant to local planners. The Hazard Exposure Reporting and Analytics (HERA; https://www.usgs.gov/apps/hera/) web tool translates the flooding extents and uncertainties into community exposure, highlighting the population and property at risk, among other features. The HERA web tool expresses the consequences of unmitigated coastal hazards in terms of dollars and cents, which represents a critical exercise in developing effective return-on-investment strategies to improve coastal infrastructure (e.g., via beach nourishments, construction of coastal protection structures, improving drainage, and managed retreat) and safeguard human health and services.

In line with these efforts, the objectives of this report are to:

- present the global-to-local scale downscaling methodology used to define the flood hazards and assess the exposure of people, property, infrastructure, and other systems within the Southern California Bight to future sea level rise and coastal storms.
- describe and evaluate the hazards, exposure, and vulnerability associated with various scenarios that combine the full spectrum of SLR combined with plausible future coastal storms for each of the five coastal counties of Southern California.

2: Study Area

Five counties, from north to south, comprise the coast of Southern California: Santa Barbara, Ventura, Los Angeles, Orange, and San Diego Counties. The Southern California Bight (SCB) extends from the U.S. / Mexican border northward to Point Conception and encompasses ~500 km of partially-protected, open coast shoreline (fig. 1). The active, complex tectonic setting along the Pacific and North American plate boundary has resulted in the region being fronted by a narrow continental shelf, a series of islands, beaches often backed by semi-resistant bedrock sea cliffs, and a highly irregular complex bathymetry that hosts a plethora of submerged seamounts, troughs, and canyons (Christiansen and Yeats 1992; Hogarth et al. 2007). The presence of seamounts, knolls, canyons, and the Channel Islands significantly alters the deep-water wave climate to a more complicated nearshore wave field (O'Reilly and Guza, 1993;

O'Reilly et al., 1999; Rogers et al., 2007; Adams et al., 2008). The islands block waves approaching from many directions, yielding a large wave energy shadow zone. Additionally, complex shallow water bathymetry adjacent to the islands, seamounts, and canyons scatters, focuses, and dissipates wave energy, resulting in highly variable wave energy distribution patterns along the coast. Though swell dominates nearshore wave energy, locally-generated seas contribute as much as ~40% to the total wave energy spectrum (Crosby et al., 2016; Hegermiller et al., 2017A).

Tides are mixed and semi-diurnal with a mean diurnal range of 1.7 m (5.6 feet; NOAA, 2017). Offshore waves can reach ~8 m during the most extreme events (CDIP, 2017) and therefore, even with dissipation across the shelf, wave-driven water levels (i.e., set-up and run-up) are still the dominant contributors to extreme coastal water levels across the region, contributing as much as 3 m (9.8 ft) to the total water level while storm surge and El-Niño-driven water level anomalies rarely contribute more than ~20-30 cm (7.9-11.8 inches) each (Flick, 1998; Bromirski et al., 2003).

The region hosts one of the largest economies in the United States and is heavily urbanized with 17 million residents living in the five Southern California coastal counties. Many vulnerable coastal areas are presently protected by sea walls or other flood and erosion defenses designed to withstand present-day storm impacts or even low SLRs for some of the more recent installations.

The coincident occurrence of storm-driven elevated water levels with high astronomic tides yield the greatest flooding (Storlazzi et al., 2000; Bromirski et al., 2009), whereas astronomic tide ranges along the open coast are well-predicted and not expected to vary significantly over the 21st century compared to historical levels (Flick et al. 2003). Rates of SLR and the frequency and magnitude of storm-generated water levels are less well constrained and thus are the main foci of this study.

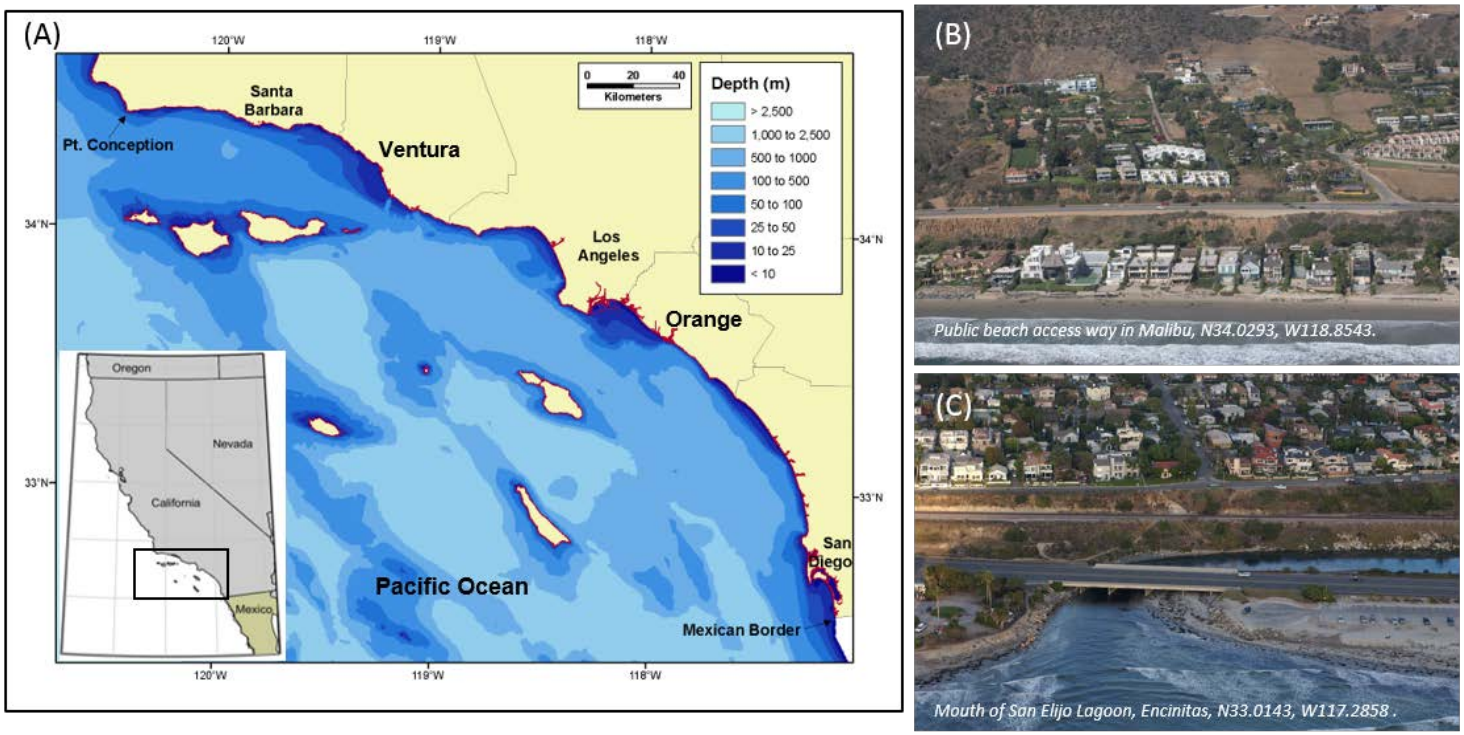

Figure 1. Overview of the study area. (A) Southern California Bight and coastal counties. (B) Aerial oblique photograph of Malibu. (C) Aerial oblique photograph of Encinitas. Both oblique photos highlight the urban infrastructure common throughout the study area. Image source: California Records Project, http://www.californiacoastline.org/

3: Model System Overview

Southern California CoSMoS is comprised of one global scale wave model and a suite of regional and local scale models that simulate coastal hazards in response to projections of 21st century waves, storm surge, anomalous variations in water levels, river discharge, tides, and sea level rise (fig. 2). A total of 40 scenarios resulting from the combination of 10 sea levels, 3 storm conditions, and one background condition (i.e., average waves, no storm) were simulated. Because scientific consensus on the magnitude of SLR projections is constantly evolving, we characterize changes in sea level by distinct increments and not by specific time periods. SLR ranged from 0 m to 2 m at 0.25 m increments plus an additional 5 m extreme. Future storm conditions represent the 1-year, 20-year, and 100-year return level coastal storm events as derived and downscaled from winds, sea level pressures (SLPs), and sea surface temperatures (SSTs) of the RCP 4.5, GFDL-ESM2M global climate model (GCM).

At the global scale, wind fields from four GCMs, using the latest 21st century climate change scenarios developed for the Coupled Model Intercomparison Project Phase 5 (CMIP5; Taylor et al., 2012), are fed into the WaveWatchIII (WWIII; Tolman et al, 2002) global wave model (see Section 4 for more details). A higher resolution Eastern North Pacific WWIII model is nested within the global WWIII model to produce a regional time-series of 21st century wave

conditions across a range of models and climate scenarios at the edge of the continental shelf (Erikson et al., 2015).

The wave conditions at the regional scale are subsequently fed into a series of nested, higher resolution wave models (i.e., SWAN) (Booij et al., 1999) that dynamically downscale the waves across the shelf to the point of wave-breaking (Section 6). Coupled to these wave models are a series of nested hydrodynamic models (i.e., DELFT3D-FLOW) (Lesser et al., 2004) that downscale the remaining physical processes from shelf to coastline, including astronomic tides, storm surge from downscaled atmospheric pressures and winds (Pierce, 2015; O'Neill et al., 2017; Pierce/Cayan/Kalansky et al., 2018 CA 4th Assessment Report), local river discharge, and seasonal water level anomalies. High resolution grids (~10-20 m (32.8-65.6 ft)) are used to simulate overland flows in areas surrounding protected embayments. Along the open coast, cross-shore XBeach (Roelvink et al., 2009, 2010) models are used every 100-200 m in the along-shore direction to explicitly simulate wave set-up and swash (i.e., run-up) due to infragravity waves, a key driver of extreme water levels during storm events on dissipative beaches (Stockdon et al., 2006). Modeled flood levels are interpolated onto regularly spaced grids and differenced from a 2 m (6.6 ft) resolution digital elevation model (DEM) to isolate areas that are not hydraulically connected to the open ocean but were wetted by the numerical model. The DEMs were developed using the most recent nearshore multibeam bathymetry and topographic LiDAR (Light Detection and Ranging) data (Danielson et al., 2016). The DEMs provide highly accurate bathy-topo for the numerical hydrodynamic flood models and are additionally used as initial conditions and calibration data in two long-term coastal change models that are run prior to the CoSMoS flood model. Further details can be found in Erikson et al. (2017).

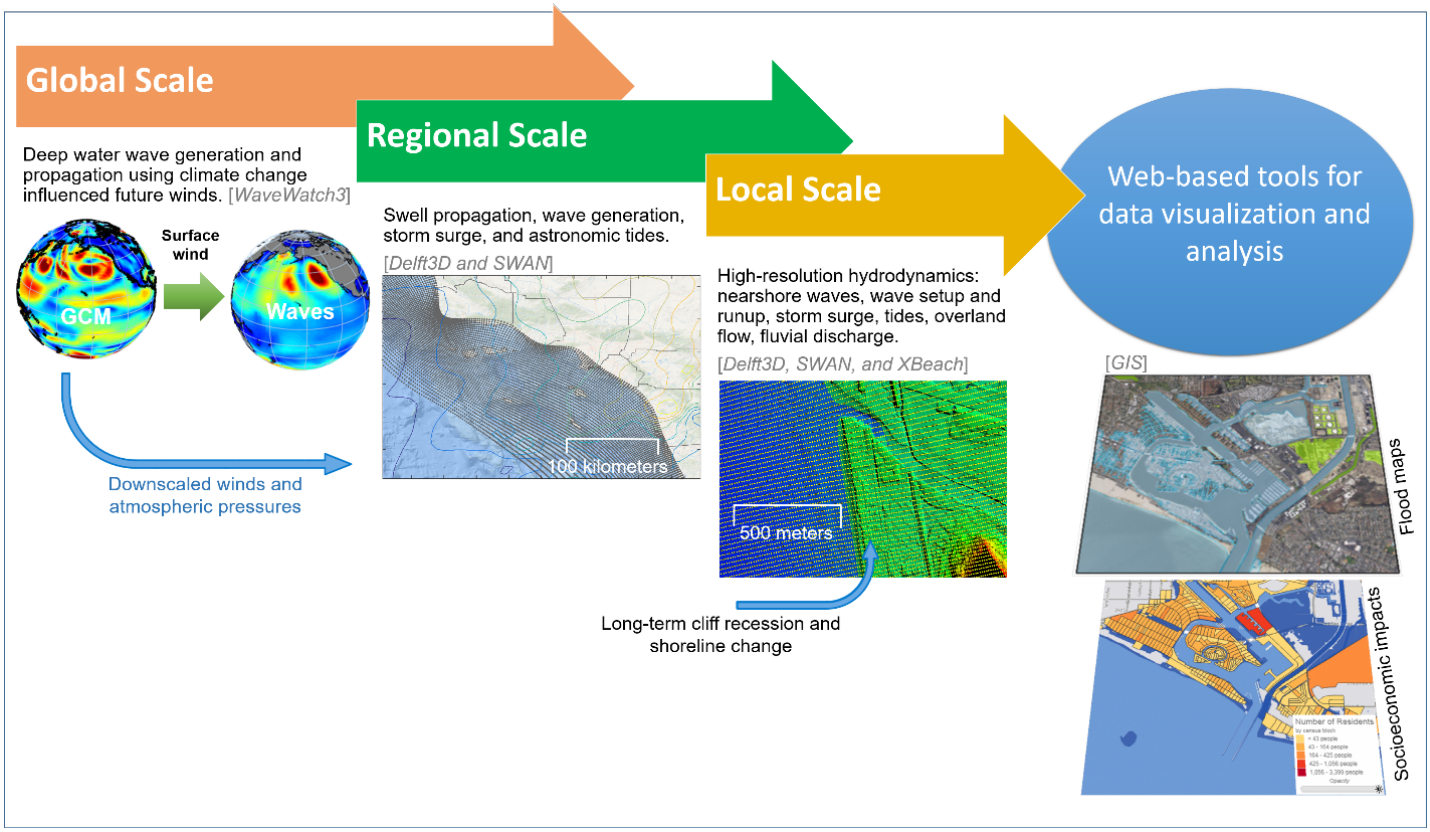

Figure 2. Overview of the Coastal Storm Modeling System (CoSMoS). Diagram illustrates the downscaling approach from the global to regional and local scales using a suite of numerical models (WaveWatchIII, Delft3D, SWAN, and XBeach). At the local scale, long-term cliff recession and shoreline change models are incorporated into the digital elevation models that are used to populate the numerical models. Dynamically modeled flood hazards at the local scale are summarized, exported, and overlaid with spatial Geographic Information System (GIS) layers and block scale census data that provide online tools for visualizing, quantifying, and evaluating exposures and vulnerabilities along the Southern California Coast. (www.ourcoastourfuture.org; https://www.usgs.gov/apps/hera/)

The explicit downscaling approach of the CoSMoS modelling system, from a global to local scale, is computationally expensive and thus does not lend itself to simulating lengthy 100-year-long continuous time-series. Instead, the model is run for predetermined scenarios of interest such as the 1-year or 100-year storm event in combination with sea level rise. Storms are first identified from time-series of total water level proxies (TWL_{px}) at the shore (Section 6.6). TWL_{px} are computed for the time period of interest, spanning the majority of the 21st century and assuming a linear super-position of the major processes that contribute to the overall total water level. TWL_{px} time-series are then evaluated for extreme events which define the boundary conditions for subsequent detailed modeling with CoSMoS.

TWL_{px} time-series are also used to force a cliff recession and shoreline change model, both of which were developed for this study (Section 5). The data-driven sandy beach evolution

(Vitousek and Barnard, 2015; Vitousek et al., 2017) and cliff retreat (Limber et al., 2015; in review) models are run at thousands of cross-shore transects spaced approximately 100 m apart along the Southern California coast. Both models use shoreline positions and oceanographic forcing to calibrate a suite of equations and develop robust relationships between forcing parameters and coastal response. Results from the two models provide time-varying beach shoreline and cliff positions, defined as the mean high-water (MHW) line and top of the cliff, respectively, that are used to evolve cross-shore profiles (Erikson et al., 2017) that are initialized by extracting elevations from the 2 m (6.6 ft) resolution DEM. The evolved cross-shore profiles are used to update the 3-dimensional DEM prior to running the thirty-six scenarios that incorporate future SLR and storms using full model physics of the CoSMoS flood model described above.

4: Projected Swell Waves Offshore of Southern California

Pacific Ocean waves were computed with the WaveWatchIII model (Tolman 2002, 1996) using near-surface winds from four global climate models (Beijing Climate Center, Meteorological Administration in China, BCC-CSM1.1; Institute of Numerical Mathematics, Russia, INM-CM4; Model Interdisciplinary Research on Climate, Japan MIROC5; National Ocean and Atmospheric Administration Geophysical Fluid Dynamics Laboratory, USA, GFDL-ESM2M) and two climate scenarios (Erikson et al., 2015; http://cmgwindwave.usgsportals.net). The two climate scenarios, Representative Concentration Pathway (RCP) 4.5 and RCP8.5, represent a future with relatively ambitious emissions reductions so that global radiative forcing is stabilized shortly after year 2100 (Thomson et al., 2011), and a future with no policy changes to reduce emissions, i.e., business as usual (Riahi et al., 2011), respectively. RCP4.5 represents a scenario of medium radiative forcing with the onset of stabilization by mid-century and reaching an increase in total global radiation of +4.5 MW/m2 by the year 2100, relative to pre-industrial (1850) conditions (Hibbard et al. 2007; Moss et al. 2010). The RCP4.5 scenario reflect societal actions that reduce greenhouse gas emissions in order to stabilize radiative forcing by 2100. It is also a mitigation scenario – the transformations in the energy system, land use, and the global economy required to achieve this target are not possible without explicit action to mitigate greenhouse gas emissions (Thomson et al. 2011).

The WWIII model (version 3.14, Tolman, 2009) was applied over a near-global grid (NWWIII, latitude 80°S–80°N) with 1°x 1.25° spatial resolution, and a one-way nested Eastern North Pacific (ENP) grid of 0.25° spatial resolution (~27 km at latitude 37°N). Bathymetry and shoreline positions were populated with the 2-minute Naval Research Laboratory Digital Bathymetry Data Base (DBDB2) v3.0 and National Geophysical Data Center Global Self-Consistent Hierarchical High Resolution Shoreline (GSHHS, Wessel and Smith, 2006). Wave spectra were computed with 15° directional resolution and 25 frequency bands ranging non-linearly from 0.04 to 0.5 Hz. Wind-wave growth and whitecapping was modeled with the Tolman and Chalikov (1996) source term package, and nonlinear quadruplet wave interactions were computed with the Hasselmann et al. (1985) formulation. Bulk wave parameter statistics (significant wave height, H_s; peak wave period, T_p; and peak wave direction, D_p) were saved at

daily time-steps (integrated over 24hrs) at each grid point and hourly at select points in deep water offshore of the continental shelf (see Erikson et al., 2015 and 2016 for further details).

Interestingly, it was found that the lower emissions scenario, RCP4.5, resulted in somewhat higher waves compared to RCP8.5 for the study region (Figure 3; Fig. 10 in Erikson et al., 2015), and thus RCP4.5 was selected as the scenario to further downscale to the local level across the Southern California bight. The decrease in deep water wave heights offshore of Southern California is believed to be related to poleward migration of storm tracks (e.g., Yin, 2015) and is consistent with several other modeling studies using GCMs to compute future wave conditions (e.g. Graham et al., 2013).

Because it was necessary to identify one GCM for further downscaling of winds and pressures that could be used to simulate individual storms with the CoSMoS model, a selection was made based on simulations of historical wave conditions (using GCM winds from 1976 through 2010) compared to temporally overlapping buoy observations. Of the four GCMs simulated, GFDL-ESM2M was shown to best represent observed wave conditions in the extremes (Fig. 4 in Erikson et al., 2015). Lower percentile waves were somewhat underestimated with a bias of about 25 cm (0.82 ft). This is commensurate with previous global scale models and thus the GFDL-ESM2M was selected as the model of choice for further downscaling and simulating future storm events.

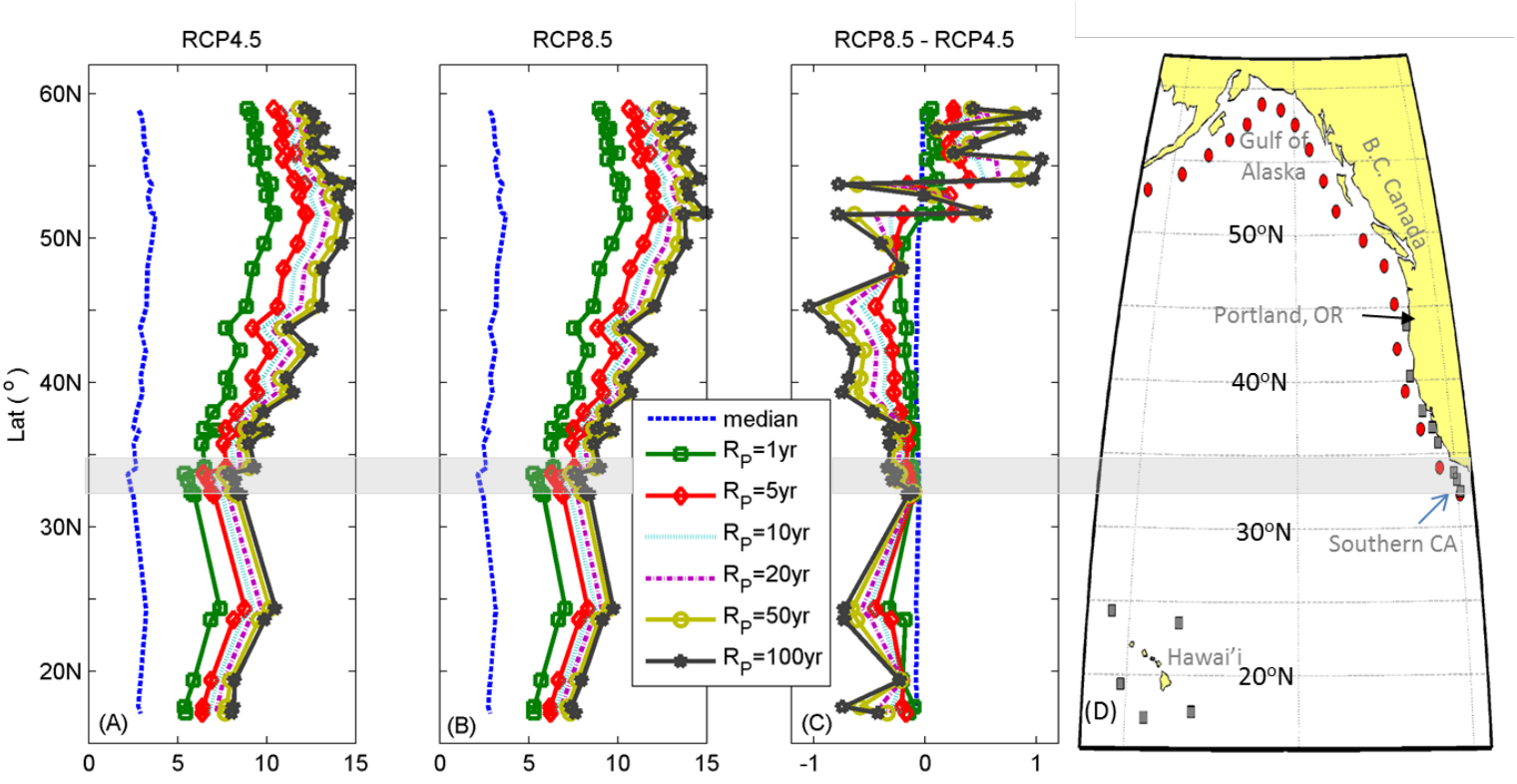

Figure 3. Changes in deep water significant wave heights offshore of the US west coast and southern Alaska as projected with dynamically downscaled waves using the WaveWatch3 model and winds from 4 global climate models spanning the years 2026-2045 and 2081-2100. (A) Four-member ensemble mean of projected median, 1-year, 5-year, 10-year, 20-year, 50-year, and 100-year return period wave heights for the mid-emissions representative concentration pathway

(RCP) or climate scenario, RCP4.5. (B) Same as in (A) but for the higher emissions RCP8.5 climate scenario. (C) Difference between projected median and extreme (1-year to 100-year) wave heights of the RCP8.5 and RCP4.5 scenarios. A negative value indicates that RCP8.5 waves are smaller compared to waves computed with wind forcing from the RCP4.5 models. (D) Overview map of the model output stations where hourly data was saved and analyzed. Gray squares indicate model output points collocated with buoys that were used to validate the model (Erikson et al., 2015).

The GFDL-ESM2M GCM is advantageous over some of the older models in that it is an earth systems model that communicates back and forth between atmosphere and ocean circulation models. The atmospheric component includes physical features such as aerosols (both natural and anthropogenic), cloud physics, precipitation, and evaporation; the oceanic model includes such processes as water fluxes, currents, sea ice dynamics, and a representation of ocean mixing.

Offshore of the SCB and in the approximate north-south center of the study area, collocated with Scripps Institution of Oceanography California Data Information Program (CDIP) buoy 067 (33.221°N, 119.881°W) the GFDL-ESM2M RCP4.5 wave model projects wave heights to be 4.9 m, 6.5 m, and 6.9 m for the 1-yr, 20-yr, and 100-yr return periods, respectively (Table 1). These values are about 1 m lower than measured waves at the same site where a maximum significant wave height of 7.76 m (wave period, T_p =14.3 s) was measured on December 28, 2006. Whilst swell waves are projected to be lower compared to the recent past, the wave period is projected to increase and the incidence angle to be more southerly. More southerly incidence angles and longer wave periods are related to the intensification of Southern Ocean wave generation, a consistent feature in global climate model predictions (Arblaster et al., 2011; Hemer et al., 2013). The projected decrease of extreme wave heights is thought to be related to a poleward shift in North Pacific extra-tropical storm tracks (Yin, 2005; Bromirski et al., 2009; Graham et al., 2013).

Table 1: Modeled and observed deep water waves at buoy CDIP067.

Parameter	1-year	5-year	10-year	20-year	50-year	100-year
GFDL-ESM2M (full 100 years up to year 2100) (Tp and Dp are means of all Hs±0.1m)						
H_s (m)	4.93	5.93	6.25	6.5	6.76	6.91
T_p (s)	16	16	17	17	16	17
D_p (deg)	294	292	291	282	282	284
Observed (September 1996 through December 2017)*						
H_s (m)	6.04	7.21	7.47	7.65	7.79	7.86
T_p (s)	15	16	14	17	ND	ND
D_p (deg)	299	296	305	306	ND	ND

A Generalized Pareto Distribution (GPD) was fit through the wave data and, in the case of the observation data, extrapolated for return periods greater than the length of the time-series. Listed T_p and D_p are the means of all instances for which the shown $H_s \pm 0.1$ m occurred.

*ND: no data.

A note on return periods: flooding is often described by its recurrence interval, and thus identification and simulation of storm events with given recurrence intervals are used throughout this study. As described by Heberger et al. (2009), the terminology can often be misleading. For example, a "100-year" flood refers to a flood that has a 1 in 100, or 1%, chance of occurring in any year – it does not mean that the flood level will occur every 100 years. See Heberger et al. (2009) and other literature for example calculations.

5: Data and Methods for Modeling Long-Term Shoreline Change

Two data-driven models to simulate cliff retreat and sandy beach evolution were developed for this study. The two models are described in the following sections; further details can be found in (Limber et al., 2015, in review; Vitousek and Barnard, 2015; Vitousek et al., 2017).

5.1 Coastal Cliff Retreat Model

Cliff retreat is defined as the landward movement of the cliff (top) edge. Coastal cliff retreat is projected at each transect using a multi-model ensemble of up to seven models that relate sea cliff retreat to wave impacts, SLR, historical cliff behavior, and cross-shore geometry (Trenhaile, 2009,2011; Walkden and Hall, 2005; Ruggiero et al., 2001; Walkden and Dickson, 2008; Hackney et al., 2011). The multi-model ensemble can mitigate the limitations of an individual model and therefore develop more robust predictions. All the models are time-dependent and were implemented using a basic forward Euler scheme (Moin, 2010) with a 1-year time step. The models can be divided into two general types. The first type consists of simple one-dimensional models that empirically relate wave impacts to cliff retreat where the cliff profile shape remains constant through time (of which there are up to six per transect). The second type is a more complex, two-dimensional model that includes a discretized, freely evolving cross-shore profile of nearshore and sea cliff morphology (of which there is one per transect). Each of the individual models is subject to unique, simplifying approximations that tailor the model to certain morphologic settings. Predictions from the simple 1-D models are based on Monte Carlo simulations of each individual model which account for the uncertainty of model parameters. Here, each model was run 100 times for each transect and SLR scenario to balance computational efficiency and the spread of the parameter space. For example, model parameter values including historical retreat rate, cliff toe (or beach) height, nearshore slope, beach slope, cliff height, and the decay constant were drawn from uncertainty ranges that were normally distributed around observed values. The ensemble gives preference to models that show less sensitivity to variations in model parameters and then weights projection uncertainty proportionally with the difference between individual model results (i.e., how well the ensemble reaches a consensus). Unlike the one-dimensional models, the 2-D profile-based models were more computationally intensive and predictions could not be made with a Monte Carlo approach. Instead, profile model behavior was assimilated into a machine learning framework (using artificial neural networks, or ANN; see Limber et al., 2016) which was used to

decrease computation time and estimate unknown model coefficients. The ANN was then used to make predictions at each transect for each SLR scenario.

Because the models are applied over large spatial and temporal scales which might require long computation times and detailed input parameters that are not available, some simplifications were necessary. The models do not explicitly distinguish between soft rock and hard rock coasts because they represent only basic physical interactions between waves and cliffs that are common to both morphologies. Smaller-scale details, such as vertical variations in rock strength on the cliff face (Carpenter et al., 2012) and seasonal variations in beach width and height, are not explicitly represented. The dynamics of progressive undercutting and sudden cliff failure are difficult to accurately model, especially with limited geotechnical data, and predicting the timing and scale of individual cliff failures is not possible on this scale. As a result, we estimate time-averaged cliff edge positions and rates – and not the timing or scale of the episodic failures that ultimately generate the long-term rates (Lim et al., 2010; Rosser et al., 2013; Barlow et al., 2012). Dynamics related to seasonal beach erosion (Yates et al., 2009) and talus deposition and subsequent removal (e.g. Castedo et al., 2012; Kline et al., 2013) are also not considered here. Finally, rainfall can affect sea cliff evolution in parts of Southern California (Young et al., 2009). Here, our predictions focus on wave-driven erosion because the relationships between rainfall, groundwater, and cliff failures are not well established. However, rainfall-induced cliff erosion and other factors that might affect cliff retreat rates, such as jointing, fractures, geologic variability, failure planes, and groundwater flow, are implicitly included in the historical cliff retreat rates used to calibrate the models.

Summary of limitations and assumptions pertaining to cliff and bluff projections:

- are determined largely from the geometry of the coastal profiles (offshore slope, cliff face slope, beach slope, cliff toe elevation, etc.) rather than the geologic characteristics of the cliffs because geologic data is not yet available (note: such data collection efforts have begun and will be used in future model applications and developments)
- long-term mean historic cliff retreat rates over the time period ~1930-2000 (USGS National Shoreline Assessment Project) are used to calibrate the models
- are time-averaged and do NOT resolve individual cliff failure events
- do not directly include the effects of rainfall or groundwater percolation, only wave impacts

5.2 Sandy Beach Shoreline Change Model

The CoSMoS-COAST sandy shoreline change model (Vitousek et al., 2017) combines geographic information, management scenarios, and forcing conditions (due to waves and SLR) with three process-based models that compute (1) wave-driven longshore transport (Vitousek and Barnard, 2015), (2) cross-shore transport due to waves (Yates et al., 2009), and (3) cross-shore transport due to SLR (Anderson et al., 2015). The model integrates the process-based models with historical shoreline observation via an Extended Kalman Filter data assimilation method (Long and Plant 2012). The model uses historical shoreline positions and oceanographic observations to calibrate a suite of equations and develop robust relationships between forcing parameters and shoreline response and projects these relationships into the future (Fig. 4).

Continuous time-series of forecasted nearshore waves (Hegermiller et al., 2016) and water levels, combined with sea level rates of change, are used to model shoreline change to the year 2100 (section 5.4). Four different management scenarios, representing all combinations of beach nourishment and the existence or non-existence of hard structures that limit erosion, were considered. The hard-structures scenario was achieved by limiting erosion to an 180,000-point polyline digitized from aerial photos (Google Earth, 2015/2016) that represents the division of beach and urban infrastructure.

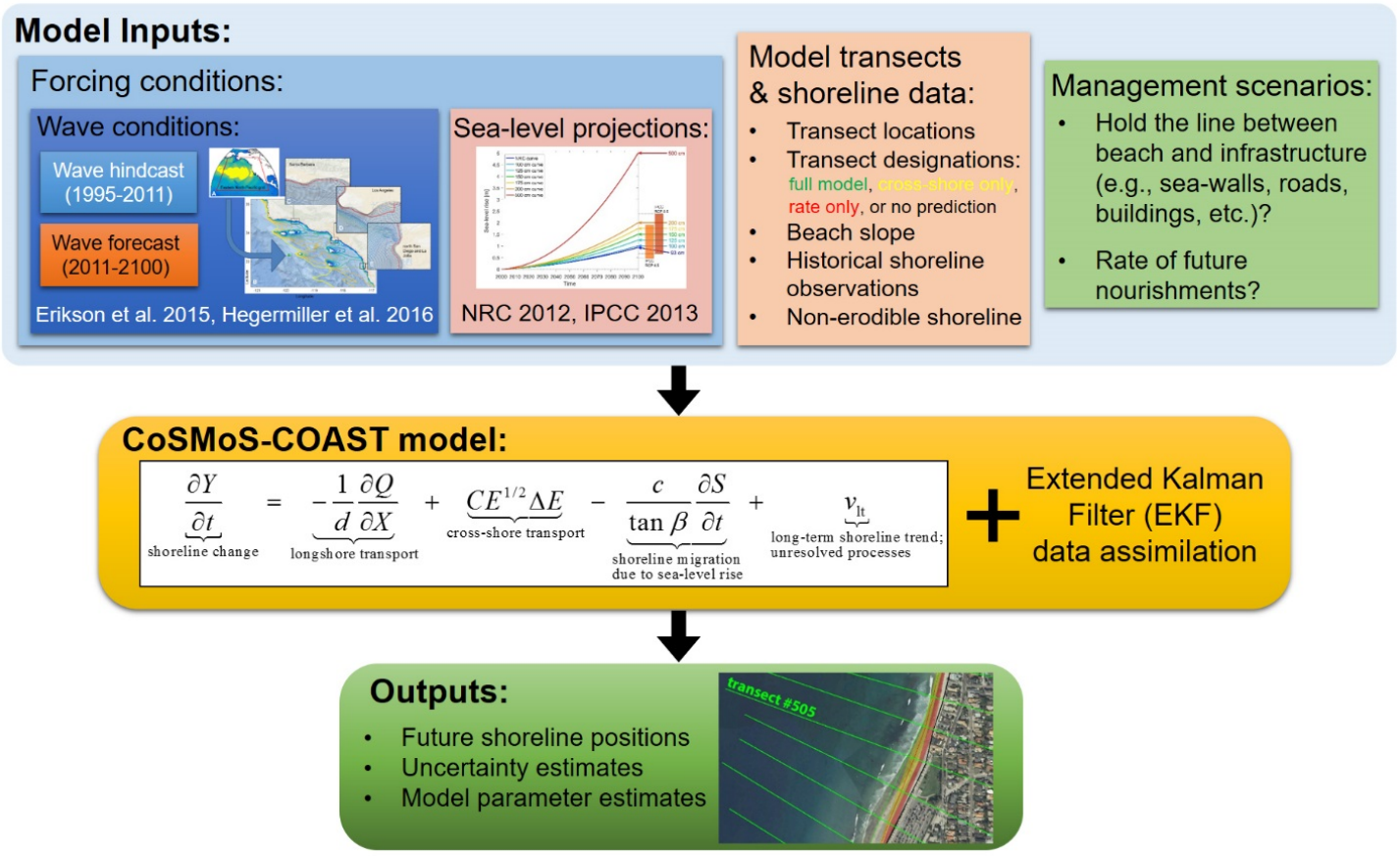

Figure 4. Overview of the CoSMoS-COAST shoreline change model. Model inputs include spatially varying hourly time-series of nearshore wave bulk statistics (wave height, period, and direction), sea level rise rates, historical shoreline change rates, beach nourishment rates, beach slopes, and information regarding armoring at each model cross-shore transect. Inputs are provided to the model (shown within the yellow box) which consists of a one-line longshore transport model, a cross-shore equilibrium transport model, a sea level driven shoreline recession model, and terms for parameterization and historical data assimilation that account for unresolved processes. Training the model with historical data is crucial to achieving accuracy. In regions where little historical data exists, model uncertainty is greater and explicitly quantified.

Summary of limitations and assumptions: Pertaining to sandy shoreline projections:

- model evaluates one-dimensional shoreline changes at a series of alongshore-spaced transects;

- model assumes an equilibrium beach profile spatially translating the mean high-water position (actual beach profile changes are not computed);
- natural and anthropogenic sediment supply is estimated from sparse shoreline data.

5.3 Sea Level Rise

SLR scenarios for the coastal change projections were represented with a second-order polynomial curve that reached 1 m or greater by the year 2100, relative to 2000 (Fig. 5). For SLR rates of 0.25 m, 0.50 m, and 0.75 m, long-term morphodynamic change simulations were run up through Jan 01, 2044, 2069, 2088, respectively, based on the National Research Council (2012) values for Southern California (2012). The 0.93 m scenario is a regional sea level projection developed specifically for Southern California by the National Research Council (2012), and, overall, the chosen sea levels are in line with the long-term predictions in the IPCC 2013 report (Church et al., 2013) as well as in other studies (e.g., Pfeffer et al., 2008; Vermeer and Rahmstorf, 2009; Horton et al., 2014). New recommendations for local coastal planning within the State of California provided by 4th Assessment authors suggest SLR of up to ~2.87 m by 2100 (Cayan et al., 2016).

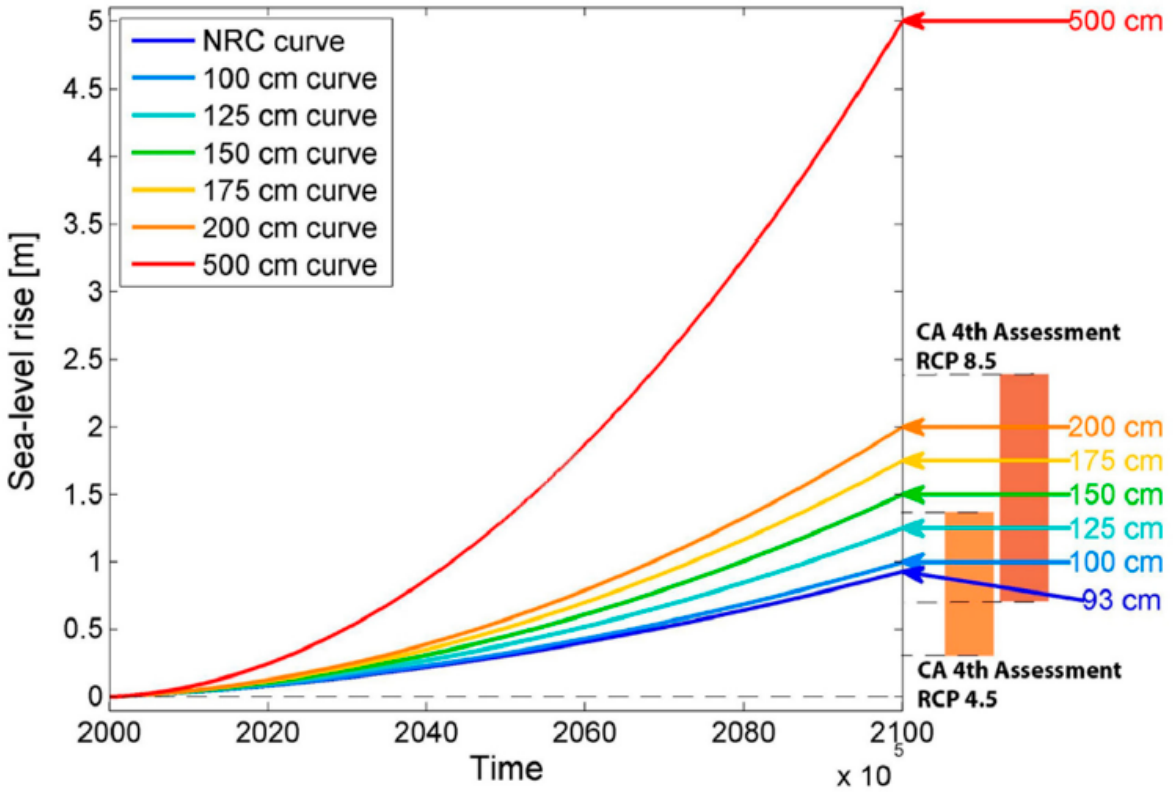

Figure 5. Rates of sea level rise used in the cliff retreat and shoreline change models. Vertical bands on the right side illustrate the range of SLR projections by 2100 from the California 4th Assessment (Cayan et al., 2016).

5.4 Oceanographic Forcing

The cliff and shoreline change models were forced with hindcasted (1980 - 2010) and projected (2010 - 2100) wave time-series (Hegermiller et al., 2016). The hindcast was generated from high resolution SWAN model runs that capture changes in the wave field due to wave refraction across complex bathymetry and shadowing, focusing, diffraction, and dissipation of wave energy by islands. The model was forced at the open boundaries by intermediate-depth Wave Information Study (WIS: http://wis.usace.army.mil) wave time-series located landward of the Channel Islands and by CaRD10 near-surface wind fields (Kanamitsu and Kanamaru, 2007). Three-hourly wave parameters (significant wave heights, mean wave period, peak wave period, mean wave direction, and peak wave direction) were output at 4,802 points along the 10 m bathymetric contour every ~100 m in the alongshore direction. The hindcast was validated against 23 collocated CDIP buoys and found to behave reasonably well with a mean root-mean-square-error (*RMSE*) of 27 cm (10.6 inches; range 14-40 cm (5.5-15.7 inches; Fig. 6)). The hindcast overestimates the peak wave period but with generally small positive *bias*. See Hegermiller et al. (2016) for further details.

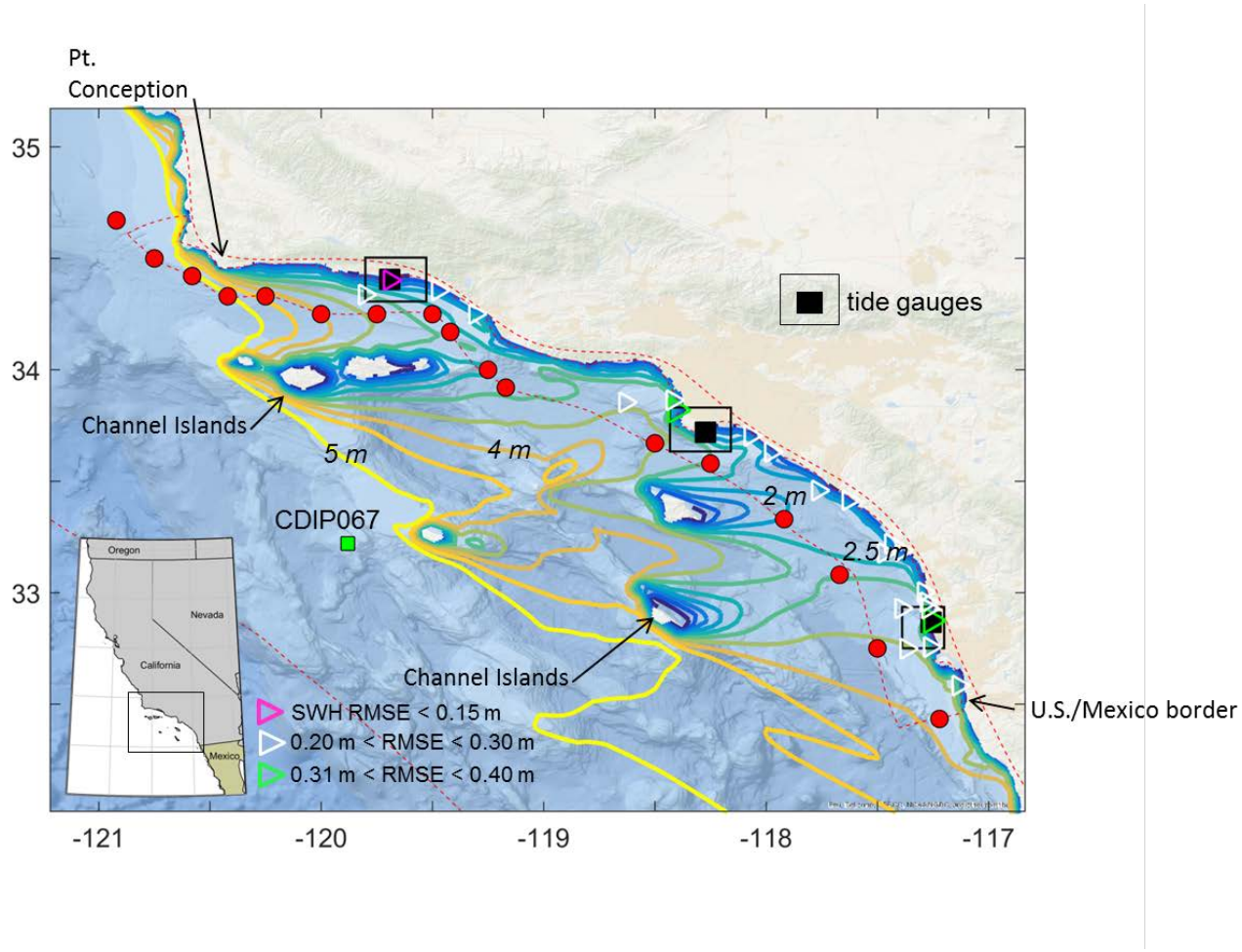

Figure 6. Root-mean-square-error (RMSE) statistics of the hindcast SWAN model used to generate continuous time-series of nearshore wave conditions for the cliff recession and shoreline change models. RMSEs were computed between modeled and measured significant wave heights in the nearshore region. Filled red circles show locations of the Army Corps of Engineers' Wave Information Study (WIS) model output points used as boundary forcings to the nearshore wave model (dashed inshore red line).

The 30-year hindcast time-series was correlated with measured and modeled (NOAA CFSRR WWIII, when observations were not available) deep-water waves at the CDIP067 buoy to generate a look-up table that relates deep-water waves to nearshore wave bulk parameters (Hegermiller et al., 2016). The look-up table, in conjunction with the dynamically downscaled waves (WWIII; Section 4) and winds (Cayan et al. CA Fourth Assessment) using GFDL-ESM2M as the forcing fields, were used to derive 15-m (50 ft) depth nearshore wave parameters at 3-hourly intervals out to the year 2100. Hindcast and projected time-series data are available for download at http://dx.doi.org/10.5066/F7N29V2V.

To estimate total water level proxies at the shore, wave run-up was computed from the hindcast and projected wave time-series and linearly superimposed onto empirically derived time-series of storm surge (SS) and other water level anomalies (SLA).

$$TWL_{px} = R_{2\%} + SS + SLA \qquad (1)$$

Projected storm surge and sea level anomalies were estimated with empirical models developed for this study. Details of these models can be found in Erikson et al. (submitted). Conditional dependencies of H_s, T_p, D_p, SS, SLA are accounted for through the use of internally consistent boundary conditions from a single GCM; for this study, NOAAs GFDL-ESM2M, RCP4.5 was selected based on evaluation of projected offshore wave conditions as described in Section 3.

6: Data and Methods for Modeling Flood Hazards

In contrast to the *TWL* proxies (described in the previous section) that were computed to aid in identification of extreme storms (section 6.5) and to provide temporally continuous boundary conditions for the cliff recession and shoreline change models (section 5), flood hazard modeling is done explicitly and deterministically with a suite of numerical models, accounting for changes in water levels and currents and without assuming a linear superposition of waves and water levels. For all flood hazard simulations, projected deep water waves, computed with the global scale wave model (Section 4), are propagated to shore with a suite of regional (Tier I) and local (Tiers II and III) models that additionally simulate regional and local wave growth (seas) in combination with long-term and event-driven morphodynamic change and water level changes due to astronomic tides, winds, sea level pressure, steric effects, and sea level rise.

The regional Tier I model consists of one Delft3D hydrodynamic FLOW grid for computation of currents and water level variations (astronomic tides, storm surge, and steric effects) and one SWAN grid for computation of wave generation and propagation across the continental shelf. Wave conditions from the global wave model are applied at the open-boundaries of the SWAN model. The FLOW and SWAN models are two-way coupled so that tidal currents are accounted for in wave propagation and growth and, conversely, orbital velocities generated by waves impart changes on tidal currents.

Employing high resolution grids for fine-scale modeling of the entire study is not possible using desktop computers and therefore Tier II was segmented into 11 sections. Each sub-model consists of two SWAN grids and multiple FLOW grids. Wave and water level time-series of the Tier I model are applied at the open boundaries of each Tier II sub-model. See Section 6.3 for more details on Tier II.

Tier III consists of more than 4,000 cross-shore XBeach (eXtreme Beach) models that simulate event-driven morphodynamic change, water level variations, and infragravity wave run-up every ~100 m (328 ft) alongshore. Wave run-up is the maximum vertical extent of wave uprush on a beach or structure above the still water level and, in cases where infragravity waves exist, the reach of wave run-up can be significantly further inland compared to wave run-up driven by shorter incident waves (Roelvink et al., 2009, 2010). The U.S. west coast is particularly susceptible to infragravity wave run-up due to the prevalence of breaking long-period swell (low wave steepness) across wide, mildly sloping (dissipative) beaches that result in a shoreward decay of incident wave energy and accompanying growth of infragravity energy.

6.1 Regional Scale Wave and Hydrodynamic Model - Tier I

6.1.1 Grids, Model Settings, and Bathymetry

The WAVE and FLOW modules of the Delft3D version 4.01.00 were used to simulate waves and hydrodynamics, respectively. The WAVE module allows for two-way coupling (communication) between wave computations and FLOW hydrodynamics and simulates waves with the numerical model SWAN (Simulating Waves Nearshore, Delft University of Technology). SWAN is a commonly used third-generation spectral wave model specifically developed for nearshore wave simulations that account for propagation, refraction, dissipation, and depth-induced breaking (Booij et al., 1999; Ris, 1999).

Delft3D-FLOW, developed by WL/Delft Hydraulics and Delft University of Technology, is a widely used numerical model that calculates non-steady flows and transport phenomena resulting from tidal and meteorological forcing (Lesser et al., 2004). Details on model settings and calibration can be found in Erikson et al., 2017.

Tier I SWAN and FLOW models consist of identical structured curvilinear grids that extend from shore to ~200 km (124.2 miles) offshore in water depths >1,000 m (>3,280 ft) and range in resolution from 1.2 x 2.5 km (0.75 x 1.6 miles) in the nearshore to 3.5 x 5 km (2.2 x 3.1 miles) in the offshore (dashed black line in Fig. 7). The two-way coupled model was run in a spherical coordinate system and with FLOW in a vertically-averaged mode (2DH). Bathymetry was derived from the National Geophysical Data Center (NGDC) Coastal Relief Model (http://www.ngdc.noaa.gov/mgg/coastal/coastal.html).

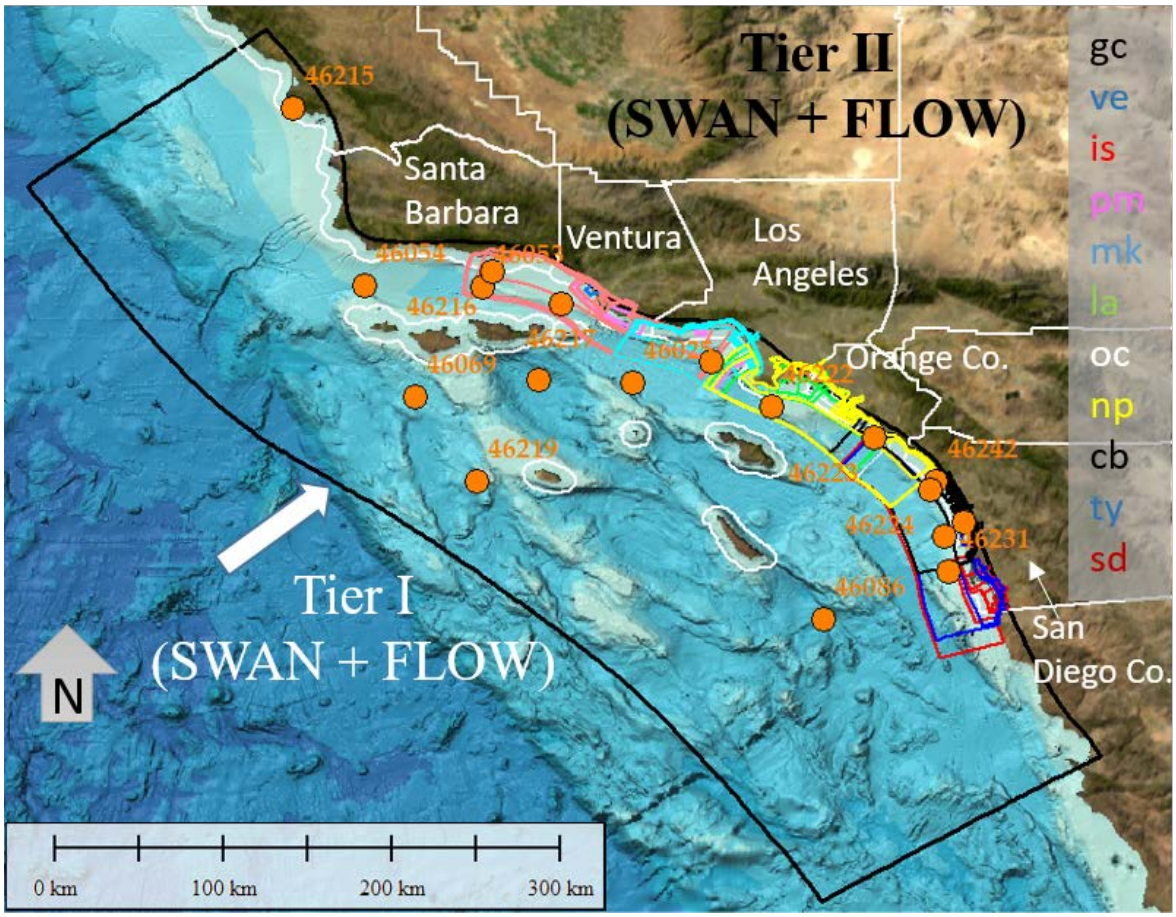

Figure 7. Map showing Tier I (black outer line) and Tier II (nearshore outlines) model grid extents. Wave observation buoys used in model validation are shown with orange circles. Labels on the right are color coordinated to indicate the brief names of each Tier II model domain.

6.1.2 Boundary Forcing

Tidal forcing

Spatially varying astronomic tidal amplitudes and phases derived from the Oregon State University (OSU) TOPEX/Poseidon global tide database (Egbert et al., 1994) were applied along all open boundaries of the Tier I FLOW grid. A total of 13 constituents were represented: M2, S2, N2, K2, K1, O1, P1, Q1, MF, MM, M4, MS4, and MN4.

Sea level anomalies

Sea level anomalies due to large-scale meteorological and oceanographic processes unrelated to storms were applied along all open boundaries of the Tier I FLOW grid. Elevated sea level anomalies (SLAs) are often observed in conjunction with El Niño events (Flick, 1998; Storlazzi and Griggs, 1998; Bromirski et al., 2003) and yield water levels of 10-20 cm (3.9-7.9 inches) above normal for several months (Cayan et al., 2008).

In an effort to maintain simplicity, correlations of measured SLAs with sea surface temperature anomalies (SSTAs) were developed and used in conjunction with GFDL-ESM2M projected SSTs to estimate future variations in SLAs (Appendix A).

Atmospheric forcing

Space- and time-varying wind (split into eastward and northward components) and sea level pressure (SLP) fields were applied to all grid cells at each model time-step. The wind and SLP fields were input as equidistant points spaced 10 km apart and interpolated within the Delft3D model to the SWAN and FLOW grids. An average pressure of 101.3 kiloPascals (14.69 lbs/in^2) was applied to the open boundaries of the meteorological grid.

Winds and SLPs stem from a recently (2015) derived 10 km (6.2 mile) resolution dataset of hourly winds and sea level pressures. The California Reanalysis Downscaling at 10 km (CaRD10) is a reconstruction of the high-spatial resolution / high-temporal scale analysis of atmosphere and land covering the state of California for global change studies (Kanamitsu and Kanamaru, 2007). CaRD10 data is generated by dynamically downscaling coarse atmospheric data using Scripps' Experimental Climate Prediction Center Hydrostatic Global to Regional Spectral Model (G-RSM). The downscaling includes scale-selective bias corrections to suppress large scale errors, yet stays true to the large scale forcing fields and does not use any observations except sea surface temperatures (SSTs) to adjust the results. Two sub-sections of the CaRD10 database were used for CoSMoS application to the Southern California study region: 1) a hindcast period derived from dynamical downscaling of the National Centers for Environmental Prediction (NCEP) Global Forecast System (GFS) model Global Reanalysis (available years 1975 to 2010 at 32 km, 3 hourly resolution), and 2) a future period (2011 – 2100 at 2.5° x 1.5°, 3-hourly resolution) derived from the same RCP4.5 GFDL-ESM2M GCM used in the global-scale wave downscaling.

Deep water wave forcing

Deep water wave parameters (H_s, T_p, and D_p) obtained with the WWIII model for the CDIP067 buoy were applied along all open boundaries of the Tier I SWAN grid. Alongshore variations in deep water wave forcing available with the WWIII model outputs were small, particularly with respect to incident wave directions which are critical to accurate computations of wave propagation from deep water to the SCB nearshore region where sheltering effects are important (Rogers et al. 2007), and thus non-varying wave boundary forcings were applied to the Tier I model.

6.2 Local Scale 2D Wave and Hydrodynamic Model – Tier II

6.2.1 Grids, Model Settings, Bathymetry, and Topography

Eleven local scale sub-models, each consisting of two SWAN grids and multiple FLOW grids, are included in Tier II (Fig. 7). San Diego and Los Angeles Counties each include three sub-models, Orange and Ventura Counties include two sub-models, and Santa Barbara includes one sub-model. Physical overlap exists between sub-models along-shore extents in order to avoid erroneous boundary effects in regions of interest.

Each Tier II hydrodynamic FLOW sub-model consists of one 'outer' grid and multiple two-way coupled 'domain decomposition' (DD) structured grids. DD allows for local grid refinement where higher resolution (~10-50 m (32.8-164.0 ft)) is needed to adequately simulate the physical processes and resolve detailed flow dynamics and overland flood extents. Communication between the grids takes place along internal boundaries where higher resolution grids are refined by 3 or 5 times that of the connected grid. This DD technique allows for two-way communication between the grids and for simultaneous simulation of multiple domains

(parallel computing), reducing total computation time while maintaining high resolution computations.

In the landward direction, Tier II DD FLOW grids extend to the 10 m topographic contour; exceptions exist where channels (e.g., the Los Angeles River) or other low-lying regions reach far inland. The number of DD FLOW grids ranges from 4 to 13, depending on local geography, bathymetry, and overall setting. Grid resolution ranges from approximately 130 m x 145 m (across and along-shore, respectively) in the offshore region to as fine as 5 x 15 m (16.4 x 49.2 ft) in the nearshore and overland regions.

Wave computations are done with the SWAN model using two grids for each Tier II sub-model: one larger grid covering the same area as the 'outer' FLOW grid and a second finer resolution two-way coupled nearshore nested grid. The nearshore SWAN grids extend from at least the 30 m isobath to well inland of the present day shoreline. The landward extension is included to allow for wave computations of the higher SLR scenarios.

All model settings of the Tier II domains are identical to those used for Tier I runs with the exception of the time-step (10 seconds) and threshold depth (1 cm) in the hydrodynamic FLOW models. The threshold depth is used within the model to assign a grid cell as either wet or dry. For the flooding and drying scheme, the bottom is assumed to be represented as a staircase of tiles centered around the grid cell water level points. If the total water level drops below 1 cm, then the grid cell is set to dry. The grid cell is again set to wet when the water level rises and the total water depth is greater than the threshold.

Model grid bathymetry and topography were generated using the 2 m (6.6 ft) resolution DEM (USGS Coastal National Elevation Database, CoNED) in the near and onshore regions, and the 1/3 arc-second NOAA coastal relief model (http://www.ngdc.noaa.gov/dem/squareCellGrid/map) seaward of the 3 nautical mile (~5.6 km; 3.5 mile) limit. The 2 m CoNED DEM was constructed from the most recent available bare-earth topographic and bathymetric lidar and multi- and single-beam sonars. The DEM was constructed to define the shape of nearshore, beach, and cliff surfaces as accurately as possible, utilizing dozens of bathymetric and topographic data sets. The vast majority of the data was derived from the Coastal California Data Merge Project which includes lidar data collected from 2009 through 2011 and multi-beam bathymetry collected between 1996 and 2011, extending out to the three nautical mile limit of California's state waters (NOAA, 2016; https://catalog.data.gov/dataset/2013-noaa-coastal-california-topobathy-merge-project). Harbors and some void areas in the nearshore were filled in with bathymetry from either more recent multi-beam surveys, 1/3 arc-second NOAA coastal relief model data, or single-beam bathymetry. Following compilation of the topography and bathymetry data, the DEM was 'hydro-enforced' to provide water flow connectivity between open sluices, canals, and under bridges and piers.

6.2.1 Boundary Forcing

Water level and Neumann time-series, extracted from Tier I simulations, were applied to the shore parallel and lateral open boundaries of each Tier II 'sub-model outer' grid, respectively. Several of the sub-models proved to be unstable with lateral Neumann boundaries; for those cases one or both of the lateral boundaries were converted to water level time-series or left unassigned. The open boundary time-series were extracted from completed Tier I simulations so that there is no communication from Tier II to Tier I (i.e., one-way communication).

The water level time-series extracted from Tier I and applied at the open boundaries of the 'nested' sub-models included variations due to tides, SLAs, and storm surge, the latter of which is computed with spatial and time-varying winds and SLPs across the continental shelf. In order to account for further contributions of winds and SLPs to storm surge related wind set-up at the shore and local inverse barometer effects (IBE, rise or depression of water levels in response to atmospheric pressure gradients), the same 10 km (6.2 mile) hourly resolution winds used in Tier I are also applied to each grid cell in the Tier II sub-models.

6.2.2 Fluvial Discharge Model

At the time of this study, there were no available time-series of 21st century discharge rates associated with the RCP 4.5 scenario, and therefore a set of relations based on historical observations were established to estimate future discharges associated with future coastal storms. The approach does not assume that a 100-year fluvial discharge event coincides with a 100-year coastal storm event, but instead employs atmospheric patterns common to both events with the aim to obtain more realistic joint occurrences.

A set of gauged and ungauged rivers considered most relevant in influencing coastal flooding were selected and included in the Tier II sub-models. A total of 41 rivers (Fig. 8) were identified and separated into two groups: 1) gauged rivers for which we were able to identify a relationship between peak flows and an independent atmospheric variable available as part of GCM model outputs, and 2) subordinate river for which relations with assigned primary rivers were used to estimate future flows. Seven gauged rivers for which an identifiable relationship between peak flows and sea level pressure gradients were attainable were identified as 'primary / parent representations' (Table 3). As many as 15 sub-ordinate rivers were assigned to each of these primary rivers, using USGS-defined hydrologic units, local water district maps, and previous studies that have evaluated similar relationships (Warrick and Farnsworth, 2009).

Table 3. Primary and sub-ordinate rivers within the Southern California study area.

Primary rivers	Sub-ordinate river
Atascedero	Jalama, Gaviota, Refugio, El Capitan, Devereux, Goleta
Mission Creek	Arroyo Burro, Mission, Carpinteria, Rincon
Ventura	Santa Clara
Calleguas	Malibu
Santa Margarita	San Juan, San Mateo, San Onofre, Los Flores, San Luis Rey, Buena Vista, Agua Hedionda, Batiquitos, San Elijo, Del Mar, Pensaquitos, San Diego, Sweetwater, Otay, Tijuana
Rio Hondo	Ballona, Dominguez, Bolsa Chica, Newport Bay
Santa Ana	Los Angeles, San Gabriel

Future peak discharge rates of the primary rivers were estimated by developing observation-based least-squares linear regression equations relating peak discharges to sea level pressure gradients (SLPs) and then using future SLPs from the GFDL-ESM2M RCP4.5 GCM as the predictor in the derived linear equations. Variants of SLPs were tested against observed peak discharge rates, defined as the 99.95th percentile flow rate from at least 14-year records (60-year mean record length), measured at the seven primary USGS gauging sites. Reasonably strong linear relationships ($0.50 \leq r \leq 0.99$, $0.001 \leq p - value \leq 0.076$) were found between maximum SLP gradients (ΔSLP) and peak discharge. ΔSLP were computed with the CaRD10 reanalysis over 1, 3, and 5 days prior to peak discharge and within 0.667°, 1°, and 5° radii of the gauging station. All combinations were tested; best fits were obtained with the 3-day window and 0.67° search radius for all but two (Santa Ana and Santa Margarita) gauging sites for which a 1° radius was best. The greater search radius of the Santa Ana and Santa Margarita Rivers is consistent with the larger watershed areas (~>3 times) associated with each of these rivers compared to the other 5 watersheds.

An idealized dimensionless hydrograph was developed from data of 9 gauging stations within the study area. These stations had data available at 15 minute or better sampling resolution and at least 3 events exceeded the 99.95th percentile during the record period. Events that exceeded the 99.95th percentile were selected, normalized by the peak flow, and fit with a lognormal distribution. Lognormal distributions are often used to develop unit hydrographs as they have been shown to predict peak flows and time to peak well (e.g., Ghorbani et al., 2007). The mean of the mean and mean variance of all 9 fitted distributions were used to define the idealized hydrograph. The hydrograph is skewed toward rapid initial increases in flow and subsequent slower rates of decreasing discharge rates. The total duration is on the order of 0.7 days (17 hours) for flows that exceed 10% of the peak discharge.

The time-varying discharges were added to the Delft3D Tier 2 model domains (for example, fig. 8B,C) as point discharges coincide with USGS gauging stations. For the few cases where gauge locations were outside model boundaries, discharge points were placed in the furthest upland

position, upstream of tidal influence. For each storm event, the lowest SLP (characterizing storm passage and maximum surge) within the entire Southern California model domain were synchronized with peak tide water levels. Winds fields and resultant waves, from the same downscaled GCM data as SLPs, were thus dictated by the timing of the SLP low; this storm-pressure forcing relationship was also assumed for fluvial discharge parametrization.

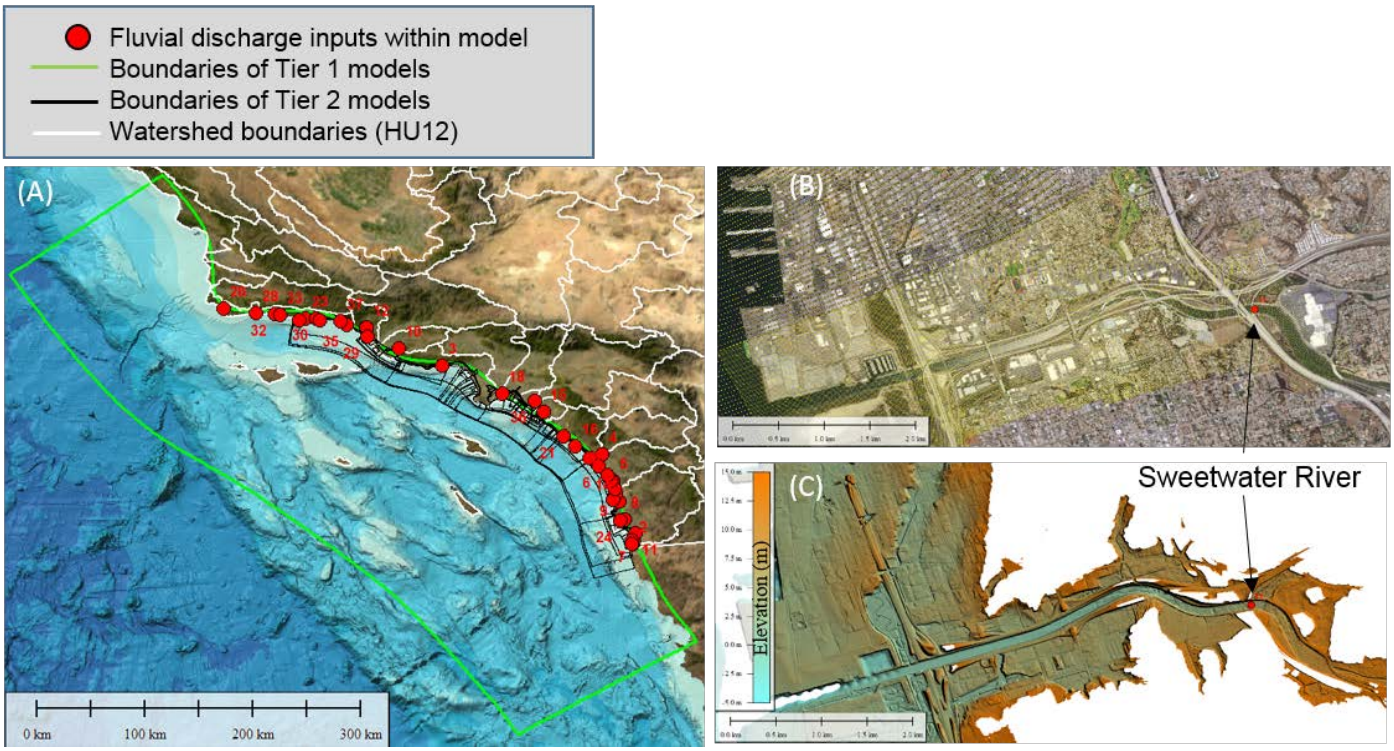

Figure 8. Overview of fluvial input locations to the Tier II model domains. (A) Map showing all input discharge locations. (B-C) map view of a Tier II grid, input location, and digital elevation model of the San Diego region. (see Erikson et al. 2017 for a full list of rivers included in the simulations).

6.3 Local Scale 1D Wave and Hydrodynamic Model – Tier III

6.3.1 Grids, Model Settings, Bathymetry, and Topography

Nearshore hydrodynamics, wave set-up, total wave run-up and event-based erosion were simulated with the XBeach (eXtreme Beach) version 1.21.3667 (2014) model (Roelvink et al., 2009, 2010). XBeach is a morphodynamic storm impact model specifically designed to simulate beach and dune erosion, overwash, and flooding of sandy coasts. XBeach was run in a profile mode, at 4,466 cross-shore transects numbered consecutively from 1 at the U.S.-Mexico border to 4,802 north of Point Conception. Profiles across harbor mouths, inlets, etc. were excluded from the XBeach simulations. Each of the profiles extend from the approximate -15 m (-49.2 ft) isobath to at least 10 m (32.8) above NAVD88 but are truncated in cases where a lagoon or other waterway exists on the landward end of the profile. Cross-shore profiles obtained from the

DEM (see previous section) were resampled using an algorithm that evaluates long wave resolution at the offshore boundary, depth to grid size ratio, and grid size smoothness constraints to obtain optimum grid resolution while reducing computation times. Final profile grid resolutions are between 25 m and 35 m in the offshore and 5 m in shallow nearshore and land regions. Further details on settings are provided in Erikson et al. (2017A).

6.3.2 Boundary Forcing

Time-series of water levels (hourly) and waves (20-minute intervals) extracted from completed Tier II runs were applied at the seaward ends (-15 m isobaths) of each of the profile models. Water level variations represented the cumulative effect of astronomic tides, storm surge (including IBE and wind set-up), SLAs, and SLR. Neumann boundaries set to zero were used along the lateral boundaries: a condition that has been shown to work well with quasi-stationary situations where the coast can be assumed to be uniform alongshore outside the model domain (Roelvink et al., 2009, 2010).

6.3.3 Long- and Short-term Morphodynamic Change

Incorporating long-term morphodynamic change into the flood modeling in CoSMoS was done by evolving the original (0 m SLR) cross-shore profiles to their future positions (Erikson et al., 2017) as predicted by the long-term recession of the cliff top and the mean-high-water (MHW) contour, derived from the cliff and shoreline models, respectively (section 5; Vitousek et al., 2017; Limber et al., in review). The selected long-term management scenario assumed that beach nourishment would cease but that existing cliff armoring and flood/beach protection infrastructure remains in place (i.e., the "hold-the-line" scenario). The resulting 'evolved' profiles were then used to simulate inundation and run-up with the Tier III XBeach model. No adjustments were made to the depth and topography representations in the Tier II Delft3D high resolution grids that were used to simulate inland flooding (Section 6.3).

Morphodynamic change due to individual storms is computed with the XBeach model for each particular scenario (SLR combined with a coastal storm). The event-based erosion extent simulated by XBeach is dependent on the hydrodynamics across the entire active and wetted profile, bordered on the landward side by the run-up extent. Sediment transport is computed in XBeach with the Soulsby-van Rijn (Soulsby, 1997) transport formula and bore averaged equilibrium sediment concentrations. A median grain diameter of 0.25 mm and sediment thickness of 2 m was assumed for all profile models. Bottom roughness is set to a uniform Chezy value of 65, horizontal background viscosity of 0.01 m^2/s, and a flooding and drying threshold depth of 1 cm, similar to Tier II. Initial profile sections of steepness in excess of 32° (angle of repose of natural sand) are assumed to be hard structures or cliffs and set to be immobile (not allowed to erode or accrete during the storm). All simulations are run with a morphological acceleration factor of 10 to speed up the morphological time scale relative to the hydrodynamic time scale and thus reduce computation time.

6.4 Testing and Validation

The model setup and simulation scheme was tested by comparing model outputs to observed water level variations due to astronomic tides and non-tidal residuals (storm surge and other anomalous water levels), wave heights, wave run-up, and short-term morphologic change.

The root-mean-square-difference (*rmsd*) and *bias* were calculated,

$$rmsd = \left[\frac{\sum_{i=1}^{N}(obs_i - mdl_i)^2}{N}\right]^{1/2}$$

$$bias = \frac{1}{N}\sum_{i=1}^{N}(mdl_i - obs_i)$$

where *obs* is the observation data, *mdl* is the model data, *i* is the individual time point data, and *N* is the total number of time-points analyzed. The *rmsd* represents the standard deviation of the residuals (difference between the observed and modeled values). The *bias* describes the model's overall offset from observations.

6.4.1 Water Levels

The models' ability to replicate tidal variations was tested over a month long time period (October to November 2010) to capture full variations in spring and neap cycles. Modeled tidal variations are compared to NOAA predicted tides at the 4 tide stations within the SCB: La Jolla (station ID: 941030), Los Angeles (station ID: 9410660), Santa Monica (station ID: 9410840), and Santa Barbara (station ID: 9411340) (see fig. 4 for locations). Comparisons between time-series of the modeled and predicted tides are very good at all 4 stations, being less than 6 cm (2.4 inches) for both the rmsd and bias (Fig. 9).

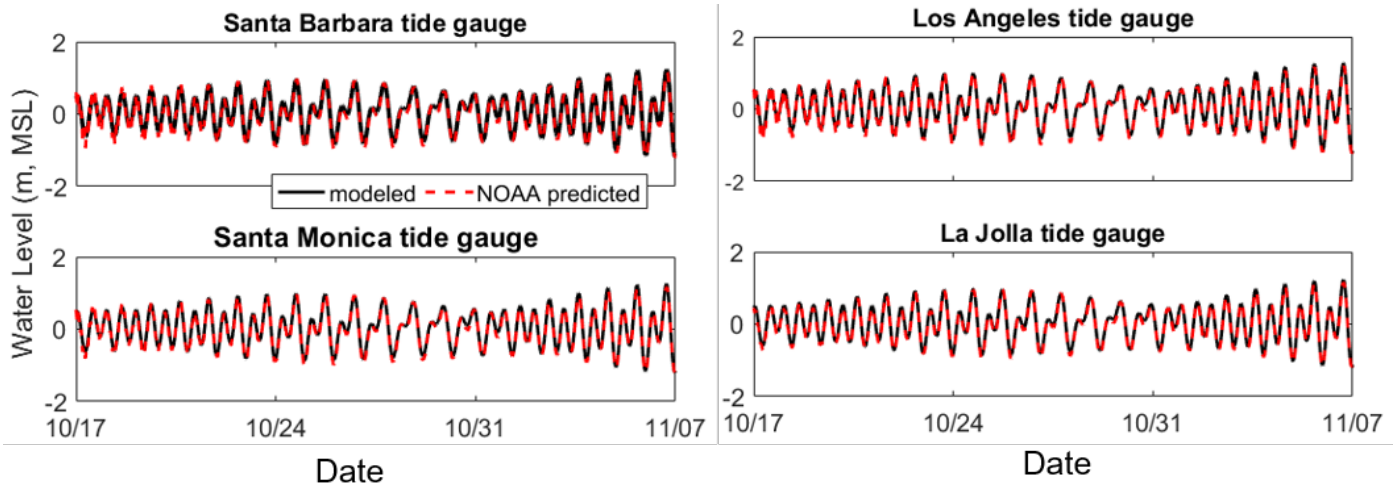

Figure 9. Comparison of modeled and NOAA-predicted tides at the Santa Barbara, Santa Monica, Los Angeles, and La Jolla tide gauges for a month long simulation in 2010.

The accuracy of modeled water levels associated with storms was investigated for the January 2010 storm. The storms were selected as test cases because offshore wave measurements, wind, and sea level pressure reanalysis data (CaRD10) were available to provide model forcing. Observation time-series at stations located within the bounds of the grids were readily available. The January 2010 storm produced water levels approaching 40 cm (15.7 inches) above

normal at Southern California tide gauges (Fig. 10). Root-mean-square differences ranged from 7-9 cm (2.8-3.5 inches) for the northern gauges of Santa Barbara, Santa Monica, and Los Angeles, with a bit more at the La Jolla gauge at 16cm (fig. 10). The model under-predicted water levels at the Santa Barbara, Santa Monica, and Los Angeles gauges by 4-5 cm (1.6-2.0 inches; bias) and over-predicted the water levels at the La Jolla gauge (bias=12 cm (4.7 inches)), indicating satisfactory model performance.

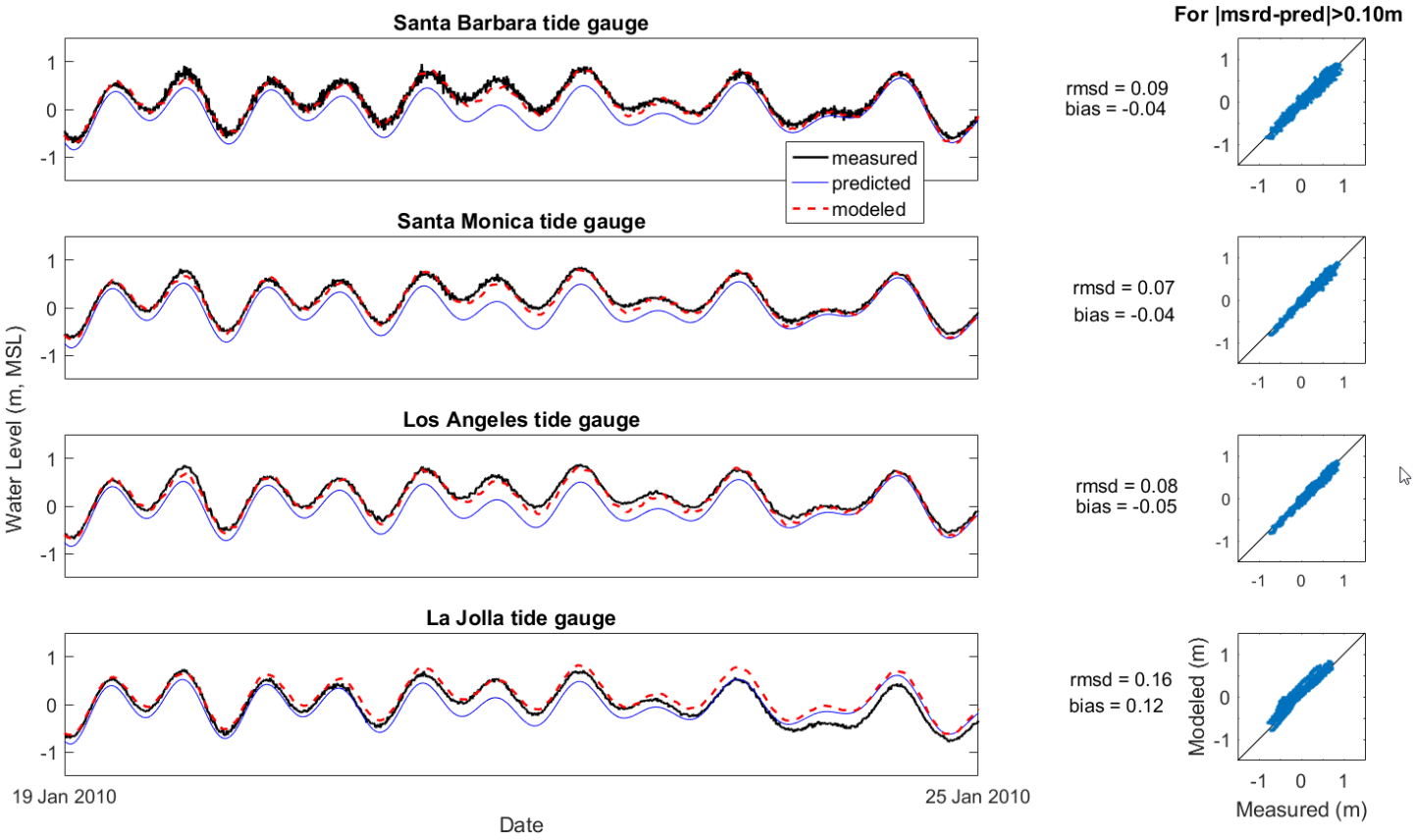

Figure 10. Comparison of modeled and measured water levels at the Santa Barbara, Santa Monica, Los Angeles, and La Jolla tide gauges during the January 2010 storm. Time-series plots show the predicted tide levels (blue), measured water levels including tides and non-tidal residuals (black), and modeled water levels (dashed red line). Right-hand plots compare modeled and measured total water levels using data points for which the non-tidal residuals are greater than 10 cm.

6.4.3 Waves

Wave model accuracy was tested against the January 2010 storm by comparing hindcast wave heights, periods, and directions to observed values at 18 buoys within the Southern California Bight (see fig. 7 for buoy locations and Table 4 and fig. 11 for observation-model comparisons). In addition to *rms* values, non-dimensional Wilmott skill scores are used to aid in quantifying model skill of wave simulations (Willmott, 1981). Skill scores range from 0 to 1, with 1 being perfect agreement between the model and observations. As a general guide, a skill score between 0.8-1 is considered great, a score between 0.6-0.8 is considered good, and a score of 0.3-0.6 is fair. These are highlighted as green, yellow, and gray in Table 4, respectively, where computed model skill and the collocation of the finest grid corresponding to each buoy location are listed.

The model's ability to simulate wave heights is generally good (yellow text in Table 4) to great (green text in Table 4), and in conjunction with the *rms* values, shows that model performance increases with the finer TierII grids (e.g., gc, is, mk, ty). Root-mean-square values range from 19-51 cm (7.5–20.1 inches) for the Tier II grids and from 28-67 cm (11.5-26.4 inches) for the Tier I

grids. Peak wave directions are quite good with *rms* values less than 3 degrees. Peak wave periods are modeled with good to fair skill (0.48<skill<0.69). The lower skill compared to wave height skill scores is likely a reflection of the 'jumpy' nature of peak wave periods in multimodal regions such as these (e.g., Hegermiller et al., 2017A, B). Skill scores of mean wave period are likely to show better performance, but are not listed here as it is the peak periods that are used for boundary conditions to Tier II XBeach models.

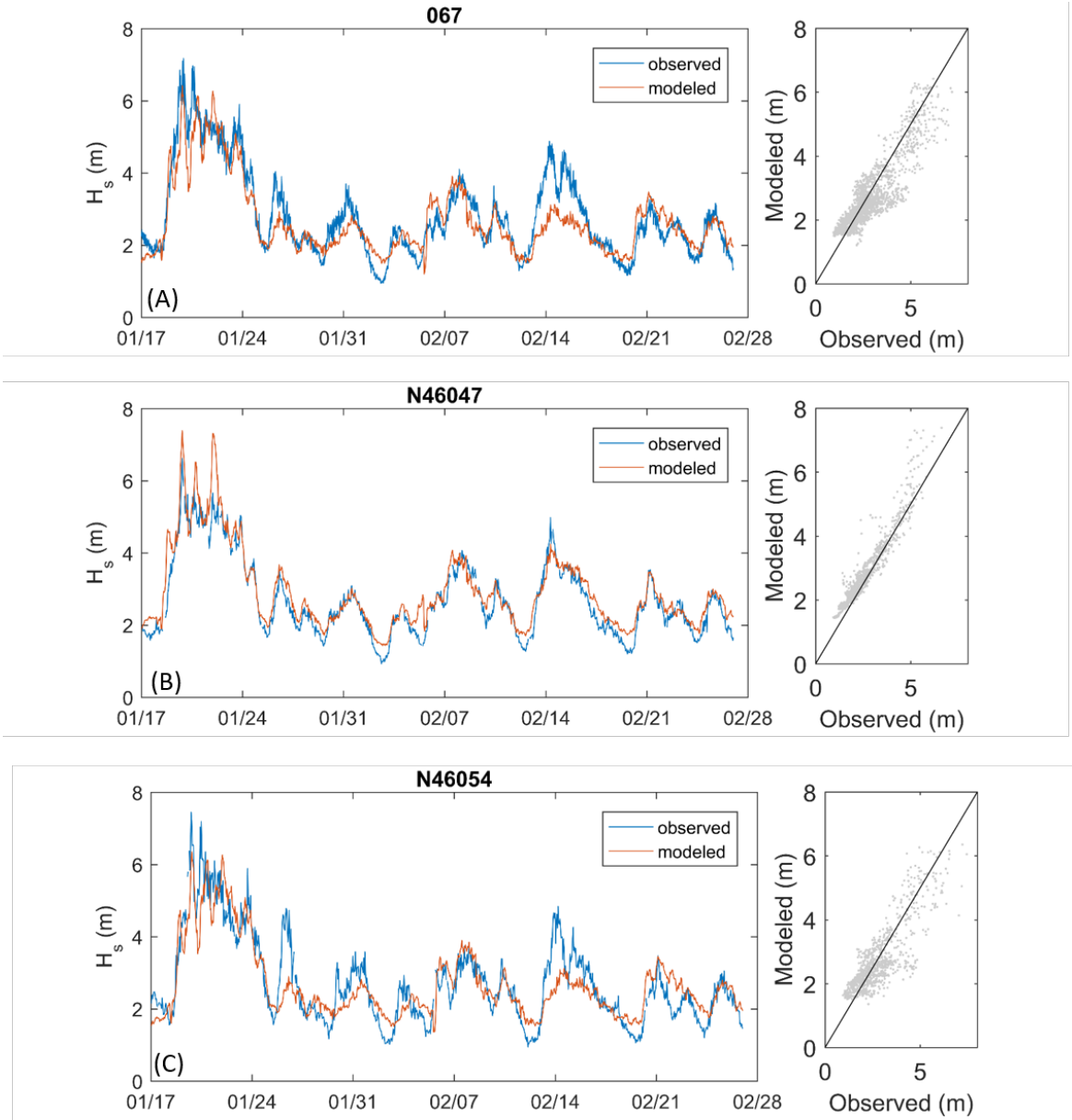

Figure 11. Comparison of measured and modeled wave heights at 3 buoy locations within the Southern California Bight.

Table 4. Comparison of modeled and measured waves for the January 2010 storm. Skill scores >0.80 are considered to be great and are shown in green; skill scores between 0.6 and 0.8 are considered good and are shown in red.

NDBC ID	CDIP ID	Latitude (degrees N)	Longitude (degrees W)	Grid	Significant wave height		Peak wave period		Peak wave direction	
					rms, meters (inches)	skill	*rms*, seconds	skill	*rms*, degrees	count
46086	-	32.49083	118.03472	tierI	0.37	0.92	2.02	0.62	-	982
46069	-	33.67444	120.21167	tierI	0.60	0.96	2.57	0.66	-	93
46054	-	34.26472	120.47694	tierI	0.62	0.91	1.81	0.61	-	981
46053	-	34.25250	119.85333	gc, is	0.25	0.75	1.88	0.63	-	978
46025	-	33.74944	119.05278	tierI	0.28	0.76	2.19	0.55	-	983
46221	28	33.85500	118.63400	mk	0.25	0.83	2.36	0.53	1.7	1,966
46242	43	33.21980	117.43940	cb, ty	0.19	0.55	3.08	0.51	1.2	1,614
46224	45	33.17778	117.47215	cb, ty	0.27	0.74	2.66	0.48	1.5	1,944
46219	67	33.22480	119.88180	tierI	0.67	0.79	1.82	0.69	2.2	1,964
46215	76	35.20382	120.85931	tierI	0.50	0.89	2.25	0.60	2.0	1,968
46222	92	33.61791	118.31701	mk	0.27	0.88	2.09	0.58	2.3	1,963
46231	93	32.74700	117.37000	sd	0.31	0.90	2.20	0.55	2.4	1,968
46223	96	33.45800	117.76700	cb	0.25	0.79	2.30	0.52	1.9	1,947
46225	100	32.93342	117.39083	cb	0.27	0.84	2.37	0.54	1.9	1,968
46216	107	34.33300	119.80300	gc, is	0.29	0.88	1.79	0.54	2.0	1,968
46217	111	34.16692	119.43465	gc, is	0.22	0.69	2.26	0.50	2.3	1,941
46241	161	33.00300	117.29200	cb, ty	0.25	0.71	2.27	0.56	1.9	1,968
46238	167	33.76000	119.55000	tierI	0.51	0.89	1.78	0.62	2.3	1,967

Wave run-up was evaluated by running XBeach for a time period of available run-up measurements at Ocean Beach just south of the Golden Gate near San Francisco in central California. Run-up measurements were obtained during 3-hr daylight intervals in May 2006 when offshore waves ranged between 1-2 m (3.3-6.6 ft) and peak wave periods up to 14s (at NDBC buoy 46026) using a camera system (Barnard et al., 2007). The foreshore beach slope was mild with an average slope of 0.03. Computed *rms* values between the observed and modeled run-up height for four separate 3-hr time periods ranged from 10-16 cm (3.9-6.3 inches).

6.5 Identification of Storms for Detailed Flood Hazard Modeling

The model system, which aims to account for the most relevant atmospheric and oceanic processes that might contribute to future flooding and associated coastal hazards as well as the inter-related non-linear physics of each of these, requires downscaling from the global to local level and is computationally expensive. Because of the long simulation times, it is not feasible to run all Tiers for the entire 21st century time period. Instead, future storms are identified *a priori* and then these storms are run with Tiers I through III.

The storm selection process employs the same total water levels that are used as forcing for the cliff recession and shoreline change models (Section 5.4). Total water levels are derived from the super-position of wave run-up (calculated with the Stockdon et al. (2006) formulation and an average foreshore slope of 0.03), empirical storm surge, and sea level anomalies time-series. Variations in water levels due to astronomic tides and SLR are not included as they are independent of atmospheric conditions and thus should not, on a first-order basis, affect identification of storm events. It is recognized, however, that nearshore wave heights and $R_{2\%}$ are affected by tidal stage and currents, and that the phase of tides and storm surge can have an amplification effect on non-tidal residuals (Horsburgh and Wilson, 2007). These are assumed to be small relative to the TWL and thus are excluded in the identification of storm events, but are accounted for in the numerical CoSMoS model runs which simulate individual storm events during a typical spring tide.

In keeping with the approach of identifying coastal storms with specific recurrence intervals (Section 4), the 1-year, 20-year, and 100-year future coastal storm events were identified at each nearshore location (4,802 sites) and clustered with a *k*-means algorithm to delineate coastal segments where individual storms result in similar return period water levels (Erikson et al., in review). Clustering of extreme events showed that the more severe but rare coastal flood events (e.g., the 100-year event) occur for most of the region from the same storm. In contrast, different storms from varying directions were responsible for the less severe but more frequent local coastal flood events (Fig. 13). To this end, two 100-year storms (February 2044 and March 2059), two 20-year storms (February 2025 and February 2095), and three 1-year storms (March 2020, December 2056, and January 2097) were identified. Upon completion of 1-year storm simulations using the entire train of models (resolving detailed flow dynamics and wave-current interaction) for a range of SLRs, results showed a single 1-year storm (March 2020) consistently yielding the highest water levels throughout the SCB; thus, 1-year projections use contributions from that storm only. Deep water waves, SLAs, maximum and minimum wind speeds, and sea level pressures (SLPs) within the entire model domain are summarized for each of the identified storm events in Table 5. Deep water wave conditions (H_s, T_p, and D_p) listed in Table 5 are applied at all open boundaries of the Tier I wave grid. Sea level anomalies are applied uniformly to all model domains. SLPs and wind speeds vary in time and space. The

wind and SLPs vary throughout the domain; the values listed in Table 4 are the minimum and maximum values, respectively, attained somewhere within the SCB domain.

Table 5. Boundary conditions associated with each modeled scenario.

Scenario	H_s, meters (ft)	T_p, seconds	D_p, degrees	SLA, meters (inches)	Minimum SLP (kPa)	Maximum wind speed, meters/second (miles/hour)
Background	1.75 (5.7)	12	286	0	NA	NA
1-year storm #1	4.39 (14.4)	16	284	0.16 (6.3)	100.56	22.8 (51.0)
20-year storm#1	5.86 (19.2)	18	281	0.18 (7.1)	100.79	22.3 (49.9)
20-year storm#2	6.13 (20.1)	18	292	0.24 (9.4)	100.41	28.7 (64.2)
100-year storm#1	6.20 (20.3)	16	264	0.19 (7.5)	100.43	26.6 (59.5)
100-year storm#2	6.80 (22.4)	18	287	0.23 (9.1)	98.67	30.3 (67.8)

NA: not applicable

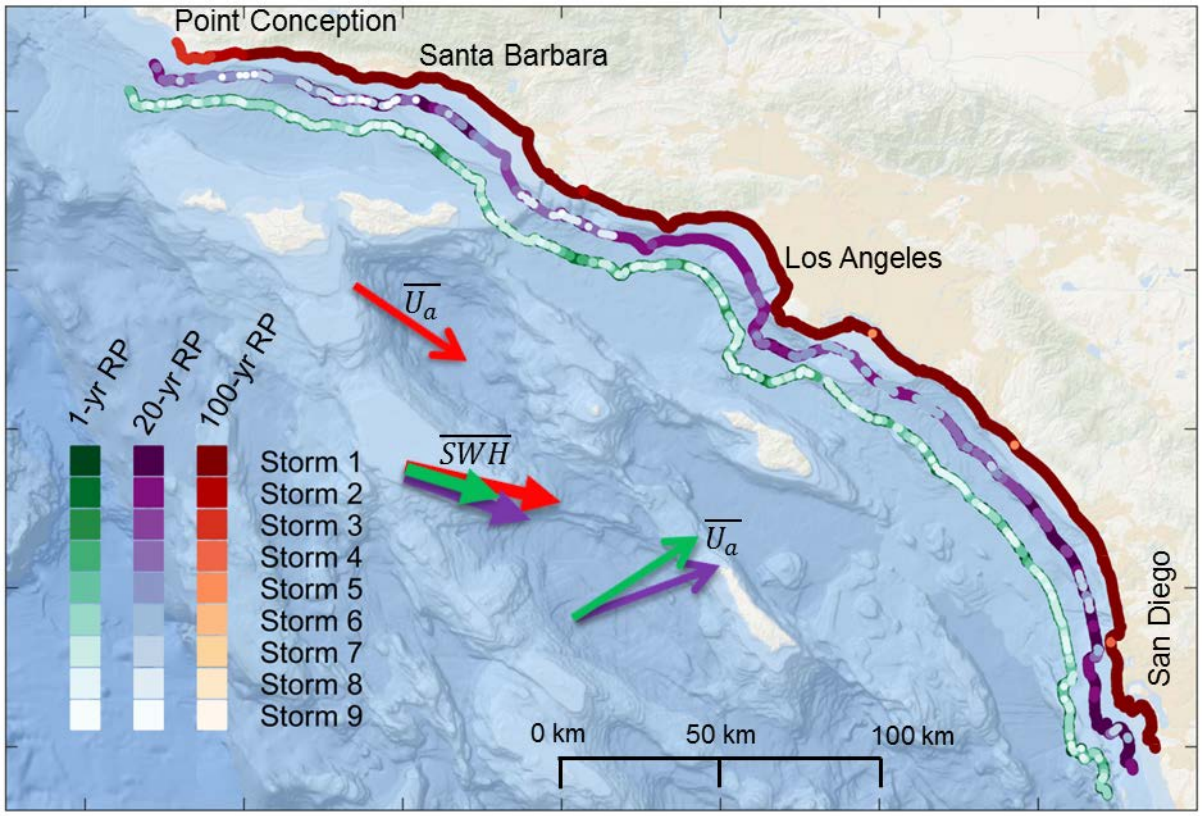

Figure 12. Map showing coastal regions that respond similarly to region-wide storms as determined through *k*-means clustering of nearshore total water level proxies. Large colored arrows show the weighted mean (Table 5) offshore wave heights and winds for the 1-yr, 20-yr and 100-yr return period coastal storms.

6.6 Determination of Flood Extents and Uncertainties

Flood extents were determined in two ways: 1) from the landward-most wet grid cell in the high resolution Delft3D grids in embayments, and 2) from maximum sustained water levels calculated with XBeach cross-shore models along the open coast. The sustained water levels (constant water levels of durations longer than 1 minute; see Erikson et al., 2017 for further explanations) are intended to capture the wave set-up at the shore which is the increase in mean water level above the still water line due to the transfer of momentum by breaking waves. Maximum run-up, computed with the Tier III XBeach model, are also output as part of the CoSMoS results, but are mapped as single points and are not included in the flood footprint. Mapped outputs are done in this way to distinguish between shorter duration wave run-up which, depending on the beach slope, may only constitute a couple of centimeters of intermittent standing water. Except where overtopping occurs or at a narrow beach that fronts a near vertical cliff or wall, sustained water levels and flood extents are seaward of the maximum run-up.

Melding of flood extents simulated with the XBeach and Delft3D high resolution models was done by interpolating (linear Delaunay Triangulation) resulting water level elevations onto a common 2 m resolution square mesh (within the Mathworks Matlab environment). In some

areas, such as Mission Beach in San Diego County, where both XBeach and high resolution grids exist to capture flooding from either or both the landward or seaward side, XBeach results were given precedence.

This post-processing step was done for all storms simulated as part of a given scenario. For the 20-year storm for example, two individual storm events were modeled in order to ensure that local effects such as shoreline orientation with respect to incident storm direction were taken into account. For those cases where more than one storm was modeled, all resulting 2 m gridded flood maps were overlain and maximum water levels were saved at each grid cell to generate a single, composite flood map for a given scenario.

Resulting water elevation surfaces were differenced from the high resolution DEM to isolate areas where the water level exceeds topographic elevations, indicating flooding. Though the DEM is of rather fine resolution at 2 meters, it does not capture narrow coastal structures like seawalls and levees. To remedy this, levees or 'thin dams' were manually digitized onto the model grid from available GIS layers. Efforts were made to include all known structures; in cases where it is later discovered that a levee or flood protection structure was not fully represented, either by its existence or wrong elevation, the information is added to the OCOF tool under 'known issues'.

For scenarios that include SLR, 2 m DEMs that incorporate long-term morphodynamic changes were used. These DEMs were constructed by replacing original DEM data within the active beach zone with results of the long-term morphodynamic models. The active beach zone was populated with data from the evolved >4,000 cross-shore transects and additionally with data from sub-profiles spaced ~10 m apart in between the primary cross-shore transects. Shoreline and cliff profile changes of the primary cross-shore transects were projected onto 2 m cross-shore resolution sub-profiles; all cross-shore transect and sub-cross-shore transect data (Easting, Northing, elevation (ΔZ)) were then spatially interpolated within the active beach zone of the original DEM to portray total morphological change.

The resulting flood maps were then processed to exclude isolated wetted areas not hydraulically connected to the ocean; these disconnected areas were flagged as low-lying vulnerable areas below the flood elevation.

Maps of associated maximum flood durations, velocities, and wave heights were processed in a similar manner to that of the flood depths and extents in that they were gridded onto a common 2 m mesh and then combined. Data that fell outside the flood map extents were removed so that the footprints of all maps are identical.

6.6.1 Vertical Land Motion

Spatially variable measurements of vertical land motion, based on GPS data and statistical and physical tectonic models, largely attributed to tectonic movement of the San Andreas Fault System from Howell et al. (2016), were also incorporated into the model results. Maximum rates of uplift (0.4 mm/yr (0.016 inches/yr)) and subsidence (0.6 mm/yr (0.024 inches/yr)) within our study area equate to a maximum of 3.4 cm (1.4 inches) of uplift and 5.2 cm of subsidence for the 1m SLR scenario based on the National Research Council (2012) SLR projections for Southern California (2012) of ~1 m of SLR by the year 2100. In the future, these rates could be refined through the use of more spatially-resolved data sources (e.g., InSAR) to complement the GPS data which is fairly sparse along the Southern California coast. But, in general, even the

highest rates of vertical motions that have been recorded in the San Francisco Bay Area (Burgmann et al., 2006) and more locally in the Santa Ynez mountains (Wehmiller et al., 1979) rarely exceed more than 2 and 6 mm/yr, respectively, and therefore are quite small relative to the expected rates of SLR by the middle and end of the 21st century.

6.6.2 Uncertainties, Limitations, and Assumptions

Uncertainties in the numerical model outputs and DEM measurements were added to the VLM estimates to produce spatially varying offsets that were added and subtracted to/from the modeled flood elevations to produce 'potential flood maps'. This was done for each of the 40 scenarios, so that a total of 120 (40*(1+2) = 120) mapped vulnerabilities were generated. Numerical model errors were estimated to be ±50 cm (±19.7 inches). This value is greater than the root-mean-square and absolute errors computed between model results and measurements (Section 6.5) but was used in an effort to mitigate for the fact that the number of storms tested are few and the geographic scope is large compared to where measurements for validation are available. Uncertainties associated with the baseline DEM were set at ±0.18 m (±7.1 inches), equivalent to the 95% confidence level for topographic lidar measurements in open terrain (Dewberry, 2012).

Other limitations and assumptions pertaining to flood extents:

- CoSMoS includes estimates of fluvial discharge, but the storms selected and modeled are based on coastal storm intensities (not riverine flooding per se)
- Hydrographs are idealized and peak fluvial discharges are first-order estimates
- The model scheme assumes that maximum wave heights coincide with high spring tides and peak fluvial discharge occurs shortly after high tide
- Flood depths and extents between cross-shore transects modeled along the open coast with Tier III XBeach are along-shore interpolations and are not exact representations of model outputs
- Culverts or other manmade and natural underground pathways between coastal waters and land are not accounted for in the modeling

7: Data Dissemination and Outreach for Communicating Hazards and Assessing risk

7.1 Our Coast Our Future (OCOF)

Our Coast Our Future (OCOF) is the web application for data visualization, synthesis, and access to all output products from the CoSMoS modeling (www.ourcoastourfuture.org; Fig. 14A). The OCOF web tool provides the full suite of high resolution coastal flooding projections from CoSMoS, allowing a user to compare different SLR and storm scenarios in a Google Maps-style interface. The Southern California expansion also incorporates the cliff retreat and shoreline change projections for the region.

The OCOF project (www.ourcoastourfuture.org), started in 2011 as a collaborative, user-driven project, focused on providing San Francisco Bay Area coastal resource managers and planners

locally-relevant online maps and tools to help understand, visualize, and anticipate vulnerabilities to SLR and storms. OCOF continues to be led by USGS who provides final CoSMoS output products and Point Blue Conservation Science (Point Blue) who developed, maintains, and expands the cyberinfrastructure and content. USGS and Point Blue work in partnership with local, regional, state, and federal partners to provide technical assistance, outreach, and engagement with local stakeholders. The Southern California expansion of CoSMoS was tightly integrated with and leveraged related ongoing efforts across California. This included 4 years of work and outreach in the San Francisco Bay region from the original OCOF project, taking full advantage of the existing cyberinfrastructure and lessons learned from active end-users. In partnership with USC Sea Grant, this project also leveraged stakeholder engagement via three collaborative coastal resilience projects in the San Diego and Los Angeles regions (Section 7.1.3).

7.1.1 Data Processing and Integration for Online Visualization and Download

All CoSMoS data for San Diego, Orange, Los Angeles, Ventura, and part of Santa Barbara County (to Point Conception) were loaded and processed for use in the OCOF web tool. The CoSMoS data included all 40 scenarios (0 to 200 cm sea level rise in 25 cm increments plus 500 cm with storms (none, annual, 20-year, and 100-year)) for flood extent and uncertainty (termed "minimum and maximum flood potential" in the web tool), flood depth, water surface elevation, low lying flood prone areas, wave run-up, wave height, current velocity, and flood duration.

OCOF also incorporates shoreline change projections from the cliff retreat and shoreline change models which included the 10 SLR scenarios (no storms), as well as management options based on assumptions described in detail in Section 8.1.1. The cliff retreat projections included an option for "hold the line" infrastructure management or not (20 total). Finally, the tool incorporates shoreline position data that also covers the 10 sea level rise scenarios (no storms) with both "hold the line" and an additional management option for "beach nourishment", for a total of 40 scenarios.

(A)

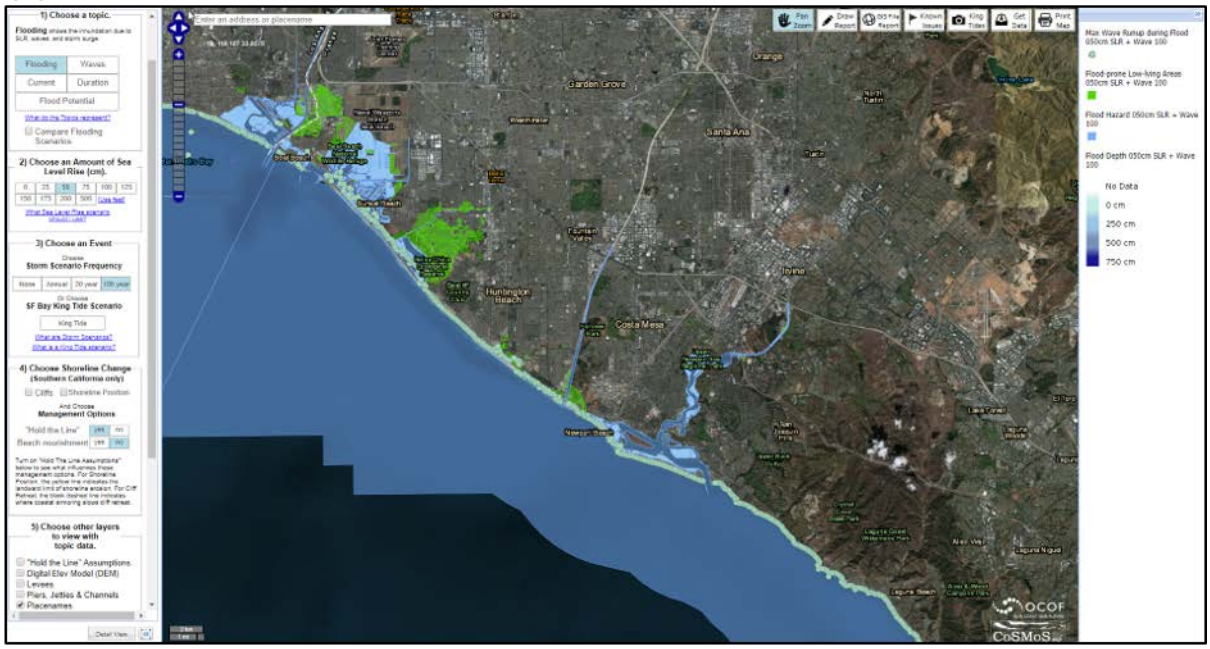

(B)

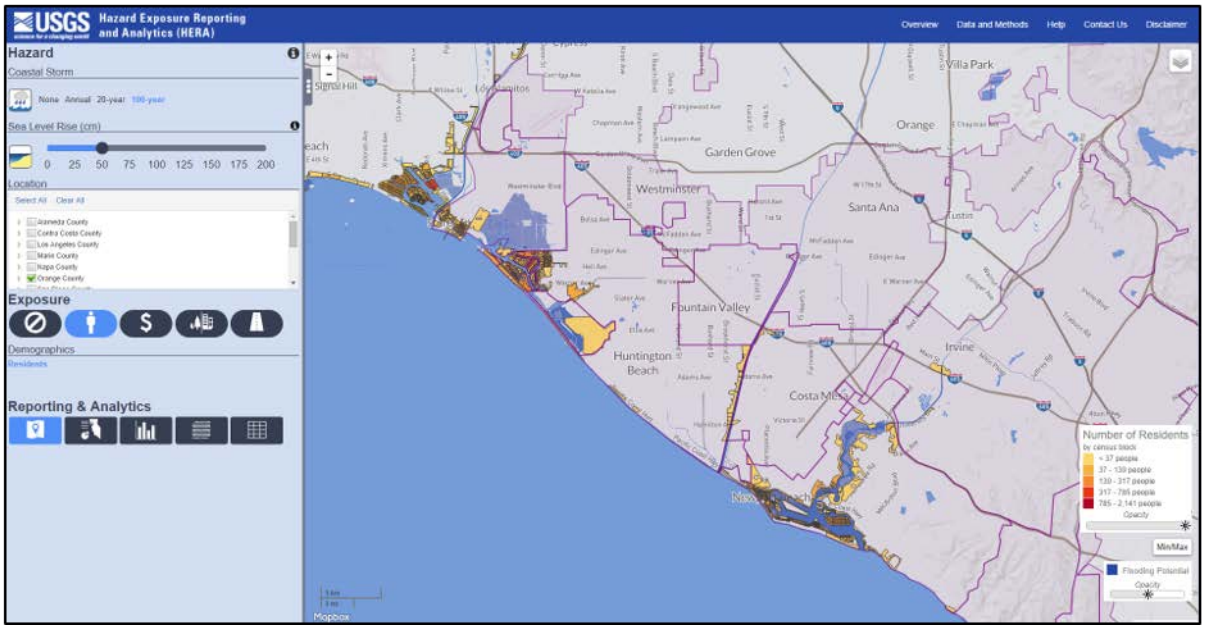

Figure 13. Web applications for data visualization, synthesis, socio-economic analyses, and data download. (A) Hazard maps (www.ourcoastourfuture.org). (B) Hazard exposures and socio-economic data (https://www.usgs.gov/apps/hera/). Both applications contain a suite of tools and options for visualizing and analyzing the model results. Example screen grabs are for the Orange County area.

These data layers, depending on their form, were processed to be compatible with the rest of OCOF data infrastructure, loading into precached raster tiles, PostgreSQL/PostGIS vector and

raster data, GeoTIFFs and ESRI SHP files for download packages, GeoServer web service definitions, and other OCOF custom metadata support forms.

The tool organizes model results into 5 topics to make it easier for OCOF users to work with this data: *Flooding* for showing projected flood extent and depth, *Waves* for wave height, *Current* for current velocity, *Duration* for how long areas are flooded, and *Flood Potential* for the uncertainty of flood extent projections.

Addition of data for the 5 Southern California counties doubled the size of the amount of data now available through OCOF.

In the past, the tool has provided zipped data available for download by request. Previously, those packages were organized in very large files, making it hard for users to work with the CoSMoS data. OCOF has reorganized the CoSMoS data into county packages, organized by scenario and data layer.

7.1.2 Changes to OCOF User Interface

As part of the Southern California expansion, a variety of changes were made to the user interface to support users across two sections of California as well as adding access to the new shoreline change data for Southern California. Because many existing users work in and identify with county jurisdictional boundaries, we added an initial "Where do you want to explore?" navigation pane that allows users to select and quickly navigate to their geography of interest. This also helps illustrate the current geographic extent of CoSMoS data availability. The navigation through the 5 topics (Flooding, Waves, Current, Duration, and Flood Potential) and 40 SLR and storm scenarios is seamless regardless of whether the user is in Northern or Southern California. We added a new section to the navigation panel called "Choose Shoreline Change" and is marked for Southern California only. In this section, you have the ability to turn on Cliffs and Shoreline Position layers as well as the ability to choose "Hold the Line" and Beach Nourishment management options.

We were able to begin a complete user interface redesign for the project to clean up some of the specific issues we've encountered during expansion of the project. Examples of updates include (1) expanding the topics to include shoreline change projections, (2) additional infrastructure to allow users to load and view their own GIS layers, and (3) improvements to on-the-fly summary reports generated for user-defined polygons. We look to funding in future projects to allow us to finish this effort.

7.2 Hazard Exposure Reporting and Analytics (HERA)

Geospatial data summarizing various population, business, land cover, and infrastructure indicators were used to estimate community exposure to a given hazard zone in HERA (Jones et al. 2016; Fig. 14B). Residential populations were estimated using block-level population counts compiled for the 2010 US Census (U.S. Census Bureau 2010). Demographic factors such as age, ethnicity, and tenancy can amplify an individual's sensitivity to hazards (Wood et al. 2012); therefore, the 2010 block-level data was used to estimate demographic attributes related to these socioeconomic indicators of sensitivity.

Business populations and regional trends of exposure were estimated in HERA using employee counts organized by North American Industry Classification System (NAICS) codes (U.S. Census Bureau 2010) at individual businesses using a georeferenced, proprietary employer

database (Infogroup 2012). Business types based on NAICS codes are generalized in this analysis into five classes: (1) government and critical facilities, (2) manufacturing, (3) services, (4) natural resources, and (5) trade.

Land cover indicators include the amount and type of land in hazard zones based on 30-m resolution data extracted from the 2011 National Land Cover Database (NLCD) (Homer et al. 2015). The HERA application currently focuses on land classified in NLCD as either wetlands or developed.

Hazard exposure of critical facilities and infrastructure was estimated in Jones et al. (2016) using the length of rail and road networks (infrastructure) and the number of schools, medical facilities, police stations, and fire stations (facilities). These facilities are considered critical because they provide public safety services or house vulnerable populations. Data sources for critical facilities and infrastructure include a wide array of county and federal sources which are summarized by Jones et al. (2016).

For each variable, geographic information system (GIS) software was used to overlay data representing community boundaries, the community indicator, and a specified hazard zone. Two variables for each asset were estimated at the community level: (1) a total amount (or length, in miles, for road and rail networks) of an asset in a hazard zone and (2) a community percentage. For resident and employee populations in hazard zones, the community percentage reflects the exposed amount compared to the total amount within a community. For the business types, percentages reflect the number of businesses of a certain type divided by the total number of that business type in the community. For the demographic attributes, community percentages reflect the percentage of a specific attribute relative to the total number of residents in the hazard zone, not the community total. Spatial analysis of vector data focused on determining if points (businesses and critical facilities), lines (roads and rails), or polygons (census blocks) were inside hazard zones. If census block polygons overlapped hazard polygons, final population values were adjusted proportionately using the spatial ratio of each sliver within or outside of a hazard zone.

7.3 Stakeholder Engagement and Outreach

7.3.1. “Traditional” Stakeholder Engagement

USGS partnered with USC Sea Grant (through funding from the California State Coastal Conservancy (SCC)), to lead extensive outreach and engagement both in advance of the release of model results and once modeling results were publicly available. We were able to provide technical resources for the Regional AdaptLA project, the Southern California Coastal Impacts Project, the Santa Barbara Coastal Ecosystem Vulnerability Assessment Project, and the Resilient Coastlines Project of Greater San Diego. Workshop attendees typically included planners, engineers, emergency management, and environmental scientists from coastal cities, counties, utilities, state agencies, non-governmental organizations, and the private sector.

Over the course of the Southern California project, we participated in eight workshops over 3 years, reaching all Southern California counties (Table 6). At each workshop, we provided an overview of CoSMoS and shared regional results. In addition, working with local partners active in coastal resilience and community engagement in each region, we helped develop workshops tailored to the specific needs and interests of local stakeholders. For instance, in the San Diego workshop, we included a panel highlighting local projects engaged in sea level rise

planning and a separate session providing a deeper dive into the modeling for more technical end-users. For the Los Angeles workshop, we included a presentation on adaptation strategies led by the Coastal Commission, and a community planning exercise where attendees could view the sea level rise and erosion projections on paper maps for their local community and brainstorm adaptation ideas. At the workshop in Oxnard, attendees also participated in a half-day training developed by Climate Access focused on overcoming challenges in communicating about sea level rise science, modeling, and adaptation. Workshop agendas are provided in Appendix 1. Once model results were available, we gave live, high level training and demonstration of the OCOF web tool, allowing local stakeholders immediate access to the data in their areas. To bolster the information provided at the workshops, and to reach a broader audience, we also held webinars in each county at the initial release of the 100-year flood hazard results and upon release of the final modeling results.

Table 6. Summary of outreach workshops.

Date	Location (County)	Partners	# of attendees
October 30, 2014	San Diego (San Diego)	Tijuana River National Estuarine Research Reserve, San Diego Climate Collaborative, USC Sea Grant, USGS, Point Blue Conservation Science, CA Coastal Commission	46
April 14, 2015	Carpinteria (Santa Barbara)	City of Carpinteria, USC Sea Grant, CA Sea Grant, State of California Coastal Conservancy, USGS, County of Ventura, County of Santa Barbara	67
October 21, 2015	Santa Monica (Los Angeles)	USC Sea Grant, USGS, Point Blue Conservation Science, City of Santa Monica, California Coastal Commission, State of California Coastal Conservancy, California Ocean Protection Council, Santa Monica Bay Restoration Commission, Los Angeles Regional Collaborative	65
November 18, 2015	San Diego (San Diego)	Tijuana River National Estuarine Research Reserve, San Diego Climate Collaborative, Climate Science Alliance, USC Sea Grant, USGS, Point Blue Conservation Science	60
February 23, 2015	Irvine (Orange County)	UC Irvine Sustainability Initiative, USC Sea Grant, State of California Coastal Conservancy, Southern California Coastal Water Research Project	58

November 17, 2016	San Diego (San Diego)	Tijuana River National Estuarine Research Reserve, San Diego Climate Collaborative, Climate Science Alliance, USC Sea Grant, USGS, Point Blue Conservation Science	98
February 22, 2017	Marina Del Rey (Los Angeles)	USC Sea Grant, USGS, Point Blue Conservation Science, Coastal Conservancy, Coastal Commission, Ocean Protection Council, City of Santa Monica, ESA, TerraCosta	48
June 27, 2017	Oxnard (Santa Barbara/ Ventura)	USC Sea Grant, USGS, Point Blue Conservation Science, Climate Access, California Coastal Conservancy, Ventura County, Santa Barbara County, City of Santa Barbara	65

This extensive engagement and outreach allowed us to work closely with local partners in the counties of Santa Barbara, Ventura, Los Angeles, Orange, and San Diego (Table 6) to ensure that outreach of model information was provided at the appropriate scale, was linked to ongoing local efforts, and reached as broad an audience as possible. The relationship with regional partners and local stakeholders helped us continue to build and develop effective products and tools for the critical end-user. Moreover, this partnership proved essential for a smooth release of all the final CoSMoS information and increased the visibility and use of CoSMoS by coastal stakeholders. To date, between the efforts in the San Francisco Bay and outer coast and Southern California, CoSMoS has been utilized by at least a dozen coastal cities, including the 4 largest cities (San Francisco, Los Angeles, San Diego, and San Jose) and 11 coastal counties, representing a total of 20 U.S. Congressional Districts. It is also utilized by many of the state agencies such as the California Department of Emergency Services and the California Department of Transportation. Further, CoSMoS methods and results have been vetted and presented at over 100 agency meetings and 20 professional conferences.

7.3.2 Innovative Engagement and Communication Efforts

In addition to the more traditional outreach and engagement strategies described above, USGS has also been experimenting with the use of virtual reality and 360 degree 3-D videos as another method for communicating the CoSMoS model results.

In partnership with the City of Santa Monica, USC Sea Grant, and Owlized, and building on prior work in the Bay Area led by Climate Access and Susanne Moser Research and Consulting, CoSMoS information was utilized to create virtual reality simulations of SLR off of the Santa Monica pier (mobileowl.co/samo). Viewers are stepped through a series of images that show the beach under the pier:

1) Today, also highlighting where the beach was originally positioned in the 1920s (Figure 15A)

2) The beach today with a 100-year storm (as projected by CoSMoS)

3) The beach in the future with 2 m of SLR (Figure 15B)

4) The beach with 2m of SLR and the 100-year coastal storm

5) One possible adaptation option (Figure 15C)

As viewers moved through these images, they were asked a series of questions that gauged their level of concern as the hazards increased, as well as demographic questions. Results from the survey helped inform the City of Santa Monica's local coastal planning process.

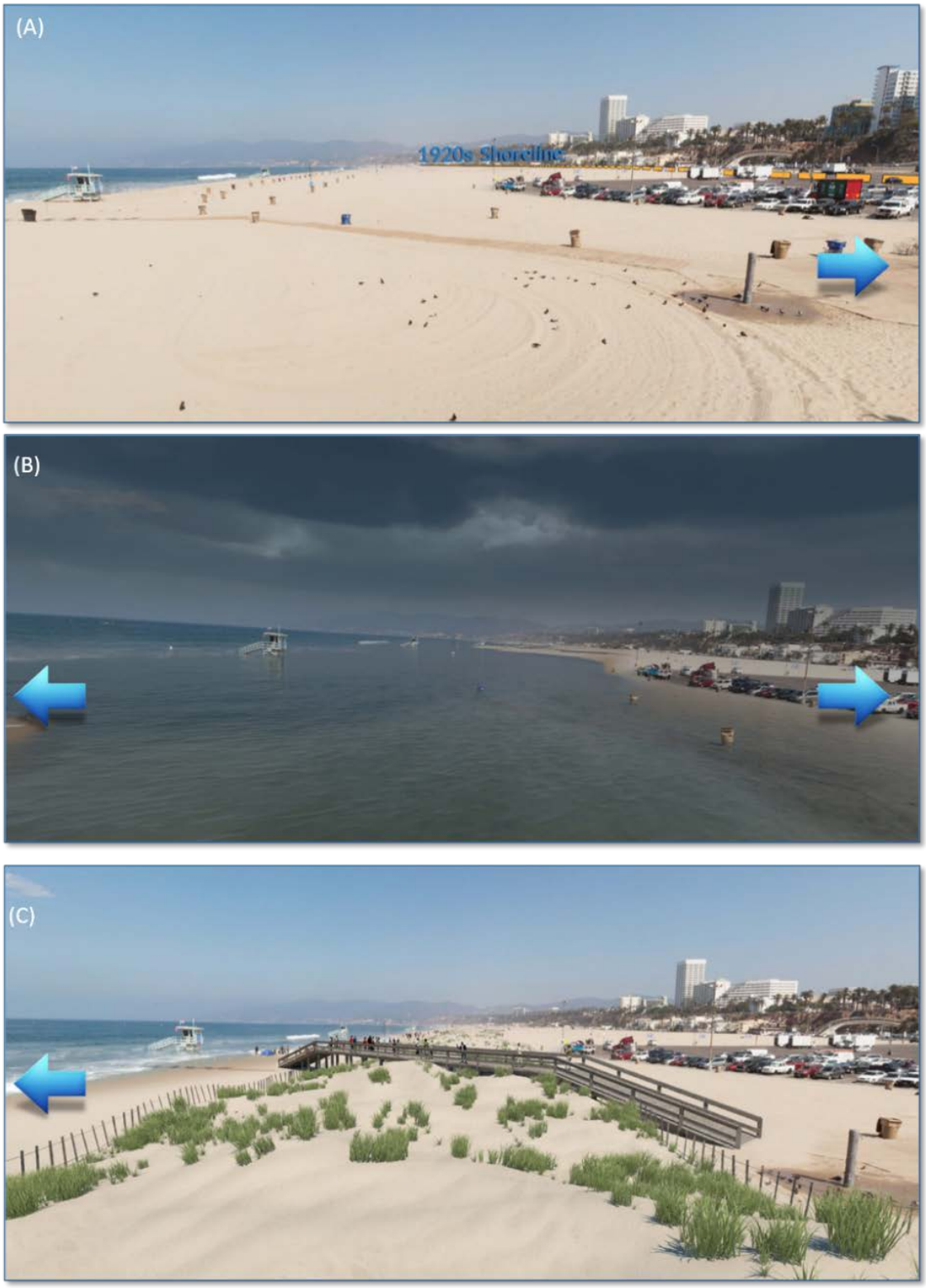

Figure 14. Virtual reality simulations of sea level rise off the Santa Monica Pier. (A) Present day conditions and including the 1920s shoreline. (B) Potential future shoreline position with a 2 m (6.6 ft) sea level rise. (C) Possible adaptation option.

We are also documenting King Tides in Los Angeles and Orange Counties by filming high resolution, live action 3-D 360 degree videos of "normal" high tides and King Tides (fig.16). We are able to use these videos to provide a glimpse of the future along the coast and to connect those with our CoSMoS projections.

Both products have been viewed by coastal stakeholders at a variety of settings. These include *in situ* on the Santa Monica pier and via the mobile app, at community meetings focused on sea level rise and coastal storm impacts, and by teachers and students in partnership with USC Sea Grant's education efforts.

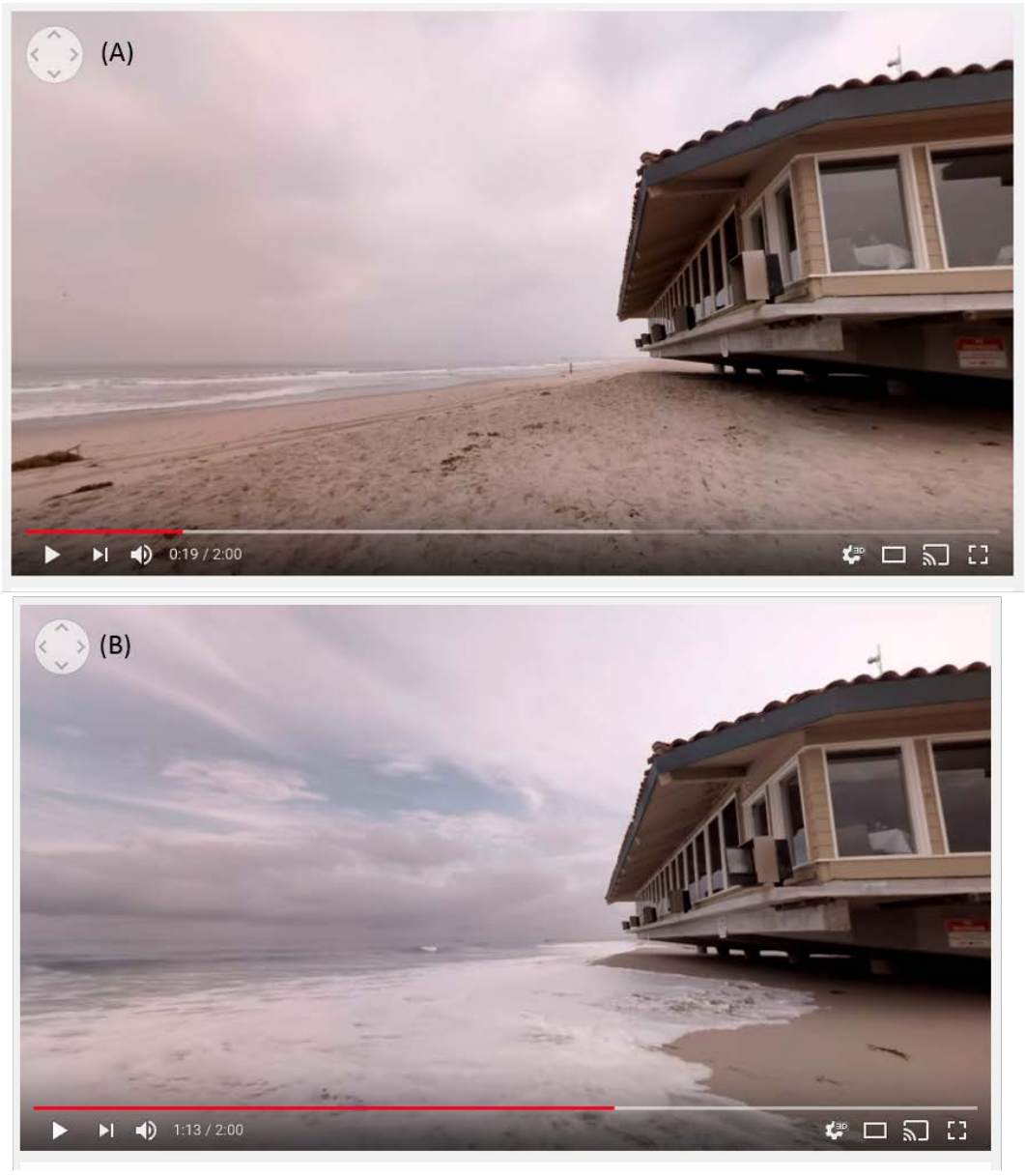

Figure 15. Moving views of normal (A) and (B) King Tide conditions. Images are from the King Tides Initiative Project.

8: Projected Hazards

8.1 Shoreline Change

SLR represents a threat to the very existence of many beaches, especially in urban environments like Southern California where landward migration is inhibited by infrastructure. Beaches are getting squeezed between a rising ocean and the landward hardscape, effectively being drowned by SLR. Therefore, it is critical to consider how the natural processes of shoreline change and cliff-retreat are influenced by different management practices in an urban setting. In this study, several different management scenarios involving beach nourishment and the existence and maintenance of hard structures to limit erosion were simulated with both the cliff recession and sandy shoreline change models. Two management scenarios were investigated for the cliff recession projections: (1) cliff recession unlimited by cliff armoring, and (2) no cliff recession where armoring currently exists (2016).

For the sandy shoreline projections, four management scenarios were simulated representing combinations of "hold-the-line" and "continued nourishment". The "hold the line" scenario represents the management decision to prevent or allow the shoreline from receding past existing infrastructure (e.g., by permitting or prohibiting shoreline armoring, respectively). If the line is held, then the modeled shoreline is constrained from eroding past a 180,000-point polyline manually digitized from Google Earth imagery that represents the division of beach and urban infrastructure or the division of the subaerial beach and coastal cliff. The "continued nourishment" scenario represents the management decision to continue or cease the long term, business-as-usual, anthropogenic beach nourishment rates computed from data spanning years 1995 through 2010. To investigate the various combinations of these management practices, all 4 combinations were simulated with the sandy coast CoSMoS-COAST model: (1) hold-the-line and no continued nourishment; (2) hold-the-line and continued nourishment, (3) no hold-the-line and no continued nourishment, and (4) no hold-the-line and continued nourishment.

8.1.1 Cliff Retreat

Applied over >2,100 transects, the ensemble cliff erosion model indicates an average bluff-top recession distance of 5 m and 30 m (16-100 ft) for the 25 cm and 200 cm SLR scenarios respectively, by 2100, and with the coastline armored as present (fig. 17), but with grater uncertainty for the higher SLRs and much variability along the coast (e.g., as much as 55 m and 230 m at individual locations for the 25 cm and 200 cm SLRs, respectively) (Barnard et al., 2018; Limber et al., 2015, 2018). Results indicate that, relative to mean historical rates, future retreat rates could increase nearly two- fold for the higher SLR scenarios.

Viewed on a county basis, Ventura and Los Angeles counties are projected to experience greater increases in cliff recession rates compared to the other counties (~165% increase for the 200 cm SLR scenario). Ranked lowest of the 5 counties is Orange County where cliff recession rates are estimated to increase by ~115% for the 200 cm SLR, compared to historical rates (Limber et al., 2018).

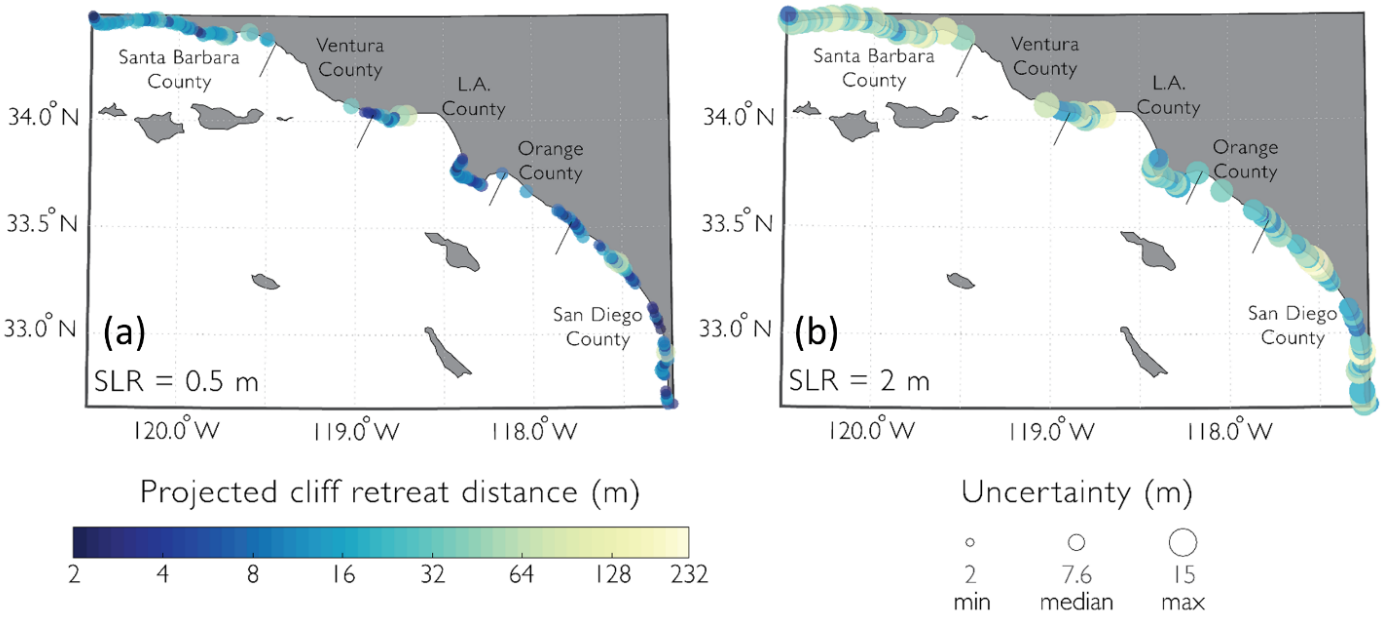

Figure 16. Map of all model results for the 50 cm and 200 cm SLR scenarios. The colors represent cliff retreat distance, and the size of the marker represents the amount of uncertainty. See Limber et al. (2018) for further details.

8.1.2 Beach Loss

The projected average beach loss ranges from ~10 to 70 m (~33-230 ft) for the 25 cm and 200 cm SLRs, depending on the management scenario. Including the additional effect of seasonal erosion[1] (driven by larger-than-average wave conditions) increases the range of average beach loss by 2100 to 110 m (360 ft) (fig. 17). This amount of beach recession may result in 30 to 67% of Southern California beaches being completely eroded up to coastal infrastructure or cliffs by 2100 (Vitousek et al., 2017).

The results also indicate that there is little overall difference between the nourished and unnourished management scenarios (i.e., scenarios 1 and 2); on average, continued nourishment scenarios only reduce the extent of erosion by ~2 to 3 m compared to the unnourished scenarios (see lighter colored sections of the bar graph in fig. 17). However, the effects are very localized and, for individual beaches receiving large nourishments, significant differences between the shoreline responses are seen in the model results. On a grander region scale however, the small differences among the management scenarios suggest that the current rate of beach nourishment is insufficient to deal with shoreline recession due to accelerated SLR. A factor lacking in this assessment, however, is the potential contribution of sediment to the total budget

[1] Average beach loss shorelines are based on a Jan 1 (mid-winter) time horizon, whereas the max seasonal erosion is based on the upper limit of the 95% confidence interval (2 std dev) using all the model-projected positions.

from cliff erosion. For example, taking an average cliff height of ~25 m and cliff erosion resulting from 200 cm of SLR (previous section), the total cliff volume loss would be up to ~300 million m^3 by 2100, which is the same order of magnitude as the projected volume of sandy beach loss reported in Erikson et al. (2017) using results from the CoSMoS-COAST model. Thus, it is possible, particularly if cliffs were left unarmored and allowed to recede, that the volume lost from coastal cliffs could mitigate some of the beach loss by supplying sediment to Southern California's littoral cells.

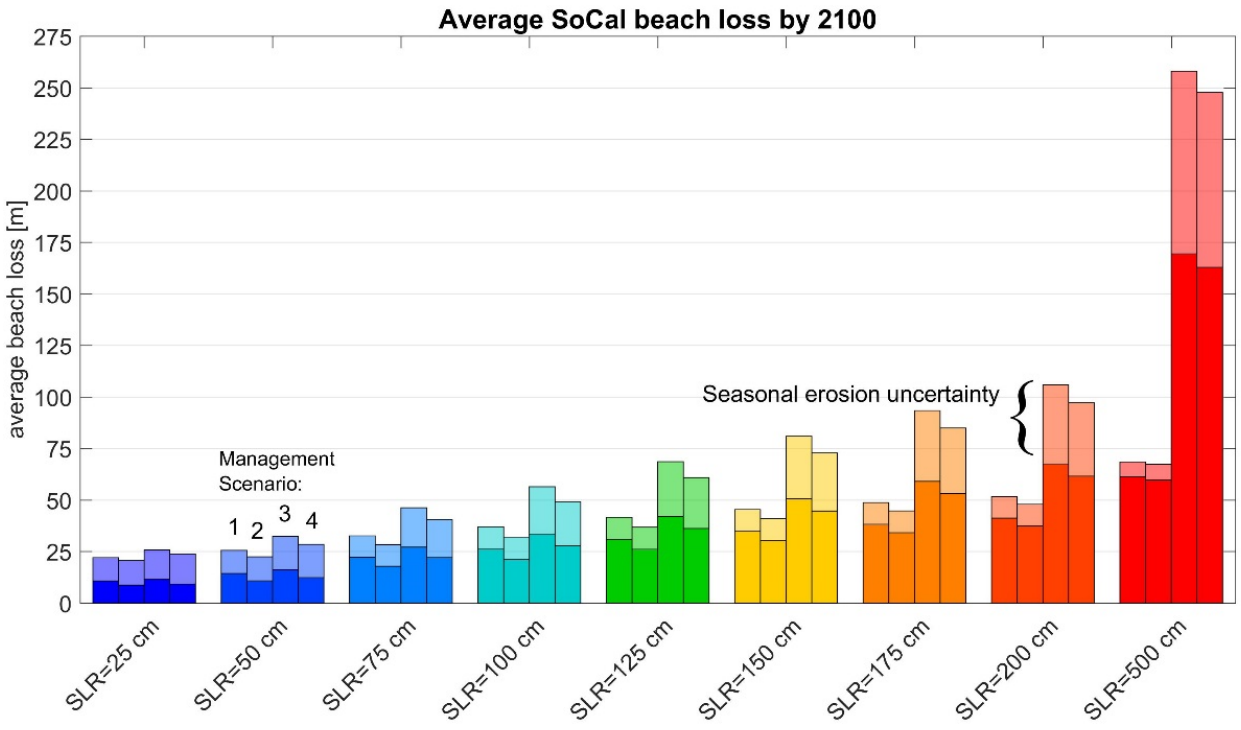

Figure 17. Average sandy coast beach loss in Southern California as simulated with the CoSMoS-COAST model under different SLR and management scenarios (Vitousek et al., 2017). The management scenarios are (1) hold-the-line and no nourishment, (2) hold-the-line and continued nourishment, (3) no hold-the-line and no continued nourishment, and (4) no hold-the-line and continued nourishment. The color scheme used for each SLR scenario is the same as in Figure 5.

8.2 Flood Hazards

8.2.1 Projected Peak Fluvial Discharge Rates

Projected peak fluvial flow rates (section 6.3.2) associated with the annual, 20-year, and 100-year coastal storms range from 2-1,300 m^3/s (70-46·10^3 ft^3/s) and average 570 m^3/s (20·10^3 ft^3/s). Projected discharge rates are listed in Table 7 for sites collocated with gauged streams and expressed as percent of observed maxima. For example, discharge rates at Santa Ana River (92-year record: February 1923 through December 2014) reached a maximum of 575 m^3/s (20.3·10^3 ft/s) in March of 1938. Peak flows are projected to reach 180 m^3/s (6.4·10^3 ft^3/s), 860 m^3/s (30.4·10^3 ft^3/s) and 960 m^3/s (33.9·10^3 ft^3/s) for the 1-year, 20-year, and 100-year projected coastal storm events at this site and thus correspond to ~30%, 150% and 165% of the observed historical maximum.

Table 7. Peak flow rates corresponding to Southern California CoSMoS projected coastal storm events, expressed in terms of percent of historically measured maxima.

USGS gauging station ID	Station name	Measured maximum (m^3/s) (ft^3/s)	Length of record (years)	Flow rates as % of observed maximum for shown coastal storm event		
				1-year	20-year	100-year
11119750	Mission Ck.	39 (1,377)	43.7	84	79	173
11105510	Malibu Ck.	255 (9,005)	4.9	114	83	152
11092450	Los Angeles R.	555 (19,600)	83.3	16	76	84
11078000	Santa Ana R.	575 (20,305)	92.0	32	149	166
11046000	Santa Marg. R.	623 (22,001)	91.9	69	87	64
11023000	San Diego R.	267 (9,429)	33.3	49	104	68

Overall, projected discharges range from ~30% (Santa Ana River, 1-year coastal storm event) to 170% (Mission Creek, 100-year coastal storm event) of measured maxima (Table 8). The projected peak discharge rates are mostly lower than historically observed maxima, but exceed historical maxima in 6 of the 18 cases listed in Table 8. Several studies with particular focus on droughts and precipitation indicate that snow pack levels will decrease, rainfall will either remain the same or decrease, and fluvial discharges will decrease in California as global temperatures rise (e.g., Cayan et al. 2008; Flint and Flint, 2014). While these recent studies tend toward projected decreases in flow rates and snow pack, other studies indicate more intense precipitation events (e.g., Naz et al., 2017; Trenberth, 1999) and increasing air temperatures that could potentially cause greater peak discharge rates on daily to hourly time-scales as simulated in this work.

Coastal zone flood extents that might be exasperated when riverine discharge is conjoined with coastally derived flooding as simulated in this study, has not yet been quantified and analyzed in detail. Such analyses, in comparison to not including the co-occurrence of the two events, are planned for the near future. At this time, cursory and qualitative evaluations suggest that the co-occurrence of elevated coastal and fluvial events are limited to river mouths with catchments of relatively greater relief in close proximity to the coast, and that flooding is exasperated in the lower reaches where fluvial plumes meet ocean-derived water levels.

8.2.2 Flood Extents

Lacking any storms or excessive riverine discharge, a SLR of only 25 cm is expected to affect all 5 counties and permanently flood ~10 km^2 throughout Southern California. Santa Barbara and Ventura counties are the least prone where slightly more than 1 km^2 (0.5 $miles^2$) of coast is expected to be underwater. San Diego is the most vulnerable at this near-term SLR with an expected ~4 km^2 of permanently inundated land. For higher SLRs, up to 100 cm, and the 500 cm SLR, Orange County is the most affected with permanent inundation of 10 to 95 km^2 (4 to 35 $miles^2$). Ventura, Los Angeles, and San Diego Counties are similarly exposed while Santa Barbara County, due largely to the high cliffs and bluffs that front the coastline, is less vulnerable with a maximum flooded area of ~20 km^2 (<10 $miles^2$) (Table 6, fig. 18). Considering the recent projections of plausible SLR by 2100 (~2.9 m, Cayan et al., 2017), permanently flooded

areas are expected to range from ~10 km² (<5 miles²; Santa Barbara) to 60 km² (~25 miles²; Ventura County), using a simple linear interpolation between the modeled 200 cm and 500 cm SLRs.

In the absence of any SLR, the 100-year coastal storm is estimated to flood 6.5 km² (2.5 miles²), 15 km² (6 miles²), 3.5 km² (1.5 miles²), 3.5 km² (1.5 miles²), and 10.0 km² (4 miles²) in Santa Barbara, Ventura, Los Angeles, Orange, and San Diego Counties, respectively. For the low-end SLR of 25 cm, flooding increases >10-fold (from >1 km² to 15.5 km² (0.5-6.0 miles²)) when the 100-year coastal storm in Ventura County is included (Table 7). While substantially lower in a relative perspective, the areas flooded increase by 3 to 7 times for the other counties when the 100-year storm is added to the 25 cm SLR (compare Tables 6 and 7).

Table 6: Area (km²) flooded due to sea level rise alone

	Sea level rise (cm)								
County	**25**	**50**	**75**	**100**	**125**	**150**	**175**	**200**	**500**
Santa Barbara	1.1	1.4	3.2	6.0	6.4	7.0	8.2	8.8	19.6
Ventura	1.2	2.3	3.7	6.5	19.1	23.0	37.0	49.4	91.3
Los Angeles	2.6	4.6	7.6	9.5	12.6	15.2	19.2	15.2	85.0
Orange	1.4	4.0	6.2	10.2	14.8	21.9	25.6	37.5	95.5
San Diego	3.7	5.0	7.5	9.6	14.9	20.1	29.9	35.8	88.9

Table 7: Area (km²) flooded due to sea level rise and the 100-year projected coastal storm

	Sea level rise (cm)								
County	**25**	**50**	**75**	**100**	**125**	**150**	**175**	**200**	**500**
Santa Barbara	7.0	7.4	7.8	8.6	9.3	10.1	13.1	15.9	21.0
Ventura	15.6	17.5	20.4	27.2	41.5	45.8	51.0	62.4	96.1
Los Angeles	6.8	10.4	13.2	16.3	19.2	23.1	28.6	39.0	97.7
Orange	4.8	9.8	12.9	21.1	26.2	30.7	54.0	58.8	105.1
San Diego	10.5	13.2	17.8	22.8	30.4	35.7	44.3	50.1	94.7

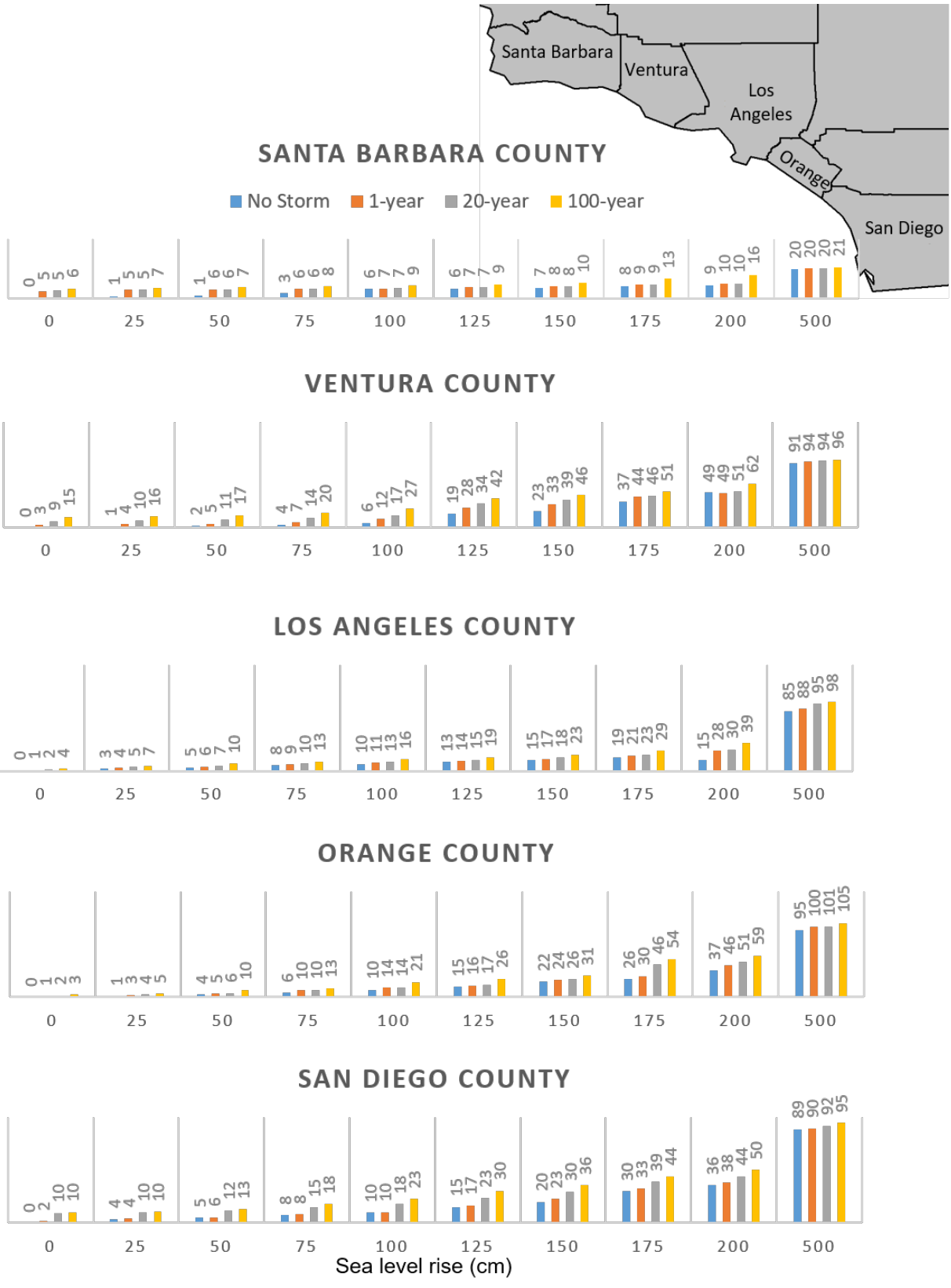

Figure 18. Areas (km^2) flooded due to sea level rise alone and in combination with 1-year, 20-year, and 100-year projected coastal storms, grouped by county.

9: Projected Exposures

Integration of modeled shoreline retreat and flood hazards with geospatial demographic and socio-economic data shows that ~20,000-164,000 residents, 160-1,500 km (100-930 miles) of road, up to 22 km^2 (8.5 $miles^2$) of agricultural land, and up to 35 km^2 (13.5 $miles^2$) of wetlands (assuming no accretion) are at risk of being permanently flooded in Southern California with a 25 cm to 200 cm SLR. Building replacement values are estimated to be between $3.5 billion and $26 billion (present-value, unadjusted for inflation). Including the 100-year coastal storm increases resident exposures by 50-110% (31,000-256,000), length of road by ~50-115%, and building replacement values by 40-90%.

Discretizing the analyses into the county and community level allows for identification of location specific exposures that might be addressed in local and regional management and adaptation strategies. Here, we summarize county-level exposure statistics of a select set of elements at risk (number of residents, length of road, building replacement costs, grazing and cropland, and wetlands) and highlight the most vulnerable communities within each county. Additional elements at risk and a vast amount of community-level assessments and data are analyzed and available for download on the HERA website.

9.1 Residents

Residents within Los Angeles, Orange, and San Diego counties are at greater risk to coastal flooding compared to the other two counties (Ventura and Santa Barbara) within coastal Southern California. Overall, 80% to 90% of residents that are at risk of being flooded for any combination of SLR and coastal storm in Southern California reside within Los Angeles, Orange, or San Diego counties (fig. 19A). For the lowest modeled 25 cm SLR and no coastal storm, more than 18,000 residents are at risk of being permanently flooded in these three counties: ~5,200 in Los Angeles (more than half of whom reside in Long Beach); 6,000 in Orange (primarily in Newport Beach); and ~7,200 in San Diego (primarily within the City of San Diego). Fewer than 1,500 residents are at risk in Santa Barbara and Ventura combined for the same 25 cm SLR, no coastal storm scenario.

Including the 100-year storm in combination with the 25 cm SLR increases resident exposures by ~175% (from ~5,200 to 14,300 residents), 60% (from 6,000 to 9,600 residents), and 55% (from 7,200 to 11,200 residents) for Los Angeles, Orange, and San Diego Counties, respectively, compared to the 25 cm SLR with no storm. The communities most affected within each county are Long Beach, Newport Beach, and San Diego City, similar to the 25cm SLR scenario with no storm. These exposure levels represent between 0.5% (City of San Diego) to 8% (Newport Beach) of the total population within each community. It is worth noting that, in the absence of any SLR, the number of residents at risk of flooding due to the 100-year storm is greater than the exposure risk of the 25 cm of SLR scenario without any storms.

At the higher level of a 200 cm SLR and 100-year coastal storm (bottom right pie chart in fig. 19A), resident exposures increase by more than 500% compared to the 25 cm SLR with no storm. 50% to 60% of the increase is attributable to the storm (comparing exposures of the 200 cm SLR without a storm to the 200 cm SLR and 100-year storm). For this 200 cm SLR in combination with a 100-year storm, >40% of the exposed population reside in Orange County (~110,000 residents primarily in Huntington Beach). The next most vulnerable counties are Los

Angeles with ~56,000 residents (~31,000 in Long Beach, ~7% of the community population), San Diego with ~52,500 residents (~32,000 in San Diego City, 2.5% of the community population), Ventura with ~26,000 in residents (~9,000 in Port Hueneme, 40% of the community population), and Santa Barbara with ~12,000 (~5,000 in Carpinteria, 35% of the community population).

9.2 Infrastructure

9.2.1 Building Replacement Value

Replacement of buildings (residential and commercial) are projected to be highest in the three most southerly counties: Los Angeles, San Diego, and Orange. Together, these 3 counties are expected to hold more than 85% of the cost burden associated with coastal flooding in Southern California (fig. 19B). Replacement values range from ~$1.0-$7.0 billion in Los Angeles (primarily in Long Beach), ~$1.0-$6.5 billion in San Diego (primarily in San Diego City), and $1.0-$9.4 billion in Orange (primarily in Huntington Beach) counties for the 25 to 200 cm SLRs. Expected replacement costs are less than $2.5 billion and $1 billion in Ventura (unincorporated Ventura) and Santa Barbara (Santa Barbara City) counties, respectively, for the 200 cm and lower SLR.

Including the 100-year storm in combination with the 25 cm SLR increases the cost burden by ~140% (up to ~$2.3 billion), 60% (up to ~$1.9 billion), and 55% (up to ~$2 billion) for Los Angeles, Orange, and San Diego counties, respectively. Within each of the 3 counties, the communities of Malibu, San Diego, and Newport Beach are expected to share the greatest burden. In Ventura and Santa Barbara counties, which are less vulnerable to flooding by SLR alone, incorporating the 100-year storm with the 25 cm SLR increases building replacement costs by ~145% and ~450% respectively; the high percentage values are a reflection of the relatively low costs associated with just the SLR scenario, increasing the cost from <$0.1 billion to ~$0.4 billion in Santa Barbara County and from $0.2 to $0.4 billion in Ventura County. The communities most affected are Carpinteria, unincorporated Ventura, and Oxnard.

For the 200 cm SLR, including the 100-year storm increases the cost burden by 30% (for a total of $9 billion), 60% ($15 billion), and 45% ($9 billion) for Los Angeles, Orange, and San Diego counties, respectively, compared to 200 cm of SLR alone. The communities most affected are Long Beach, Huntington Beach, and San Diego City. Expected replacement costs are relatively lower in Ventura and Santa Barbara counties where the burden is expected to be <$3.5 billion and $2 billion in Ventura (unincorporated Ventura) and Santa Barbara (Santa Barbara City) counties, respectively, for the 200 cm plus 100-year storm event.

Note that the values presented here assume total loss of all buildings in flooded areas, regardless of depth or lot coverage. Flood depths are available from the model (and OCOF site) and, in combination with a database of building foundation elevations, could be used to develop depth-damage curves for more refined evaluations of building replacement costs.

9.2.2 Length of Road

As with exposure of residents and building replacement costs, roads within the three most southerly counties are at most risk due to coastal flooding (fig. 19C). For just the 25 cm SLR, it is expected that ~60 km (~40 miles), 55 km (35 miles), and 35 km (20 miles) of road will be submerged in Orange, Los Angeles, and San Diego counties, respectively. The communities most affected are Newport, Huntington Beach, Long Beach, and San Diego City. Raising SLR to 200 cm increases the length of submerged roads to ~410 to 440 km in each of the counties. Impacts to the northern counties are comparatively smaller where ~5 to 230 km (~3 to 145

miles) and ~2 to 45 km (1 to 30 miles) of road are anticipated to be permanently flooded by a 25 cm and 200 cm SLR in Ventura and Santa Barbara counties, respectively.

Including the 100-year storm in combination with the 25 cm SLR increases the length of road flooded by ~100% (for a total of 75 km (~45 miles)), 90% (105 km (65 miles)) and 55% (95 km (60 miles)) for San Diego, Los Angeles, and Orange counties, respectively. The communities of San Diego City, Long Beach, and Huntington Beach are expected to be most affected. Intermittent flooding of roads within Ventura and Santa Barbara counties is expected to affect a total of ~20 km (15 miles) and 50 km (30 miles) of road, representing an additional ~15 km (10 miles) and 40 km (25 miles) compared to permanent flooding by SLR alone. Roads within the unincorporated areas of Ventura and Santa Barbara counties are anticipated to be most affected.

For the 200 cm SLR, including the 100-year storm increases roadway flood potential by 30% (Ventura and San Diego counties) to 140% (Santa Barbara County). Intermittent flooding by 100-year coastal storm events is expected to affect an additional 65 km (40 miles) (Santa Barbara County) to 280 km (175 miles) (Orange County) in excess of permanently flooded roads under a 200 cm SLR. The most affected counties are Orange, Los Angeles, and San Diego, where a total of 690 km (430 miles), 650 km (405 miles), and 550 km (340 miles) are projected to be permanently underwater or intermittently flooded.

9.3 Agriculture and wetlands

Pastures and croplands in Ventura, Orange, and San Diego counties are more vulnerable to flooding compared to agricultural lands in Los Angeles and Santa Barbara counties (fig. 19D). Permanent flooding of agricultural lands is expected to range from <1 km^2 to >20 km^2 (<10 $miles^2$) throughout Southern California with a SLR rise of 25 cm to 200 cm. At the lower-end SLR, San Diego county is expected to experience the greatest flooding, constituting 70% of all flooded agricultural land in Southern California, albeit a small actual area of ~0.5 km^2 (<0.5 $miles^2$). With an increase in SLR, Orange County is expected to experience greater portions of the total, at ~50% (1 km^2; <0.5 $miles^2$) to 55% (1.5 km^2 (<1 $miles^2$) primarily in Seal Beach) for the 75 cm and 100 cm SLR scenarios. For the higher SLRs, the greatest impacts are projected to be in Ventura County where nearly 20 km^2 (<10 $miles^2$; 85% of total; majority in unincorporated Ventura) of agricultural lands are expected to be permanently flooded with the 200 cm SLR.

Including the annual coastal storm in conjunction with SLR exhibits a similar pattern to that of the no storm case in that the counties most affected transitions from San Diego to Orange to Ventura from the lower to higher SLR scenarios. In contrast to the no storm and annual storm cases, the 100-year storm consistently floods relatively larger areas of agricultural lands in Ventura County independent of SLR. Slightly less than ~10 km^2 (~4 $miles^2$) of agricultural land are projected to be flooded with the 100-year storm in combination with SLR up to 100 cm; thereafter, the areas increase incrementally to a maximum of nearly 25 km^2 (~10 $miles^2$) with the 200 cm SLR and 100-year costal storm. Less than 3 km^2 (~1 $mile^2$) of agricultural land in each of the remaining counties are projected to be affected.

A total of ~30-35 km^2 (~10-15 $miles^2$) of wetlands are projected to be permanently flooded in Southern California, given SLR ranging from 25 cm to 200 cm (fig. 19E); the majority of affected lands are within San Diego County at ~20 km^2 (<10 $miles^2$; 75% of the region total) to ~25 km^2 (10 $miles^2$; 65% of the region total) for the lower and higher-end SLRs, respectively. The small increase in area flooded (20 to 25 km^2), compared to the substantial increase in sea level, is a

reflection of the low-lying inter-tidal topography near the coast and increasing inland relief. This pattern of small increases in wetland flooding is also reflected with the annual and 100-year storm events. Inclusion of the 100-year storm event with 25 cm and 200 cm SLR only increases flooded areas by <2 km^2 (<1 $mile^2$) in each of the counties. Overall, the maximum flooded wetland areas for the 200 cm SLR in combination with the 100-year storm are ~25 km^2 (~10 $miles^2$) in San Diego (64% of the total), followed by 10 km^2 (<5 $miles^2$) in Ventura (20% of total), and <5 km^2 (<2 $miles^2$) in Orange (9% of total), 2 km^2 (<1 $miles^2$) in Santa Barbara (5% of total), and 1 km^2 (<0.5 $miles^2$) in Los Angeles (2% of total) counties.

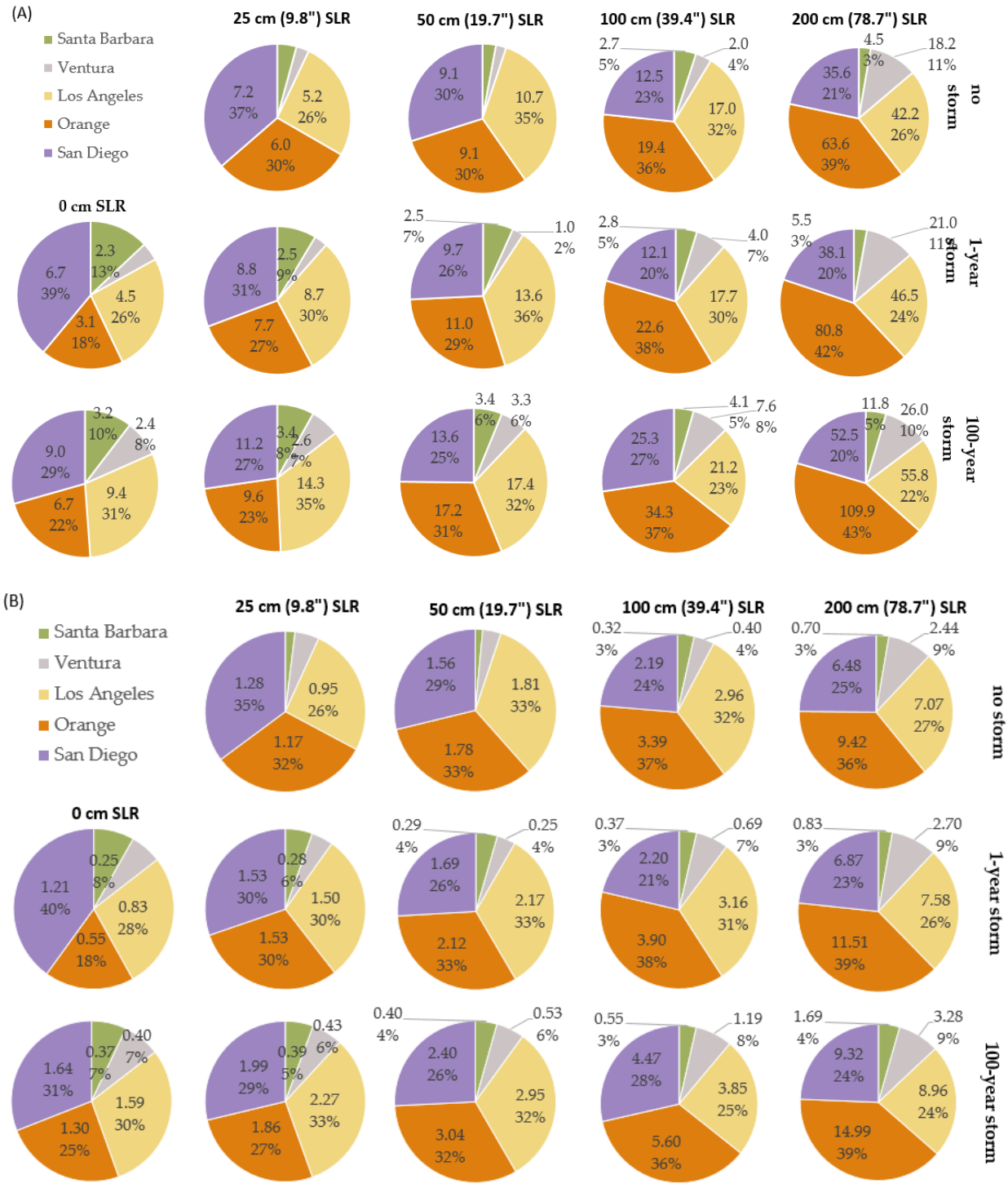

Figure 19. Pie charts showing the relative proportions of specific elements affected within each Southern California coastal county by flood hazards caused by SLR scenarios from 25 cm to 200 cm in combination with no storm, and the annual and 100-year projected storms. (A) County residents (•1,000) exposed to coastal flood hazards. (B) Building replacement costs ($billion).

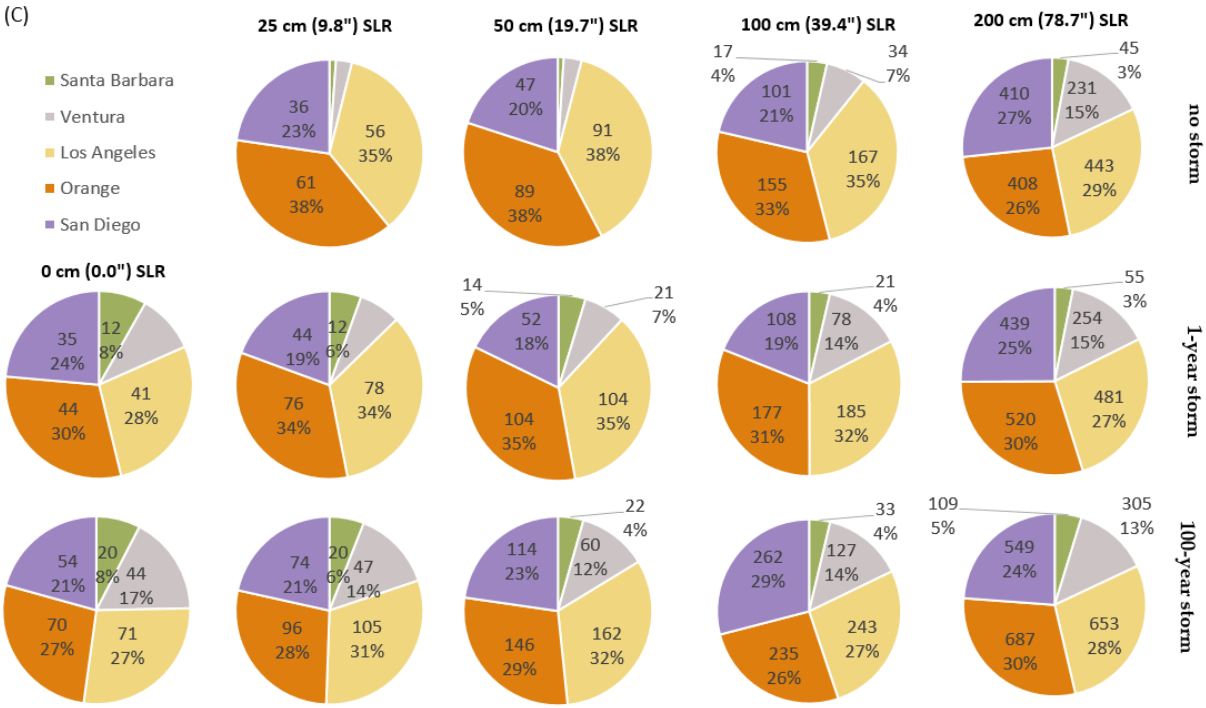

Figure 19 continued. (C) Same as in 19A but for length of road flooded.

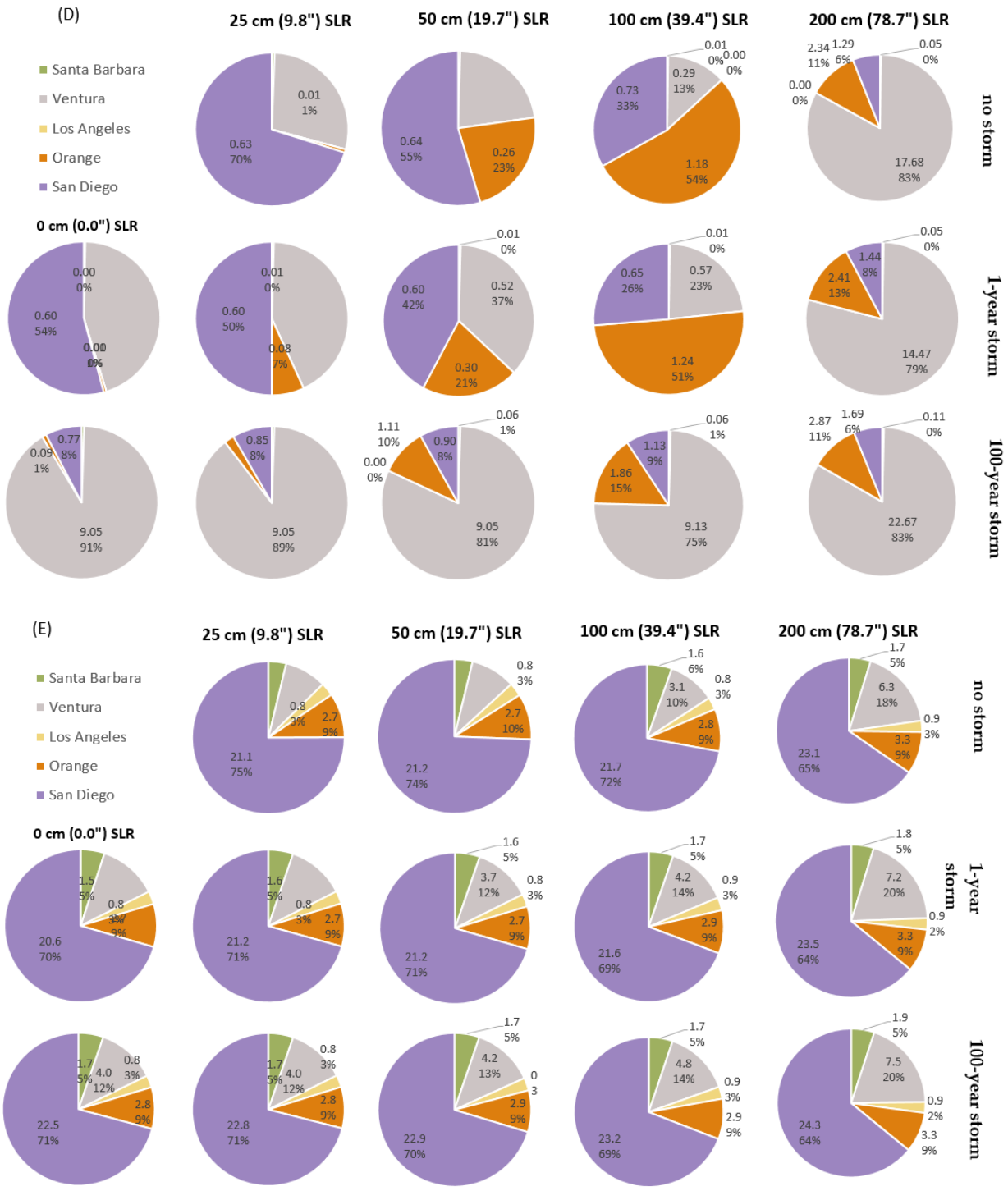

Figure 19 continued. (D) Same as in 19A but for length cropland area. (E) Same as in 19A but for wetland area.

10: Conclusions and Future Directions

The overarching concept of CoSMoS is to leverage projections of global climate patterns over the 21st century from the most recent Global Climate Models (GCMs). Coarse resolution GCM projections are downscaled to the local level and used as boundary conditions to sophisticated ocean modeling tools that simulate complex physics to accurately predict local coastal water levels and flooding for the full range of expected SLR (n= 10: 0-2 m in 0.25 m increments, and 5 m) and storm scenarios (n= 4: average daily/background conditions, annual, 20-year and 100-year). Resulting model projections include spatially explicit estimates of flood extent, depth, duration, uncertainty, water elevation, wave run-up, maximum wave height, maximum current velocity, and long-term shoreline change and bluff retreat.

The model system produces coastal flood projections suitable to aid local climate adaptation planning. The results are provided to the public via two heavily vetted and beta-tested web tools, one focused on physical exposure (Our Coast, Our Future (OCOF): www.ourcoastourfuture.org) and the other on socioeconomic impacts (Hazard Exposure Reporting and Analytics (HERA): https://www.usgs.gov/apps/hera/).

Model results show that, across Southern California, 100-200 cm of SLR is projected to permanently inundate 40-150 km^2 of land and that adding a 100-year coastal storm would flood an additional 55% (150 to 230 km^2 (60-90 miles^2)) to 129% (40 to 100 km^2 (15 to 40 miles^2)). More near-term projections of 25 cm (by ~2030; Sweet et al., 2017) are shown to permanently flood ~10 km^2 (4 miles^2) with an intermittent flood extent increasing the area affected by nearly 350% (10-45 km^2 (4-17.5 miles^2)) when the 100-year storm is also considered. The results demonstrate that, if sea level continues to rise, many areas will be impacted by flooding in both the long- and short-term and that storm conditions combined with even relatively small amounts of SLR expected within just a few decades will substantially increase the exposure hazard.

Translated to socioeconomic impacts, ~20,000-165,000 residents, 160-1,540 km (100-955 miles) of road, up to 22 km^2 (8.5 miles^2) of agricultural land, and up to 35 km^2 (13.5 miles^2) of wetlands are at risk of being permanently flooded in Southern California with a 25-200 cm SLR. Building replacement values are estimated to be between $3.5 billion and $26 billion (present-value, unadjusted for inflation). Accounting for the 100-year storm exposes 55-105% additional residents (41,000-255,000), floods 50-115% additional length of roads (340-2,300 km (210-1,430 miles)), and increases building replacement costs by 40% to 90%.

Residents and infrastructure within Los Angeles, Orange, and San Diego counties are at greater risk to coastal flooding compared to the other two counties (Ventura and Santa Barbara). Overall, more than 80% of residents and infrastructure that are at risk of being flooded for any combination of SLR and coastal storm are in those 3 counties. The most vulnerable communities are: San Diego, Coronado, Imperial Beach, and National City in San Diego county; Huntington Beach and Newport Beach in Orange county; and Long Beach, Los Angeles, and Malibu in Los Angeles county.

While residents and infrastructure in Santa Barbara and Ventura counties are *relatively* less vulnerable to flooding compared to the three southernmost counties, residential exposure and building replacement costs are non-trivial. In the case of SLR alone from 25-200 cm, between 1,400 and 22,700 residents are expected to be flooded and with a burden of $0.2-$3.1 billion in

building replacement costs. Including the 100-year storm increases Santa Barbara and Ventura counties' residential exposure risk and cost burden by 65-330% and 60-230%, respectively.

Of the 5 Southern California counties, Ventura county is most prone to flooding of agricultural land (pasture and croplands) at higher SLRs with or without storms and in all cases of intense storms (accounting for 50-90% of the total), while San Diego county (accounting for more than 65% of the total) is most prone to wetland flooding for all combinations of SLR coastal storms. Across all counties, a total of <1-20 km^2 (0.3-8 $miles^2$) and 30-40 km^2 (12-15 $miles^2$) of agricultural land and wetlands, respectively, are projected to be permanently flooded by SLRs between 25-200cm.

Integrated into the coastal flooding scenarios are projections of long-term coastal change. A 25-200 cm SLR would result in an average beach loss of ~10-70 m (33-230 ft) in Southern California, potentially completely eroding up to 67% of the beaches. Bluff retreat projections indicate a spatial average of ~5-30 m (16-100 ft) of cliff top recession for the 25-200 cm SLRs, but with much variability along the coast and increasing uncertainty with the higher SLRs. The results suggest that for the higher SLR scenarios, future retreat rates could increase nearly two- fold relative to spatially averaged historical rates.

To communicate the availability, potential uses, and implications of these model results, numerous workshops and outreach activities tailored to the specific needs and interests of local stakeholders were held in all five Southern California counties. At each workshop, an overview of the CoSMoS model and regional results were provided; additionally, demonstrations and hands-on trainings of the web tools were conducted, allowing local stakeholders immediate access to data in their respective areas of interest. Attendees typically included planners, engineers, emergency management, and environmental scientists from coastal cities, counties, utilities, state agencies, non-governmental organizations, and the private sector.

The methods and approach outlined in this report are being applied to remaining sections of the California coast and the Pacific northwest region. The results continue to be analyzed and improvements to the methods continue to evolve and are being incorporated in upcoming applications, including site specific modifications as necessary. Results from previous CoSMoS modeling work in San Francisco Bay have been used to identify communities that might benefit from working together across geo-political boundaries on region-wide adaptation strategies (Hummel et al., 2017). Such community clustering techniques could be applied to Southern California to help identify communities with similar adaptation challenges and to enhance regional efforts that aim to facilitate planning and investment prioritization.

11: References

Adams, P.N., Inman, D.L., and Graham, N.E., 2008. Southern California Deep-Water Wave Climate: Characterization and Application to Coastal Processes. Journal of Coastal Research: 24(4), 1022 – 1035.

Anderson, T.R., Fletcher, C.H., Barbee, M.M., Frazer, L.N., and Romine, B.M.. Doubling of coastal erosion under rising sea level by mid-century in Hawaii. *Natural Hazards* (2015).

Arblaster, J.M., Meehl, G.A., and Karoloy, D.J., 2011. Future cliate change in the Southern Hemisphere: Competing effects of ozone and greenhouse gases. Geoph. Res. Ltrs., 38, L02701, 6pp.

Barlow, J., Lim, M., Rosser, N., Petley, D., Brain, M., Norman, E., and Geer, M., 2012. Modeling cliff erosion using negative power law scaling of rockfalls. Geomorphology, 139, 416-424.

Barnard, P.L., Erikson, L.H., Foxgrover, A.C., Limber, P.L., O'Neill, A.C., and Vitousek, S., 2018. Coastal Storm Modeling System (CoSMoS) for Southern California, v3.0, Phase 2 (ver. 1g, May 2018): U.S. Geological Survey data release, https://doi.org/10.5066/F7T151Q4

Barnard, P. L., van Ormondt, M., Erikson, L.H., Eshleman, J., Hapke, C., Ruggiero, P., Adams, P. N., and Foxgrover, A. C., 2014. Development of the Coastal Storm Modeling System (CoSMoS) for predicting the impact of storms on high-energy, active-margin coasts. Natural Hazards, 31 p., doi: 10.1007/s11069-014-1236-y

Barnard, P.L., Hoover, D.J., Hubbard, D.M., Snyder, A., Ludka, B.C., Allan, J., Kaminsky, G.M., Ruggiero, P., Gallien, T.W., Gabel, L., McCandless, D., Weiner, H.M., Cohn, N., Anderson, D.L. and Serafin, K.A., 2017. Extreme oceanographic forcing and coastal response due to the 2015-2016 El Niño. Nat. Comm., 8 (14365), 8 pp.

Barnard, P.L., O'Reilly, B., van Ormondt, M., Elias, E., Ruggiero, P., Erikson, L. H., Hapke, C., Collins, B. D., Guza, R. T., Adams, P. N., and Thomas, J., 2009. The framework of a coastal hazards model: a tool for predicting the impact of severe storms. U.S. Geological Survey Open-File Report 2009-1073, 19 pp., http://pubs.usgs.gov/of/2009/1073/

Barnard, P.L., O'Reilly, Bill, van Ormondt, Maarten, Elias, Edwin, Ruggiero, Peter, Erikson, L.H., Hapke, Cheryl, Collins, B.D., Guza, R.T., Adams, P.N., and Thomas, J.T., 2009. The framework of a coastal hazards model; a tool for predicting the impact of severe storms: U.S. Geological Survey Open-File Report 2009-1073, 21 p. [http://pubs.usgs.gov/of/2009/1073/].

Barnard, P.L., van Ormondt, M., Erikson, L.H., Eshleman, J., Hapke, C., Ruggiero, P., Adams, P.N., and Foxgrover, A.C., 2014. Development of the Coastal Storm Modeling System (CoSMoS) for predicting the impact of storms on high-energy, active-margin coasts. Natural Hazards, Volume 74 (2), p. 1095-1125, http://dx.doi.org/10.1007/s11069-014-1236-y.

Barnard, P.L., Eshleman, J., Erikson, L., and Hanes, D.M., 2007. Coastal processes study at Ocean Beach, San Francisco, CA; summary of data collection 2004-2006: U. S. Geological Survey Open-File Report 2007-1217, 171 p. [http://pubs.usgs.gov/of/2007/1217/].

Booij, N., Ris, R. C., and Holthuijsen, L. H., 1999. A third-generation wave model for coastal regions. 1. Model description and validation. Journal of Geophysical Research, 104(C4), 7649–7666. https://doi.org/10.1029/98JC02622

Bromirski, P. D., Cayan, D. R., and Flick, R. E., 2005. Wave spectral energy variability in the northeast Pacific. Journal of Geophysical Research, 110, C03005. https://doi.org/10.1029/2004JC002398

Bromirski, P.D., Flick, R.E., and Cayan, D.R., 2003. Storminess variability along the California coast: 1858–2000, Journal of Climate, 16(6), 982–993.

Bürgmann, R., Hilley, G., Ferretti, A., Novali, F., 2006. Resolving vertical tectonics in the San Francisco Bay Area from permanent scatter InSAR and GPS analysis. Geology 34 (3), 221–224.

Camus, P., Menéndez, M., Méndez, F. J., Izaguirre, C., Espejo, A., Cánovas, V., … Medina, R., 2014. A weather-type statistical downscaling.

Carpenter, N. E., Stuiver, C., Nicholls, R., Powrie, W., and Walkden, M., 2012. Investigating the recession process of complex soft cliff coasts: an Isle of Wight case study. *Coastal Engineering Proceedings*, *1*(33), 123.

Castedo, R., Murphy, W., Lawrence, J., and Paredes, C., 2012. A new process–response coastal recession model of soft rock cliffs. *Geomorphology*, *177*, 128-143.

Cayan, D., J. Kalansky, S. Iacobellis, D. Pierce, 2016. Creating Probabilistic Sea Level Rise Projections to support the 4th California Climate Assessment. White Paper for the 2016 Integrated Energy Policy Report. http://docketpublic.energy.ca.gov/PublicDocuments/16-IEPR-04/TN211806_20160614T101823_Creating_Probabilistic_Sea_Leve_Rise_Projections.pdf

Christiansen R.L., and Yeats, R.S., 1992. Post-Laramide geology of the U.S. Cordilleran region. In: Burchfiel BC, Lipman PW, and Zoback ML (eds), The Cordilleran Region: conterminous U.S.: the geology of North America [DNAG] Vol. G-3: Geol. Soc. America, 261–406.

Church, J.A., et al. "Sea Level Change." In: Climate Change 2013: The Physical Science Basis. Contribution of Working Group I to the Fifth Assessment Report of the Intergovernmental Panel on Climate Change [Stocker, T.F., D. Qin, G.-K. Plattner, M. Tignor, S.K. Allen, J. Boschung, A. Nauels, Y. Xia, V. Bex and P.M. Midgley (eds.)]. Cambridge University Press, Cambridge, United Kingdom and New York, NY, USA.

Crosby, S. C., O'Reilly, W. C., and Guza, R. T., 2016. Modeling long period swell in southern California: Practical boundary conditions from buoy.

Danielson, J.J., Poppenga, S.K., Brock, J.C., Evans, G.A., Tyler, D.J., Gesch, D.B., Thatcher, C.A., and Barras, J.A., 2016. Topobathymetric elevation model development using a new

methodology—Coastal National Elevation Database: Journal of Coastal Research, SI no. 76, p. 75–89, doi: 10.2112/SI76-008

Egbert, G. D., Bennett, A. F. and Foreman, M. G. G.. TOPEX/POSEIDON tides estimated using a global inverse model. *Journal of Engineering*. **53**(7), 573–588, doi:10.1016/j.coastaleng.2005.12.005 (2006).

Erikson, L.H., Barnard, P.L., O'Neill, A.C., Vitousek, S., Limber, P., Foxgrover, A.C., Herdman, L.H., and Warrick, J., 2017A. CoSMoS 3.0 Phase 2 Southern California Bight: Summary of data and methods. U.S. Geological Survey, doi: 10.5066/F7T151Q4

Erikson, L.H., O'Neill, A., Barnard, P.L., Vitousek, S., Limber, P., 2017B. Climate change-driven cliff and beach evolution at decadal to centennial time scales. *Coastal Dynamics 2017*, Paper No. 210, p. 125-136, http://coastaldynamics2017.dk/proceedings.html

Erikson, L.H., Hegermiller, C.E., Barnard, P.L. and Storlazzi, C.D., 2016. Wave projections for United States mainland coasts. U.S. Geological Survey pamphlet to accompany Data Release, 172 pp., doi: 10.5066/F7D798GR

Erikson, L.H., Hegermiller, C.A., Barnard, P.L., Ruggiero, P. and van Ormondt, M., 2015. Projected wave conditions in the Eastern North Pacific under the influence of two CMIP5 climate scenarios. *Ocean Modeling*, Volume 96, p. 171-185, doi: 10.1016/j.ocemod.2015.07.004

Flick, R. E., 1998. Comparison of California tides, storm surges, and mean sea level during the El Niño winters of 1982–1983 and 1997–1998. Shore and Beach 66(3):7–11.

Flint, L.E. and Flint, A.L., 2014. California Basin Characterization Model: A Dataset of Historical and Future Hydrologic Response to Climate Change, (ver. 1.1, May 2017): U.S. Geological Survey Data Release, https://doi.org/10.5066/F76T0JPB.

Ghorbani, M.A., Singh, V.P., Sivakumar, B., et al.. Appl Water Sci (2017) 7: 663. https://doi.org/10.1007/s13201-015-0278-y

Graham, N.E., Cayan, D.R., Bromirski, P.D., Flick, R.E., 2013. Multi-model projections of twenty first century North Pacific winter wave climate under the IPCCA2 scenario. Clim. Dyn. 40,1335–1360.

Hackney, C., Darby, S. E., and Leyland, J., 2013. Modelling the response of soft cliffs to climate change: A statistical, process-response model using accumulated excess energy. Geomorphology, 187, 108-121.

Heberger, Matthew, Heather Cooley, Eli Moore, and Pablo Herrera (Pacific Institute), 2012. The *Impacts of Sea Level Rise on the San Francisco Bay*. California Energy Commission. Publication number: CEC-500-2012-014.

Hegermiller, C.A., Rueda, A., Erikson, L. H., Barnard, P. L., Antolinez, J. A. A., and Mendez, F. J., 2017A. Controls of multimodal wave conditions in a complex coastal setting. Geophysical Research Letters, 44. https://doi.org/10.1002/2017GL075272

Hegermiller, C.A., Antolinez, J.A.A., Rueda, A.C., Camus. P., Perez, J., Erikson, L.H., Barnard, P.L. and Mendez, F.J., 2017B. A multimodal wave spectrum-based approach for

statistical downscaling of local wave climate. *Journal of Physical Oceanography*, doi: 10.1175/JPO-D-16-0191.1

Hegermiller, C.A., Erikson, L.H. and Barnard, P.L, 2016. Nearshore waves in Southern California: hindcast and modeled historical and 21st-century projected time-series. U.S. Geological Survey data release, doi: 10.5066/F7N29V2V

Hemer, M. A., Y. Fan, N. Mori, A. Semedo, and X. L. Wang, 2013. Projected changes in wave climate from a multi-model ensemble. *Nature Climate Change*, **3,** 471-476.

Hogarth L., Babcock J., Driscoll N., Dantec N., Haas J., Inman D., and Masters P., 2007. Long-term tectonic control on Holocene shelf sedimentation offshore La Jolla, California. Geology 35(3):275.

Homer, C.G., Dewitz, J.A., Yang, L., Jin, S., Danielson, P., Xian, G., Coulston, J., Herold, N.D., Wickham, J.D., Megown, K., 2015. Completion of the 2011 National Land Cover Database for the conterminous United States-Representing a decade of land cover change information. Photogramm. Eng. Remote Sens. 81 (5), 345–354.

Horsburgh, K. L. and Wilson, C.. Tide–surge interaction and its role in the distribution of surge residuals in the North Sea. J. Geophy. Res. 112, CO8003 (2007).

Horton, B. P., Rahmstorf, S., Engelhart, S. E., and Kemp, A. C.. "Expert assessment of sea-level rise by AD 2100 and AD 2300." *Quaternary Science Reviews*, *84*, (2014):1-6.

Howell, S., Smith-Konter, B., Frazer, N., Tong, X., and Sandwell, D., 2016. The vertical fingerprint of earthquake cycle loading in southern California. Nt. Geosc. 9, 611-614.

Hummel, M., Wood, N.J., Schwelkert, A., Stacey, M.T., Jones, J., Barnard, P.L., Erikson, L., 2017. Clusters of community exposure to coastal flooding hazards based on storm and sea level rise scenarios – implications for adaptation networks in the San Francisco Bay region. Reg. Env. Change, Springer Nature, 13 pp. https://doi.org/10.1007/s10113-017-1267-5

Infogroup, 2012. Employer Database: Infogroup Online Dataset. http://www.referenceusagov.com/. (Accessed 20 October 2012).

Jones, J.M., Wood, N., Ng, P., Henry, K., Jones, J.L., Peters, J., Jamieson, M., 2016. Community Exposure in California to Coastal Flooding Hazards Enhanced by Climate Change, Reference Year 2010: U.S. Geological Survey Data Release. http://dx.doi.org/10.5066/F7PZ56ZD.

Kanamitsu, M. and H. Kanamaru, H., 2007. 57-year California Reanalysis Downscaling at 10km (CaRD10) Part 1. System Detail and Validation with Observations, J. Climate, 20, 5527-5552.

Kline, S. W., Adams, P. N., and Limber, P. W., 2014. The unsteady nature of sea cliff retreat due to mechanical abrasion, failure, and comminution feedbacks. *Geomorphology*, *219*, 53-67.

Lesser, G.R., Roelvink, J.A., van Kester, J.A., Stelling, G.S., 2004. Development and validation of a three dimensional, morphological model. Coast Eng 51:883–915

Lim, M., Rosser, N. J., Allison, R. J., and Petley, D. N., 2010. Erosional processes in the hard rock coastal cliffs at Staithes, North Yorkshire. *Geomorphology*, *114*(1), 12-21.

Limber, P. W., and Murray, A. B., 2011. Beach and sea-cliff dynamics as a driver of long-term rocky coastline evolution and stability, Geology, 39(12), 1147–1150.

Limber, P., Barnard, P., Hapke, C., 2015. *Towards projecting the retreat of California's coastal cliffs during the 21st century*. Proceedings of Coastal Sediments 2015 Conference, World Scientific, Singapore.

Limber, P., Barnard, P.L., Vitousek, S., and Erikson, L.H., 2018. A model ensemble for projecting multi-decadal coastal cliff retreat during the 21st century. J. Geoph. Res.–Earth Surf.

Long, J. W., and Plant, N. G., 2012. Extended Kalman filter framework for forecasting shoreline evolution, Geophys. Res. Lett., 39, L13603, doi:10.1029/2012GL052180.

National Research Council (NRC), 2012. *Sea-level rise for the coasts of California, Oregon, and Washington: past, present, and future*. Committ

O'Reilly, W.C., Guza, R.T., and Seymour, R.J., 1999. Wave prediction in the Santa Barbara Channel. Proc. 5th California Islands symposium, mineral management service, Santa Barbara CA, March 29–31.

O'Reilly, W. C., and Guza, R. T., 1993. A comparison of two spectral wave models in the Southern California bight. Coastal Engineering, 19(3-4).

O'Neill, A. C., Erikson, L. H., and Barnard, P. L., 2017. Downscaling wind and wavefields for 21st century coastal flood hazard projections in a region of complex terrain. Earth and Space Science, Volume 4, pp. 314–334, doi: 10.1002/2016EA000193

Pfeffer, W.T., Harper, J.T., and O'Neel, S., 2008. Kinematic constraints on glacier contributions to 21st-century sealevel rise. Science 331:1340–1343

Pierce, Cayan, Kalansky, et al., 2018. CA 4th Asssessment Report.

Porter, K., Wein, A., Alpers, C., Baez, A., Barnard, P.L., Carter, J., Corsi, A., Costner, J., Cox, D., Das, T., Dettinger, M., Done, J., Eadie, C., Eymann, M., Ferris, J., Gunturi, P., Hughes, M., Jarrett, R., Johnson, L., Dam Le-Griffin, H., Mitchell, D., Morman, S., Neiman, P., Olsen, A., Perry, S., Plumlee, G., Ralph, M., Reynolds, D., Rose, A., Schaefer, K., Serakos, J., Siembieda, W., Stock, J., Strong, D., Sue Wing, I., Tang, A., Thomas, P., Topping, K., Wills, C. and Jones, L., 2011. Overview of the ARkStorm scenario. U.S. Geological Survey Open-File Report 2010-1312, 183 pp., https://pubs.usgs.gov/of/2010/1312/

Riahi, K., Krey, V., Rao, S., Chirkov, V., Fischer, G., Kolp, P., Kindermann, G., Nakicenovic, N., and Rafai, P., 2011. RCP 8.5: Exploring the consequence of high emission trajectories. Climatic Change, 109(1-2), 33-57.

Ris, R.C., Booij, N., and Holthuijsen, L.H., 1999. A third-generation wave model for coastal regions: Part II –Verification.: Journal of Geophysical Research, 104(C4), 7667-7682.

Ris, R.C., Booij, N., and Holthuijsen, L.H., 1999. A third-generation wave model for coastal regions: Part II –Verification.: Journal of Geophysical Research, 104(C4), 7667-7682.

Roelvink, D., Reniers, A. J. H. M., Van Dongeren, A., Van Thiel de Vries, J., Lescinski, J., and McCall, R., 2010. *XBeach model description and manual*. Unesco-IHE Institute for Water Education, Deltares, and Delft University of Tecnhology. Report.

Roelvink, D., Reniers, A., Van Dongeren, A., van Thiel de Vries, J., McCall, R., and Lescinski, J., 2009. Modelling storm impacts on beaches, dunes, and barrier islands. Coast Eng 56(11–12):1133–1152

Rogers W., Kaihatu J., Hsu L., Jensen R., Dykes J., and Holland K., 2007. Forecasting and hindcasting waves with the SWAN model in the southern California Bight. Coastal Engineering 54(1):1–15

Rosser, N. J., Brain, M. J., Petley, D. N., Lim, M., and Norman, E. C., 2013. Coastline retreat via progressive failure of rocky coastal cliffs. *Geology*, *41*(8), 939-942.

Ruggiero, P., Komar, P. D., McDougal, W. G., Marra, J. J. and Beach, R. A. Wave run-up, extreme water levels, and the erosion of

Scripps Institute of Oceanography (SIO), University of California at San Diego. Coastal Data Information Program (CDIP), 2015B. Last accessed March 2015. https://cdip.ucsd.edu/

Soulsby, R. L., 1997. Dynamics of Marine Sands, Thomas Telford, London.

Stockdon, H. F., Holman, R. A., Howd, P. A. and Sallenger, A. H.. Empirical parameterization of setup, swash, and run-up. *Coastal*

Storlazzi, C. D. and Griggs, G. B.. Influence of El Nino–Southern Oscillation (ENSO) events on the evolution of central California's shoreline. *Geological Society of America Bulletin*. **112**(2), 236–249 (2000).

Storlazzi, C.D., Griggs, G.B., 1998. The 1997–98 El Niño and erosion processes along the central coast of California. Shore and Beach, 66(3):12–17.

Thomson, A.M., Calvin, K.V., Smith, S.J., Kyle, G.P., Volke, A., Patel, P., Delgado-Arias, S., Bond-Lamberty, B., Wise, M.A., Clarke, L.E., Edmonds, J.A., 2011. RCP4.5: A Pathway for Stabilization of Radiative Forcing by 2100. Climatic Change, 109(1-2), 77-94.

Tolman, H. L., and Chalikov, D., 1996. Source Terms in a Third-Generation Wind Wave Model. *Journal of Physical Oceanography*, **26,** 2497-2518.

Tolman, H. L., Balasubramaniyan, B., Burroughs, L. D., Chalikov, D. V., Chao, Y. Y., Chen, H. S., and Gerald, V. M., 2002. Development and

Trenhaile, A.S., 2011. *Predicting the response of hard and soft rock coasts to changes in sea level and wave height*. Climatic Change, 109:599-615.

U.S. Census Bureau, 2010. American Factfinder: U.S. Census Bureau Web Site. https://factfinder.census.gov/faces/nav/jsf/pages/index.xhtml.

Vermeer M, Rahmstorf, S., 2009. Global sea level linked to global temperature. Proc Natl Acad Sci 106(51):21527–21532

Vitousek, S. and Barnard, P.L., 2015. A non-linear, implicit one-line model to predict long-term shoreline change. *In*: P. Wang, J.D. Rosati and J. Cheng (Eds.), The Proceedings of the Coastal Sediments 2015, World Scientific, 14 pp., doi: 10.1142/9789814689977_0215

Vitousek, S., Barnard, P.L., Limber, P., Erikson, L., and Cole, B., 2017. A model integrating longshore and cross-shore processes for predicting long-term shoreline response to climate change. Journal of Geophysical Research: Earth Surface, Volume 122 (4), pp. 782–806, doi: 10.1002/2016JF004065

Walkden M.J.A., and Hall, J.W., 2005. *A predictive mesoscale model of the erosion and profile development of soft rock shores*. Coastal Engineering, 52, 55-563.

Walkden, M., and Dickson, M., 2008. Equilibrium erosion of soft rock shores with a shallow or absent beach under increased SLR. *Marine Geology*, *251*(1), 75-84.

Warrick, J.A., and Farnsworth, K.L., 2009. Sources of sediment to the coastal waters of the Southern California Bight, in Lee, H.J., and Normark, W.R., eds., Earth science in the urban ocean--The Southern California Continental Borderland: Geological Society of America Special Paper 454, p. 39-52.

Wehmiller, J. F., A. Sarna-Wojcicki, Yerkes, R.F., and Lajoie, K.R., et al. (1979). "Anomalously high uplift rates along the Ventura--Santa Barbara Coast, California--tectonic implications." Tectonophysics 52(1-4): 380.

Wood, N., Ratliff, J., Peters, J., 2012. Community Exposure to Tsunami Hazards in California: U.S. Geological Survey Scientific Investigations Report 2012–5222, Reston, VA, 49.

Yates, M. L., Guza, R. T., and O'Reilly, W. C., 2009. Equilibrium shoreline response: Observations and modeling, J. Geophys. Res., 114, C09014,

Yin, J. H., 2005. A consistent poleward shift of the storm tracks in simulations of 21st century climate, Geophys. Res. Lett., 32, L18701, doi: 10.1029/2005GL023684.

Young, A. P., Guza, R. T., Flick, R. E., O'Reilly, W. C., and Gutierrez, R, 2009. Rain, waves, and short-term evolution of composite seacliffs in southern California. *Marine Geology*, *267*(1), 1-7.

APPENDIX A: Workshop Agendas

Sea Level Rise and San Diego Communities:
Science and Planning For Our Future
November 17, 2016 | 8:30am – 12:00pm
San Diego Regional Water Board, 2375 Northside Dr, San Diego, CA 92108

Participants will:

- Learn about the basics of recent sea level rise science and how to access and use the results
- Explore how San Diego is preparing for sea level rise at the local and regional levels

8:30	**Registration & Refreshments**
9:00	**Welcome** *David Gibson, Regional Water Quality Control Board, Executive Officer*
	Southern California Coastal Storm Modeling System (CoSMoS) *Moderator: Juliette Hart, U.S. Geological Survey (USGS)*
9:15	**Overview of the Southern California Coastal Storm Modeling System (CoSMoS)** *Li Erikson, U.S. Geological Survey (USGS), Research Oceanographer*
9:30	**How To View CoSMoS Results: An Intro To An Interactive Online Viewer** *Michael Fitzgibbon, Point Blue, Chief Technology Officer*
9:45	**Q & A**
	Perspectives on Resilience: How the San Diego Region is planning for sea level rise *Moderator: Laura Engeman, San Diego Regional Climate Collaborative*
10:10	**Overview of Regional Sea Level Rise Efforts in San Diego County** *Laura Engeman, San Diego Regional Climate Collaborative, Manager*
10:25	**The Del Mar Planning Strategy** *Bruce Bekkar, M.D,* *Del Mar Sea-level Rise Stakeholder-Technical Advisory Committee Member*
10:45	***The Imperial Beach Perspective on Vulnerability*** *Ed Spriggs, Imperial Beach City Councilmember*
11:05	**A Utility's Regional Perspective on Coastal Resilience** *Brian D'Agostino, San Diego Gas & Electric, Meteorologist*
11:25	**Q & A**
11:50	**Wrap-up and Close**

Afternoon Agenda

Technical Updates & Discussion

November 17, 2016 | 1:00pm – 3:00pm

San Diego Regional Water Board, 2375 Northside Dr, San Diego, CA 92108

Participants will:

- Receive technical updates for USGS's Coastal Storm Modeling System (CoSMoS)
- Discuss CoSMoS in more technical detail
- Explore new sea level rise modeling being conducted at Scripps

1:00	**CoSMoS: Cliff Model Updates** *Pat Limber, U.S. Geological Survey (USGS)*
1:20	**CoSMoS: Flood Model Updates** *Li Erikson, U.S. Geological Survey (USGS)*
1:40	**Q & A**
2:10	**New Sea Level Rise Modeling & the 4th Assessment** *Dan Cayan, Scripps Institution of Oceanography*
2:30	**Q & A**
2:50	**Wrap-up**

ADAPTLA | Sea Level Rise & Coastal Impacts Planning

Modeling Meets Planning:
Final CoSMoS Results and Next Steps in Coastal Adaptation Planning

February 22, 2017 | 1 PM – 5 PM

Agenda

1:00 - 1:10	**Welcome and Overview** Phyllis Grifman, USC Sea Grant
	Presentations
1:10 - 1:30	• Final Results: Coastal Storm Modeling System (CoSMoS 3.0) Patrick Barnard, U.S. Geological Survey
1:30 - 1:45	• Web Tool: Our Coast, Our Future Michael Fitzgibbon, Point Blue Conservation Science
1:45 - 2:00	• Web Tool: Hazard Exposure Reporting and Analytics Jeanne Jones, U.S. Geological Survey
2:00 - 2:10	• Web Tool: Climate-Smart Cities Decision Support Tool Fernando Cazares, Trust for Public Land
	Community Planning Excercise
2:10 - 2:15	• Introduction Nick Sadrpour, USC Sea Grant
2:15 - 2:25	• Adaptation Strategies Presentation Lesley Ewing, California Coastal Commission
2:25 - 3:10	• Group Excercise: Planning Evolving Coastlines
3:10 - 3:25	Break
3:25 - 3:55	• Discussion: Planning through a Regional Lens
3:55 - 4:45	**Tools Cafe** • Our Coast, Our Future • Hazard Exposure Reporting and Analytics • Climate-Smart Cities Decision Support Tool
4:45 - 5:00	**Wrap up and Adjourn**

Sea Grant | USGS science for a changing world | ESA | Coastal Conservancy | California Coastal Commission | Ocean Protection Council

Planning for Shoreline Change in Ventura and Santa Barbara
CoSMoS and Communication Training
June 27, 2017; 9 am – 4:00 pm
Channel Islands Boating Center, 3880 Bluefin Cir, Oxnard, CA 93035

8:30	Registration
9:00	Welcome, Introduction, and Workshop Goals Rachel Couch, State Coastal Conservancy Cara Pike, Climate Access
	Presentations: • Coastal Storm Modeling System (CoSMoS) Patrick Barnard, U.S. Geological Survey • Our Coast Our Future (OCOF) Michael Fitzgibbon, Point Blue Conservation Science • Hazard Exposure Reporting and Analytics (HERA) Nate Wood, U.S. Geological Survey
	Break
	Climate Communication Best Practices and Alignment
12:30	Lunch
	Connecting the Dots
	Community Based Sea Level Rise Planning
	External Engagement Scenarios
	Break
	External Engagement Scenarios Continued
3:45	Conclusion and Closing